Fluoro-Organic Lithium Salts

for Advanced Lithium Batteries

リチウム電池用フッ素化有機リチウム塩

September 2014

Fusaji Kita

喜多 房次

Contents

General Introduction

Lithium batteries including lithium-ion batteries have been used as mobile electronic devices, such as mobile phones, laptop computers, game machines including MP3 players, digital cameras, and recent smart phones. In addition to such small-size applications, lithium-ion batteries have been of great interest as power sources for hybrid electric vehicles together with pure electric vehicles over the world. The modern world cannot be described without lithium-ion batteries.

A lithium-ion battery consists of a positive and negative electrode separated by a separator absorbed an electrolyte solution. Figure 1 shows a schematic illustration of the typical lithium-ion battery. Positive-electrode materials are usually $LiCoO_2$, $Li[Li_{0.1}Mn_{1.9}]O_4$, $LiAl_{0.05}Co_{0.15}Ni_{0.8}O_2$, $LiCo_{1/3}Ni_{1/3}Mn_{1/3}O_2$, or $LiFePO_4$ [1-7] and negative-electrode materials are graphite or non-graphitized carbons [8-11]. During charge and discharge, lithium ions shuttle between the positive and negative electrodes at which lithium ions are inserted or extracted without the destruction of core structures. Such materials are called lithium insertion materials. During the past 35 years, lithium insertion materials have been developed to a quite high level [11]. One can select lithium insertion materials whose operating voltage ranges from 3 to 5 V vs. Li for a positive electrode and from 0.1 to 2 V vs. Li for a negative electrode in designing lithium-ion batteries at present.

The electrolyte solutions used in lithium-ion batteries are not aqueous solutions. Water is a highly polar (ε = 80.2 at 20°C) solvent, which dissolves a large variety of salts, giving electrolyte solutions with a high ionic conductivity. However, an aqueous electrolyte solution is thermodynamically decomposed to oxygen at 1.23 V vs. NHE and to hydrogen at 0.00 V vs. NHE, so that its potential window is too narrow. NHE stands for a normal hydrogen electrode at given solution pH. “A potential window” is also called “electrochemical window”, which is the width of the potential range in which the solvent, the electrolyte, and the electrode remain electrochemically inert. The potential window of water is

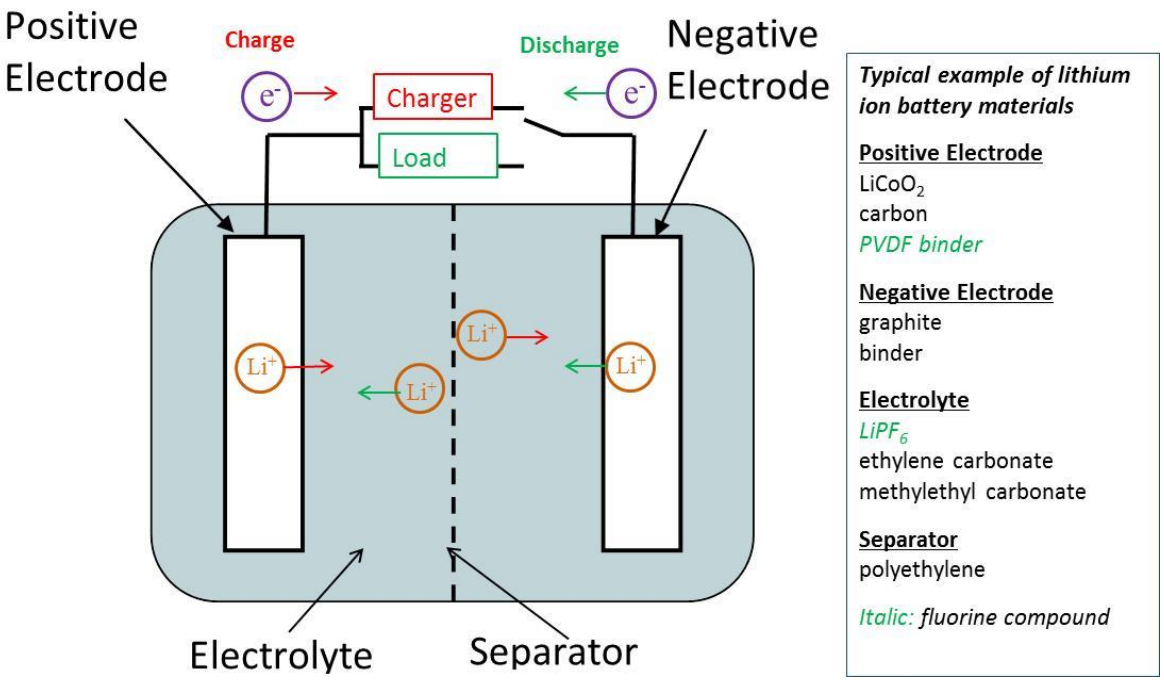

Figure 1 A schematic illustration of a lithium-ion battery consisting of positive and negative electrodes separated by a separator, in which an electrolyte solution is adsorbed. A positive electrode is usually $LiCoO_2$ mixed with a conductive carbon and PVdF binder and a negative electrode is graphite mixed with a PVdF binder. An electrolyte is usually $LiPF_6$ dissolved in the mixed solvents of ethylene carbonate and methylethyl carbonate.

about 1.3 – 1.4 V on a platinum electrode. In order to extend the potential window of an electrolyte solution, organic electrolyte solutions are used in lithium-ion batteries. The term of "Electrolyte" in this thesis is used for compounds that dissociate into anions and cations when they dissolve in solvents, providing the ionic conductivity. The electrolytes for lithium-ion batteries are lithium salts and the solvents are usually aprotic polar solvents as are listed in Table 1 [12] and shown in Fig. 2. Nonaqueous solvents used in lithium batteries are usually γ-butyrolactone (GBL, ε = 39.1 at 20°C), ethylene carbonate (EC, ε = 90.36 at 40°C), or propylene carbonate (PC, ε = 64.95 at 20°C) as a main solvent to dissolve lithium salts. The potential windows of these solvents are wider than that of water, i.e., more than 4 V. During the past 45 years, main solvents for practical lithium batteries do not change

Table 1　Properties of polar aprotic organic solvents used for lithium batteries including lithium-ion batteries.

Solvent	Dielectric constant/– (at 25 ℃)	Viscosity/cp (at 20 ℃)	Melting point /℃	Boiling point /℃
propylene carbonate (PC)	64.4	2.5	−49	243
ethylene carbonate (EC)	95.3	1.9	34−37	240
γ −butyrolactone (GBL)	39	1.7	−44	204
1,2−dimethoxyethane (DME)	5.5	0.48	−58	82
tetrahydrofuran(THF)	7.6	0.55	−108	66
dimethyl carbonate(DMC)	3.1	0.59	2	90
diethyl carbonate(DEC)	2.8	0.75	−43	127
methylethyl carbonate(MEC)	2.9	0.65	−14	107

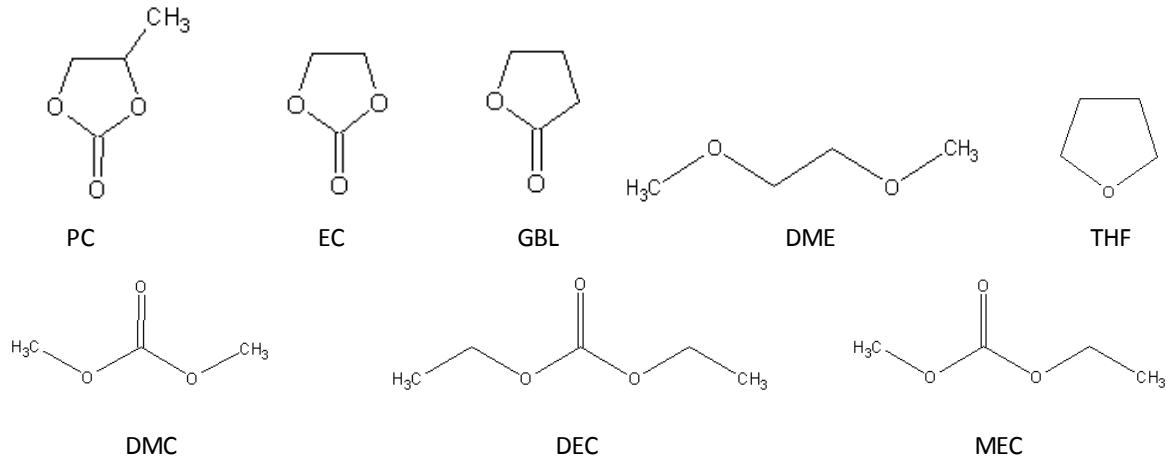

Figure 2　Lewis structures of some common solvents listed in Table 1.

in spite of several efforts to innovate polar aprotic solvents [12].

In considering lithium salts for lithium battery electrolytes,

(1) lithium salts should be highly soluble in an appropriate solvent,

and resulting electrolyte solutions should have

(2) high ionic conductivity,

(3) wide potential window, especially resistive against oxidation, and

(4) thermal and chemical stability.

In addition to the above requirements, common items for practical use are

(5) no toxicity and

(6) low cost.

Of these, ionic conductivity of battery electrolyte is straightforwardly related to battery performance, especially power capability. An electrolyte solution having a wide voltage window means that high voltage operation is possible and consequently high-energy density batteries can be made. Thermal and chemical stability not to induce thermal runaway is associated with reliable, safe long-term operation.

These requirements do not satisfy by using a single salt, such as LiCl or LiF, because the solubility even in an appropriate solvent is low due to their high lattice energy in ionic crystals. The first electrolytes used in primary lithium batteries in the 1970s are $LiClO_4$ and $LiBF_4$ in Fig. 3(a) and (b). However, lithium perchlorate solutions are thermally unstable, so that there are explosive risks with organic solvents. Lithium tetrafluoroborate solutions do not give high conductivity compared to $LiClO_4$ or $LiAsF_6$ solutions, which can initiate the polymerization of cyclic ethers due to the Lewis base BF_3 derived from BF_4^- anions.

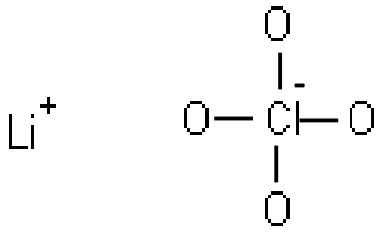

(a) $LiClO_4$
Lithium perchlorate

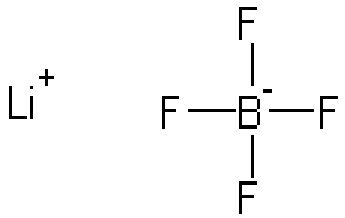

(b) $LiBF_4$
Lithium tetrafluoroborate

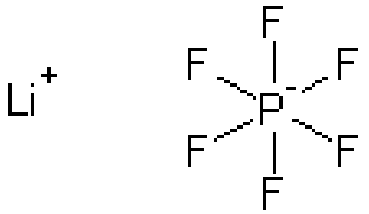

(c) $LiPF_6$
Lithium hexafluorophosphate

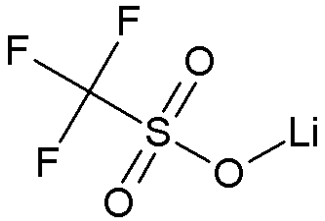

(d) CF_3SO_3Li
Lithium trifluoromethanesulfonate

Figure 3 Lewis structures of typical inorganic lithium salts and CF_3SO_3Li for lithium batteries and lithium-ion batteries.

The second electrolyte used in rechargeable lithium batteries in the 1980s is $LiAsF_6$, which is thermally stable. However, lithium hexafluoroarsenate potentially has environmental risks due to the element of arsenic. The third electrolyte used in lithium-ion batteries since the early 1990s is $LiPF_6$ in Fig. 3(c), which is thermally unstable in both the solid state and solvents, giving LiF and PF_5. The Lewis acid PF_5 initiates the polymerization of cyclic ethers and consequently degrades the electrolyte solution. Although there are thermal stability issue on $LiPF_6$ solutions, $LiPF_6$ in organic carbonates are used in lithium-ion batteries because of their outstanding stability to oxidation and conductivities among other electrolyte solutions.

In order to innovate an electrolyte solution for lithium-ion batteries, a series of trials has been done during the past 20 years. It should be noted here that all anions are thermodynamically unstable with lithium, so that the requirement for anions should be modified to "kinetically stable for a period of shell life". Possible alternatives examined are large molecular anions consisting of delocalized charges, which can be achieved by introducing electron-withdrawing substituents, such as –F, $–CF_3$, or $–C_2F_5$. The first example is CF_3SO_3Li in Fig. 3(d), supplied from 3M Company in the mid 1990s, which has been used in primary batteries, because it is thermally stable and therefore safe with its acceptable conductivity. Other examples are perfluoroalkyl or perfluoroaryl sulfonates. Koch et al. [13] report that a new dianion-type perfluoro organic lithium salt, $Li_2C_2F_4(SO_3)_2$ $[LiO(SO_2)C_2F_4(SO_2)OLi]$ in Fig. 4(a), dissolves 0.6 mol dm^{-3} in tetrahydrofuran (THF) and it shows the conductivity of 0.45 mS cm^{-1}, while similar dianion-type lithium salt $Li_2C_4F_8(SO_3)_2$ $[LiO(SO_2)C_4F_8(SO_2)OLi]$ dissolves only 0.001 mol dm^{-3} in THF and its conductivity is 0.0043 mS cm^{-1}. Dominey et al. [14-16] report that an imide salt of $(CF_3SO_2)_2NLi$ in Fig. 5(a) and a methide salt of $(CF_3SO_2)_3CLi$ show high conductivity in THF. Dominey [17] also report 0.9 mol dm^{-3} $LiCF(CF_3SO_2)_2$ in THF shows the conductivity of 8 mS cm^{-1} while $LiC(SO_2CH_3)_3$ does not dissolve in THF. Armand et al. [18, 19] report a polymer electrolyte with $(CF_3SO_2)_2NLi$. Webber [20] reports conductivity and viscosity data of CF_3SO_3Li, $(CF_3SO_2)_2NLi$ and cyclic imide $(-SO_2(CF_2)_4SO_2)NLi$ solutions in PC/DME and PC/DME/Diox solvent. Ue et al. [21] report the conductivity of many types of lithium salts including

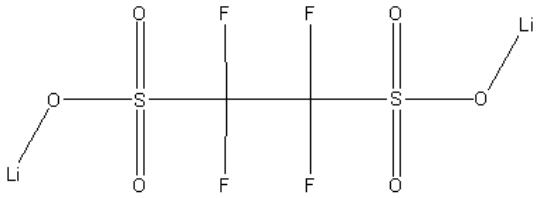

(a) $LiO_3SC_2F_4SO_3Li$
Tetrafluoro-1,2-ethanedisulfonic acid dilithium salt

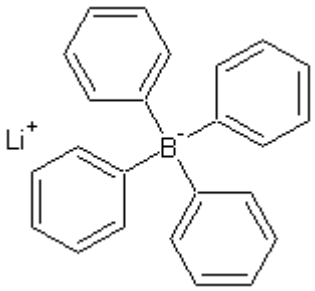

(b) $LiB(C_6H_5)_4$: $LiBPh_4$
Lithium tetraphenylborate

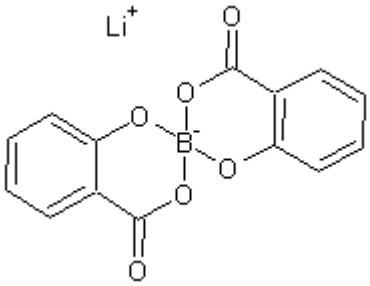

(c) $LiB(OC_6H_4COO)_2$
Lithium bis-salicylate borate

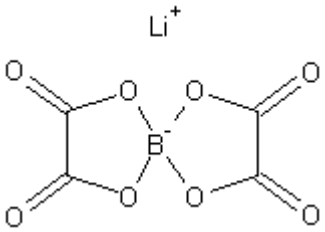

(d) $LiB(C_2O_4)_2$:LiBOB
Lithium bis(oxalate)borate

Figure 4 Lewis structures of some organic lithium salts for lithium batteries and lithium-ion batteries.

$(CF_3SO_2)_2NLi$ and its analogues. Ishikawa et al. [22, 23] report that the cycle performance of a MCMB graphite electrode is improved in $(CF_3SO_2)_2NLi$ solution of PC/DME and PC/DME/Diox solvents. Salomon et al. [24] report $(CF_3SO_2)_2NLi$ and $(CF_3SO_2)_3CLi$ in Fig. 5(b) electrolyte on their conductivity, electrochemical stability, and aluminum corrosion. Naoi et al. [25] report cycle performance of lithium metal electrode in $(C_2F_5SO_2)_2NLi$ solution in Fig. 5(c) and surface analysis. Armand et al. [26] report the characteristics of $(FSO_2)_2NLi$ (LiFSI) in Fig. 5(d).

Middleton et al. [27] report a synthetic method for a tricyano-substituted methide-type anion ($C(CN)_3^-$) as an attractive anion for lithium battery electrolyte and its lithium salt is later developed for lithium battery electrolyte by Nippon Shokubai Corporation group. The salt of $B(CN)_4^-$ is also reported by Scheers et al.

[28]. Iwaya et al. [29] report that an imide salt CTFSI, $(-O_2SCF_2CF_2SO_2-)NLi$ with five-membered ring in Fig. 5(e) showed high voltage stability.

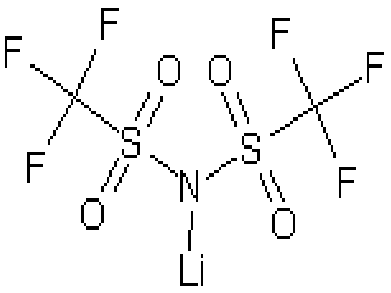

(a) $(CF_3SO_2)_2NLi$
Lithium
bis(trifluoromethanesulfonyl)imide

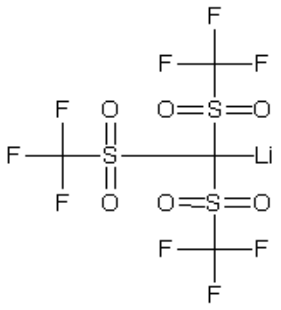

(b) $(CF_3SO_2)_3CLi$
Lithium
tris(trifluoromethylsulfonyl)methide

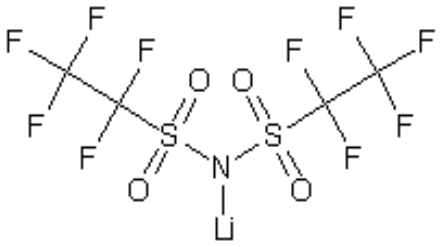

(c) $(C_2F_5SO_2)_2NLi$
Lithium
bis(pentafluoroethylsulfonyl)imide

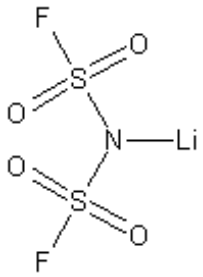

(d) $(FSO_2)_2NLi$
Lithium bis(fluorosulfonyl)imide

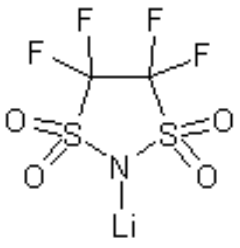

(e) CTFSI: $(-O_2SCF_2CF_2SO_2-)NLi$
4,4,5,5-tetrafluoro-1,3,2-dithiazolidine-
1,1,3,3-tetraoxide lithium salt

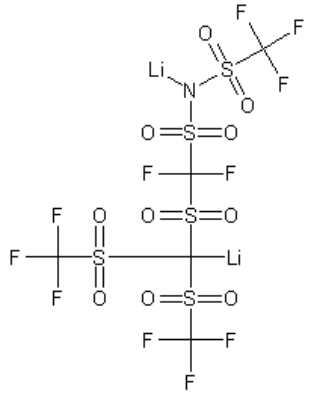

(f) $Li_2CF_2(SO_2NSO_2CF_3)(SO_2C(SO_2CF_3)_2$

Figure 5 Lewis structures of some imide or methide type of organic lithium salts for lithium batteries or lithium-ion batteries.

Sartori et al. [30] report the synthesis and properties of imide type di-lithium salts, such as $Li_2CF_2(SO_2NSO_2CF_3)_2$ [$CF_2(SO_2N(Li)SO_2CF_3)_2$], $Li_2(CF_2SO_2NSO_2CF_3)(SO_3)$ [$(CF_3SO_2N(Li)SO_2CF_2\text{-})(SO_3Li)$] and $Li_2CF_2(SO_2NSO_2CF_3)(SO_2C(SO_2CF_3)_2)$[$CF_2(SO_2N(Li)SO_2CF_3)(SO_2C(Li)(SO_2CF_3)_2$). Especially, $(CF_3SO_2N(Li)SO_2)CF_2(SO_2C(Li)(SO_2CF_3)_2$ in Fig. 5(f) shows the best cycle performance among them. Trzeciak et al. [31] report that the trivalent lithium salt Li_3BTI (2,2',2''-tris(trifluoromethyl)benzotris(imidazolate)) shows high lithium cation transference number 0.73 in ethylcarbonate(EC)/dimethyl carbonate(DMC) solution. Nie et al. [32] report the trivalent sodium salt, $C_4F_9SO_2N\text{-}(Na^+)SO_2N\text{-}(Na^+)SO_2N\text{-}(Na^+)SO_2C_4F_9$, shows higher conductivity than $(CF_3SO_2)_2NNa$ in PC/EC (1/2 by volume) and high oxidation potential of 6.0 V vs. Li. Polymer type imide salts $(CF_3SO_2N^-(M^+)[\text{-}SO_2\text{-}(CF_2)_4SO_2N^-(M^+)\text{-}]_n\ SO_2CF_3)$ (M = Li or Na) are reported by DesMarteau et al. [33, 34]. Poly-stylenesulfonyl imide type salt with $(\text{-}CH(C_6H_4\text{-}SO_2N\text{-}(Li^+)SO_2CF_3)CH_2\text{-})$ unit is reported by Armand et al. [35] as a single ion conducting polymer with high lithium cation transference number $t_{Li+} > 0.9$. Nie et al. [36] prepare different types of imide polymer $(SO_2NLiSO_2OCH_2(CF_2)_4CH_2O)_n$.

Other lithium salts, such as LiSCN, $LiTaF_6$, and Li_2GeF_6 are also reported by Johnson et al. [37] report the properties of closo-borane salts as electrolyte in organic solvents. Closo-borane salt, such as $Li_2B_{10}Cl_{10}$ and $Li_2B_{12}Cl_{12}$, shows the comparatively high ionic conductivity of about 7 mS cm^{-1} in dioxolane. Koch et al. [13] report that oxo-carbon lithium salt ($Li_2C_nO_n$), such as $Li_2C_4O_4$, shows the ionic conductivity of 8.3×10^{-4} mS cm^{-1} with the solubility 10^{-4} mol dm^{-3} in THF. Borate-type lithium salts have been reported as modified electrolyte salts and their stability is investigated as a new trial. Klemann et al. [38] report the electrochemical oxidization stability of some modified lithium salts $LiB(C_6H_5)_{4-n}(CH_3)_n$. Horowitz et al. [39] report the polyfluoro substitution effect on $LiB(C_6H_5)_4$, i.e., $LiB(C_6F_5)_4$ in Fig. 4(b). Bathel et al. [40-43] and Sasaki et al. [44,45] report benzene diolate-borate salts; $LiB(C_6H_{4-x}F_xO_2)_2$ (x = 0, 1, and 4), salicylate borate salts; $LiB(OC_6H_4COO)_2$ in Fig. 4(c), and their derivatives. Salicylate-borate salts show higher oxidation stability than benzene diolate-borate salts in an organic electrolyte solution. McBreen et al. [46] report a double salt

type of polyfluorinate lithium borate $(C_6F_5O)_3B$ and LiF. The complexation of a polyfluorinated boron compound with LiF improves the oxidation stability of boron compounds. Fujinami et al. [47-49] report a boroxine type salt $(B_3O_3)[O\text{-}CH(CH_3)_2]_3$, which shows high oxidation stability in their voltammetric study. Strauss et al. [50] report an olato cumylate-borate salt; $LiB(OC_5H_4C(CF_3)_2O)_2$. Angell et al. [51, 52] report other types of lithium salts, such as $LiB(C_2O_4)_2$ (LiBOB) in Fig. 4(d) and tetrakis(trifluoromethyl)-substituted ethylene diorate salt; $LiB(OC(CF_3)_2)_4$, and its derivatives. Zhu et al. [53] report LiDFOB ($LiF_2BC_2O_4$) as an electrolyte additive for positive electrodes. $LiPF_2(C_2O_4)_2$ and $Li_xPF_yO_z$ are also examined as electrolyte additives. Arai et al. [54] report some of $Li[B(OCORX)_4]$-type electrolytes show stability to oxidation and also to aluminum dissolution, superior to $LiPF_6$ electrolyte. Ue et al. [55] reported another modification of lithium borate salts. They have been modified $LiBF_4$ to $Li(C_2F_5)BF_3$ (LiFAB). LiFAB shows good performances comparable to $LiPF_6$ and it is much better than $LiBF_4$.

Ooike et al. [56] report that BF_3-complex-type liquid electrolyte shows high oxidation potential above 5.8 V vs. Li. National Institute of Advanced Industrial Science and Technology and Air Products Japan report that polyfluorinated icosahedral closo-borane cluster dilithium salt $Li_2B_{12}F_{12}$ shows redox reactions at overcharge potential [57].

Some aluminate-type organic lithium salts have been reported as modified electrolyte salts while the corresponding borate-type lithium salts are impossible to prepare due to their chemical instabilities. Strauss et al. [50] report the polyfluoroalkoxylated aluminate-type lithium salt $LiAl(ORf)_4$, which shows the electrochemical stability in voltage more than 5.2 V vs. Li/Li^+ for an oratecumylate aluminate salt, $LiAl(OC_6H_4C(CF_3)_2O)_2$, and its derivatives.

Koch et al. [58] report lithium phosphate $LiOP(OC(CF_3)_2C(CF_3)_2O)_2$. Zhou et al. [59] report that the cell with LiFOP ($LiPF_4(C_2O_4)$) electrolyte shows good cycle performance.

Nonflammable ionic liquid [60] has been examined as possible alternatives to current electrolyte solutions being volatile and flammable organic solvents, such as ethylene carbonate (EC) and dialkyl carbonate compound [61]. Anions in ionic

liquid are the same as those of organic lithium salts in many cases. Sakaebe et al. [62, 63] report the potential use as a lithium battery electrolyte solution of ionic liquid having quaternary ammonium ions with different lengths of linear alkyl groups and cyclic alkylene units and various counter anions, such as $(CF_3SO_2)_2N^-$, $(FSO_2)_2N^-$, and $CF_3BF_3^-$ anions. Weingarth et al. [64] report imidazorium-based ionic liquids containing $N(CN)_2^-$, $C(CN)_3^-$ and $B(CN)_4^-$. Ishikawa et al. [65, 66] report that a graphite-negative electrode does not work in ionic liquid, but it works when fluorosulfonyl imide anion $(FSO_2)_2N$ is in ionic liquid, due to the formation of an interphase layer of Li^+ and $(FSO_2)_2N^-$ on the surface of graphite-negative electrode. Armand et al. [67, 68] report the different types of anions, $(FSO_2)(RfSO_2)N^-$ for ionic liquid. Zhao et al. [69] report dendron-type lithium sulfonic salt as a functional additive agent to improve battery swelling during storage.

As have briefly been reviewed above, there are many trials on new electrolytes for lithium-ion batteries. However, they are still in a basic research stage, so that $LiPF_6$ solutions are used in lithium-ion batteries for more than 20 years. Everybody knows that $LiPF_6$ is thermally unstable and resulting PF_5 degrades the electrolyte solutions. In order to cope with the problems, materials chemistry classified in somewhere between organic and inorganic chemistry combined with electrochemistry would be necessary. For example, CF_3SO_3Li and $(CF_3SO_2)_2NLi$ are typical lithium organic salts, which have been used in primary lithium batteries. Anions have alkyl and SO_2 groups. For an alkyl group, the number of carbon can be modified in designing lithium organic salt, such as CH_3-, C_2H_5-, C_3H_7-, C_4H_9-, etc. It is also possible to replace hydrogen with halogen or others, i.e., RSO_2-, ROCO-, HO-, RO-, and phenyl-groups. A huge number of compounds is possible for lithium organic salts. When hydrogen in CH_3-SO_3Li is replaced with halogen, 20 compounds are possible, e.g., CH_2FSO_3Li, CHF_2SO_3Li and CF_3SO_3Li for fluorine. Similarly, when $CH_3CH_2CH_2CH_2$-SO_3Li is applied for F, Cl, or Br substitution, 20,000 compounds are easily designed in an organic chemical way, i.e., H_2F-CH_2-CH_2-CH_2-SO_3Li, CHF_2-CH_2-CH_2-CH_2-SO_3Li, CF_3-CH_2-CH_2-CH_2-SO_3Li, etc., ($20 \times 10 \times 10 \times 10 = 20000$). An introduction of organic chemistry to new electrolyte research is remarkable. However, synthesis and characterization of

each compound is almost impossible because time is limited. Therefore, a method to select possible electrolytes among compounds designed in a way described above is necessary.

A method selected is computational chemistry, which has been developed especially during the past 20 years. At present high-speed computers are available in a market and scientific packs to calculate electronic structures, thermodynamic properties, and spectra of compounds are easy to run on the computers. Although there is a “black box” in calculating the electronic structure of a compound, outputs can be inspected and compared to empirical basis. Therefore, computational chemistry is boldly introduced to the estimation of “thermal stability”, “oxidation potential in an electrochemical window”, and “dissociation” in advance of experimental approaches to synthesis and characterization of lithium fluoro-organic compounds.

In Chapter 1, preliminary results on conductivities of fluoro-organic lithium salts in a PC / DME mixed solvent are summarized. Electrolytes examined are polyfluoro-organic salts with a SO_2 or CO group in addition to imide or methide salts with or without SO_2 groups, and the size effect of anions upon solubility and conductivity is discussed and a strategy to develop new electrolytes for lithium-ion batteries is described.

In Chapter 2, oxidation potentials in electrochemical windows for fluoro-organic lithium salts in polar aprotic solvents are described in relation to HOMO (highest occupied molecular orbital) energies calculated by a computational method, and it will be shown that the HOMO energies of anions well correlate with the oxidation potentials empirically determined. A discussion as to which lithium salts show high oxidation potential among fluoro-organic lithium salts will be given.

In Chapter 3, the performance of prototype 14500 lithium-ion batteries consisting of a $LiCoO_2$-positive and graphite-negative electrode is described. The electrolyte selected is $((CF_3)_2CHOSO_2)_2NLi$, which is one of fluoro-organic lithium salts evaluated in chapters 1 and 2. The results will be compared with current $LiPF_6$ batteries, and it will be shown that the cycle performance of $((CF_3)_2CHOSO_2)_2NLi$ is better than that of $LiPF_6$. Possible explanation on cycle performance will be discussed in terms of solid electrolyte interface (SEI), derived

from the imide salt, formed on the graphite-negative electrode based on the XPS analysis.

In Chapter 4, the structural modification based on $LiPF_6$ is described. All possible structures are examined by a computational method, and candidate compounds are selected and then empirically examined. Although the conductivity of $LiPF_4(CF_3)_2$ electrolyte is slightly lower than that of $LiPF_6$, the oxidation potential of $LiPF_4(CF_3)_2$ in propylene carbonate (PC) is higher than that of $LiPF_6$. The performance of prototype 14500 lithium-ion batteries is also examined and shown that the cycle performance of the $LiPF_4(CF_3)_2$ batteries is superior to that of current $LiPF_6$ batteries.

References

[1] T. Ohzuku and A. Ueda, *Solid State Ionics,* **69**, 201(1994) and references cited therein.

[2] T. Ohzuku, K. Ariyoshi, Y. Makimura, N. Yabuuchi, and K. Sawai, *Electrochemistry (Tokyo, Japan),* **73**, 2 (2005) and references cited therein.

[3] T. Ohzuku and R. Brodd, *J. Power Sources,* **174**, 449 (2007) and references cited therein.

[4] W. A. van Schalkwijik and B. Scrosati, Editors, Advances in Lithium-ion Batteries, Kluwer Academic / Plenum Publishers, New York (2002).

[5] P. B. Balbuena and Y. Wang, Editors, Lithium-ion Batteries, Imperial College Press, London (2004).

[6] K. Ozawa, Editor, Lithium Ion Rechargeable Batteries, WILEY-VCH Verlag GmbH & Co. KGaA, Weinheim (2009).

[7] T. Ohzuku, Y. Iwakoshi, and K. Sawai, *J. Electrochem. Soc.*, **140**, 2490 (1993) and references cited therein.

[8] J. R. Dahn, A. K. Sleigh, Hang Shi, B. M, Way, W. J. Weydan, J. N. Rcimers, Q. Zhong, and U. von Sacken, pp. 1 - 47 in Lithium Batteries, New Materials, Developments and Perspectives, ed. by G. Pistoia, Elsevier Sciences B. V., Amsterdam, (1994).

[9] K. Sawai, Y. Iwakoshi, and T. Ohzuku, *Solid State Ionics*, **69**, 273 (1994) and references cited therein.

[10] M. S. Whittingham and A. J. Jacobson, Editors, Intercalation Chemistry, Academic Press, New York (1982).

[11] K. E. Aifantis, S. A. Hackney, and R. V. Kumar, Editors, High Energy Density Lithium Batteries, WILEY-VCH Verlag GmbH & Co. KGaA, Weinheim (2010).

[12] K. Matsuda, Z. Takehara, and Z. Ogumi, Editors, Denchi Binran (Handbook of Battery) 3rd Ed., p. 121-124, 277, and 279, Maruzen Pub. Co. Ltd., Tokyo (2001).

[13] V. R. Koch, L. A. Dominey, J. L. Goldman, and E. Lamgmure, *J. Power Sources*, **20**, 87 (1987).

[14] L. A. Dominey, J. L. Goldman, V. R. Koch, and C. Nanjundiah, p. 56 in Proceedings of the Symposium on Rechargeable Lithium Batteries, **Vol. 90-5**, The Electrochemical Society (1990).

[15] L. A. Dominey, V. R. Koch, and T. J. Blakley, *Electrochim. Acta*, **37**, 1551 (1992).

[16] V. R. Koch, L. A. Dominey, C. Nanjundiah, and M. J. Ondrechen, *J. Electrochem. Soc.*, **143,** 798 (1996).

[17] L. A. Dominey, p. 102 in the extended abstract of Seventh International Meeting on Lithium Batteries (IMLB-7), Boston, MA, May 15-20, 1994.

[18] S. Sylla, J. -Y. Sanchez, and M. Armand, *Electrochim. Acta*, **9**, 1699 (1992).

[19] F. Alloin, J. -Y. Sanchez, and M. Armand, *J. Electrochem. Soc.*, **141**, 1915 (1994).

[20] A. Webber, *J. Electrochem. Soc.*, **138**, 2586 (1991).

[21] M. Ue and S. Mori, *J. Electrochem. Soc.*, **142**, 2577 (1995).

[22] M. Ishikawa, H. Kamohara, M. Morita, and Y. Matsuda, 1D31 in the extended abstract of 63rd Spring meeting of The Electrochemical Society of Japan, Tokyo, Koganei, Sep.10-11, 1996.

[23] M. Ishikawa, H. Kamohara, M. Morita, and Y. Matsuda, *J. Power Sources*, **62**, 229 (1996).

[24] C. W. Walter, Jr., J. D. Cox, and M. Salomon, *J. Electrochem. Soc.*, **143**, L80 (1996).

[25] K. Naoi, M. Mori, Y. Naruoka, W. M. Lamanna, and R. Atanasoski, *J. Electrochem. Soc.*, **146**, 462 (1999).

[26] H. B. Han, S. S. Zhou, D. J. Zhang, S. W. Fong, L. F. Li, W. F. Feng, J. Nie, H. Li, X. J. Huang, M. Armand, and Z. B. Zhou, *J. Power Sources*, 196, 3623 (2011).

[27] W. J. Middleton, E. L. Little, and V. A. Engelhardt, *J. Am. Chem. Soc.*, **80**, 2795 (1958).

[28] J. Scheers, D. Lim, J. Kim, E. Paillard, and W.A.Henderson, P. Johansson, J. Ahn, and P. Jacobsson, *J. Power Sources* **251**, 451 (2014).

[29] M. Iwaya, K. Ikeda, N. Yoshida, and K. Hiratsuka, 1E07 in the extended abstract of The 49th Battery Symposium in Japan, Sakai, Nov.5-7, 2008.

[30] P. Murmanna, R. Schmitza, S. Nowaka, H. Goresa, N. Ignatiev, P. Sartori, S. Passerinia, M. Wintera, and R. W. Schmitza, *J. Electrochem. Soc.*, **160**, 535 (2013).

[31] T. Trzeciak, L. Niedzicki, G. Groszek, P Wieczorek, M. Marcinek, and W. Wieczorek, *J. Power Sources*, **252**, 229 (2014).

[32] J. Nie, X. Li, D. Liu, R. Luo, and L. Wang, *J. Fluorine Chem.*, **125**, 27 (2004).

[33] D. D. DesMarteau, *J. Fluorine Chem.*, **72**, 203 (1995).

[34] E. Geiculescu, J. Yang, S. Zhou, G. Shafer, Y. Xie, J. Albright, S. E. Creager, W. T. Pennington, and D. D. DesMarteau, *J. Electrochem. Soc.*,**151**, A1368 (2004).

[35] S. Feng, D. Shi, F. Liu, L. Zheng, J. Nie, W. Feng, X. Huang, M. Armand, and Z. Zhou, *Electrochim. Acta*, **93**, 254 (2013).

[36] J. Nie, T. Sonoda, and H. Kobayashi, *J. Fluorine Chemistry*, **87**, 45 (1998).

[37] J. W. Johnson and J. F. Brody, *J. Electrochem. Soc.*, **129**, 2213 (1982).

[38] L. P. Kleman, G. H. Newman, T. A. Whitney, E. L. Stogryn, and D. Farcasiu, p. 179 in Proceedings of the Symposium on Lithium Batteries, Vol. 81-4, The Electrochemical Society (1981).

[39] H. H. Horowitz, J. I. Haberman, L. P. Kleman, G. H. Newman, E. L. Stogryn and T. A. Whitney, p. 131 in Proceedings of the Symposium on Lithium Batteries, Vol. 81-4, The Electrochemical Society (1981).

[40] J. Bathel, M. Wuehr, R. Buestrich, and H. J. Gores, *J. Electrochem. Soc.*, **142**, 2527 (1995).

[41] J. Bathel, E. Carl, R. Buestrich, and H. Gores, *J. Electrochem. Soc.*, **143**, 3565 (1996).

[42] J. Bathel, R. Buestrich, E. Carl, and H. Gores, *J. Electrochem. Soc.*, **143**, 3572 (1996).

[43] J. Bathel, R. Buestrich, H. J. Gores, M. Schmidt, and M. Wuehr, *J. Electrochem. Soc.*, **144**, 3866 (1997).

[44] M. Handa, S. Fukuda, Y. Sasaki, and K. Usami, *J. Electrochem. Soc.*, **144**, L235 (1997).

[45] Y. Sasaki, S. Sekiya, M. Handa, and K. Usami, *J. Power Sources*, **79**, 91 (1999).

[46] H. S. Lee, X. Q. Yang, C. L. Xiang, J. McBreen, and L. S. Choi, *J. Electrochem. Soc.*, **145**, 2813 (1998).

[47] M. A. Mehta and T. Fujinami, *Solid State Ionics*, **113-115**, 187 (1998).

[48] M. A. Mehta, T. Fujinami, and T. Inoue, *J. Power Sources*, **81-82**, 724 (1999).

[49] M. A. Mehta , Y. Yang, T. Fujinami and T. Inoue, p. 43 in the extended Abstract of the 40th Battery Symposium in Japan, Kyoto, Nov.14-16, 1999.

[50] S. H. Strauss, A04 in extended abstract of 25th Fluorine Conference of Japan, Fukuoka, Nov.19-20, 2001.

[51] Wu Xu and C. A. Angell, Abstract of the 198th Meeting of the Electrochemical Society, Hiatt Regency, Phenix, 2000.

[52] Wu Xu and C. A. Angell, *Electrochem. Solid-State Lett,* **4**, E1 (2001).

[53] Y. Zhu, Y. Li, M. Bettge, and D. P. Abraham, *J. Electrochem. Soc.*, **159**, A2109 (2012).

[54] H. Yamaguchi, H. Takahashi, M. Kato, and J. Arai, *J. Electrochem. Soc.*, **150**, A312 (2003).

[55] Z. Zhou, M. Takeda, T. Fujii, and M. Ue, *J. Electrochem. Soc.*, **152**, A351 (2005).

[56] Y. Ooike, T. Fujinami, M. Matsui, 1B10 in the extended Abstract of the 48th Battery Symposium in Japan, Fukuoka, Nov.13-15, 2007.

[57] K. Hayamizu, M. Hattori, J. Arai, and A. Matsuo, 1E08 in the extended abstract of The 49th Battery Symposium in Japan, Sakai, Nov.5-7, 2008.

[58] V. R. Koch, p. 27 in extended abstract of The 37th Battery Symposium in Japan, Tokyo, Sep.25-27, 1996.

[59] L. Zhou, M. Xu, and B. L. Lucht, *J. Appl. Electrochem,* **43**, 497 (2013).

[60] A. Lewandowski and A. Swiderska-Mocek, *J. Power Sources*, **194**, 601 (2009).

[61] R. Hagiwara and K. Matsumoto, p. 273 in ”A guide 2010 to fluorine chemistry”, edited by the 155th committee of fluorine chemistry, Sankyo printing, Tokyo, 2010.

[62] H. Sakaebe, S. Tsudzuki, H. Matsumoto, and K. Tatsumi, 3F01 in the extended abstract of The 49th Battery Symposium in Japan, Sakai, Nov.5-7, 2008.

[63] H. Matsumoto, H. Sakaebe, K. Tatsumi, M. Kikuta, E. Ishiko, and M. Kono, *J. Power Sources*, **160**, 1308 (2006).

[64] D. Weingarth, I. Czekaj, Z. Fei, A. Foelske-Scmitz, P. J. Dyson, A. Wokaun, and R. Kotz, *J. Electrochem. Soc.*, **159**, H611 (2012).

[65] M. Ishikawa, T. Sugimoto, Y. Atsumi, M. Yamagata, M. Kikuta, E. Ishiko, and M. Kono, *ECS Transactions*, **16** (35), 67-73 (2009).

[66] M. Ishikawa, T. Sugimoto, M. Kikuta, E. Ishiko, and M. Kono, *J. Power Sources*, **162**, 658 (2006).

[67] H. B. Han, K. Liu, S. S. Zhou, S. W. Feng, J. Nie, H. Li, X. J. Huang, M. Armand, and Z. B. Zhou, #571 in the extended abstract of 218th ECS meeting, Las Vegas, Nevada, October 10-15, 2010.

[68] H. Han, Y. Zhou, K. Liu, J. Nie, X. Huang, M. Armand, and Z. Zhou, *Chem. Lett.*, **39**, 472 (2010).

[69] J. Zhao, Y. Ishigaki, M. Yamanaka, H. Fukuda, K. Aoi, 2G05 in the extended abstract of The 49th Battery Symposium in Japan, Sakai, Nov.5-7, 2008.

Chapter 1

Conductivity of Fluoro-Organic Lithium Salts in Mixed Solvent of Propylene Carbonate and 1,2-Dimethoxy Ethane

1. 1 Introduction

As was described in general introduction, an electrolyte is the most important requisite to lithium and lithium-ion batteries. An electrolyte consists of solute and solvent. A main solvent for lithium batteries and lithium-ion batteries is usually propylene carbonate (PC), ethylene carbonate (EC), alkyl carbonates, or ether such as γ-butyrolactone (GBL) because water or more generally a protic solvent having labile protons easily reacts with lithium evolving hydrogen gas [1-2]. Therefore, protic solvents, such as alcohols, organic and inorganic acids, amines, etc., are excluded in considering electrolytes for lithium batteries. Solvents of PC, EC, and GBL are called *aprotic* solvents in contrast to protic solvents [3].

Aprotic solvents are further classified in different ways: polar versus nonpolar; organic versus inorganic. Because nonpolar solvents cannot give a good electrolyte solution, polar *aprotic* solvents having high enough dielectric constant to ensure the dissociation of the dissolved salts to separate ions, PC, EC, and GBL are selected during the past 40 years as main solvents for lithium battery electrolytes. There seem to be few options in selecting a main solvent for lithium batteries at present.

A salt to dissolve in a main solvent is only limited to a lithium salt. Most of lithium salts listed in a handbook of chemistry, such as LiOH, Li_2CO_3, LiF, LiCl, LiBr, LiI, Li_2SO_4, $LiNO_3$, and CH_3COOLi, are insoluble in the main solvents, except LiBr and LiI, so that these lithium salts cannot be used in lithium batteries. Of these, a lithium salt of the small fluoride ions LiF does not dissolve in the solvents, while that of the large iodide ions LiI dissolves well [4]. Similarly, the salts consisting of small lithium ions and large anions, such as $LiClO_4$, $LiPF_6$, $LiAsF_6$,

$LiBF_4$, $LiSbF_6$, $LiAlCl_4$, and $LiB(C_6H_5)_4$, dissolve well in the aprotic solvents. $LiBF_4$ has been used in the primary Li / $(CF)_n$ batteries since the early 1970s [5]. $LiClO_4$ and $LiAsF_6$ have been used or used in the primary Li / MnO_2 and rechargeable Li / MoS_2 batteries, respectively, in 1980s [6-7]. $LiPF_6$ has largely been used in lithium-ion batteries since the mid-1990s [5, 8].

As briefly stated above, the main electrolytes for lithium-ion batteries do not change during the past 20 years, although the battery materials together with lithium-ion technology have highly been advanced especially during the past 10 years in progress of mobile information and electric-driven automobile technologies. An electrolyte innovation would be necessary in order to advance lithium-ion batteries more. There is almost no research space in simple inorganic salts consisting lithium ions and anionic species already known. New lithium salts or compounds are keys to help with innovation on an electrolyte system for lithium-ion batteries. Fluoro-organic lithium compounds may be candidate materials for lithium-ion battery electrolyte. However, an infinite number of fluoro-organic lithium compounds can be designed, prepared and examined. Therefore, a systematic research under the principles that guide an effective way to explore new electrolytes is inevitably necessary. In order to find the guiding principles, a series of experimental works has been undertaken.

In this chapter, factors affecting the solubility and conductivity are discussed from the results of preliminary examinations on the conductivity of fluoro-organic lithium salts in a mixed aprotic solvent and the guiding principles for a systematic research to innovate electrolytes for lithium-ion batteries are given.

1. 2 Experimental

1. 2. 1 Chemicals

Lithium salts available in a market are obtained from chemical companies: $LiPF_6$ is obtained from Stella Chemifa Co. Ltd., Japan; CF_3SO_3Li, $(CF_3SO_3)_2NLi$, $(C_2F_5SO_2)_2NLi$, and $C_4F_9SO_3Li$ are obtained from Sumitomo 3M Co. Ltd., Japan; $C_4F_9SO_3Li$ is also obtained from Mitsubishi Materials Electronic Chemicals Co. Ltd.,

Japan; $C_6F_{11}OC_6H_4SO_3Li$ is obtained from NEOS Co. Ltd., Japan; CF_3CO_2Li obtained from Morita Chemical Industries Co. Ltd., Japan; $(CF_3CH_2OSO_2)_3CLi$ and $(C_2F_5)_2P(=O)OLi$ are prepared at the Institute of Organic Chemistry Ukrainian Academy of Science Ukraine; $(HCF_2CF_2CH_2OSO_2)_2NLi$ and $(CF_3CF_2CH_2OSO_2)_2NLi$ prepared at the Institute of Advanced Material Study of Kyushu University, Japan; $((CF_3)_2CHOSO_2)_2NLi$ is supplied from the Institute of Advanced Material Study of Kyushu University and Central Glass Co. Ltd., Japan [9, 10]. The lithium salts obtained are used as received.

Lithium salts not available in a market are prepared from appropriate acids. $C_8F_{17}SO_3Li$ is prepared from $C_8F_{17}SO_2F$ obtained from Sumitomo 3M Co. Ltd., Japan. $C_8F_{17}SO_2F$ is mixed with water by stirring, and Li_2CO_3 solid is gradually added to the solution until solution pH reached 7. The solution is heated on a hot plate at about 100°C until water apparently disappeared. Similarly, $(CF_3CO)_2NLi$ is prepared from $(CF_3CO)_2NH$ obtained from Tokyo Chemical Industry Co. Ltd., Japan. Ten grams of $(CF_3CO)_2NH$ is dissolved in ca. 100 cm^3 of water, and Li_2CO_3 solid is gradually added until solution pH reached 7.

Lithium tetrakis(3,5-bis(trifluoromethyl)phenyl)borate, $LiB[3,5\text{-}(CF_3)_2C_6H_4]_4$ (LiTFPB) is prepared by an ion-exchange method. NaTFPB (over 99% purity) obtained from Dojindo Laboratories (Kumamoto Techno Research Park, Japan) is dissolved or suspended in a mixed solution of Li_2CO_3 aqueous solution and acetone. After shaking the mixture at 25°C for 5 min., an acetone phase containing both of sodium and lithium salts of TFPB is separated from an aqueous phase. Thus obtained acetone is again mixed with an aqueous solution of Li_2CO_3 and the solution is repeated for 10 times. After evaporating acetone from the final solution, LiTFPB is obtained. Residual sodium is less than 100 ppm in the LiTFPB salt.

All the prepared lithium salts are dried under vacuum at 130°C for 3 h and cooled to room temperature. The vacuum-dried samples are stored in glass-sample bottles over an argon-filled dry box.

1. 2. 2 Conductivity measurements

Battery-grade solvents of propylene carbonate (PC) and 1,2-dimethoxyethane

(DME) are obtained from Mitsubishi Chemical Co. Ltd., Japan and used as received. A one-to-two mixture of PC to DME by volume is used to prepare electrolytes. The concentration of lithium salts in the mixed solvents is fixed to 0.1 mol dm^{-3}. All the procedures to prepare electrolytes are performed in an argon-filled dry box.

Conductivity measurements of the electrolytes are carried out at 25°C with a conductance meter combined with a one-milliliter conductance cell (Type CM40S, Toa Electronics Co. Ltd., Japan). The conductance cell is calibrated by using a 0.1 mol dm^{-3} KCl aqueous solution and a cell constant is obtained. Other sets of experimental conditions are given in results and discussions section.

1. 3 Results and discussion

1. 3. 1 Conductivity measurements

Table 1. 1 shows the results of conductivity measurements on fluoro-organic lithium salts dissolved in the mixed solvent of PC/DME (1/2 by volume). The concentration is fixed to 0.1 mol dm^{-3}. $LiPF_6$ widely used in lithium-ion batteries is also shown in Table 1. 1 in order to compare conductivity measured. Totally 24 fluoro-organic samples were examined.

Lithium methanesulfonate CH_3SO_3Li is hardly dissolved in the mixture of PC and DME. When the hydrogen of an organic anion is substituted by fluorine, electron-withdrawing substituents, i.e., $\underline{CF_3}SO_3Li$ and $\underline{CF_3}COOLi$, they show solubility more than 0.6 mol dm^{-3} in the same mixed solvent. Koch et al. [11] report that $Li_2C_2F_4(SO_3)_2$ dissolved more than 0.6 mol dm^{-3} in tetrahydrofuran (THF). Dominy et al. [12-14] report that an imide salt $(CF_3SO_2)_2NLi$ and a methide salt $(CF_3SO_2)_3CLi$ dissolving 0.9 mol dm^{-3} in THF give high ionic conductivity. These results suggest that the electronic structures of the counter anions together with their bulkiness or size may play crucial roles in determining solubility and consequently conductivity of fluoro-organic lithium salts in an aprotic solvent.

CH_3SO_3Li and $C_6H_5SO_3Li$ are not fluoro-organic salts, which are examined in order to show the effect of fluorination upon solubility and consequently conductivity. CH_3SO_3Li is virtually insoluble and $C_6H_5SO_3Li$ is slightly soluble,

ca. 0.02 mol dm^{-3}, while corresponding fluoro-organic salts are soluble and give ionic conductivity as shown in Table 1. 1. Although $LiPF_6$ shows the highest conductivity of 4.4 mS cm^{-1} among a series of samples examined, fluoro-organic salts show conductivity ranging from 0.4 to 4.0 mS cm^{-1}, which may open a new window in terms of the electrolyte solutions for lithium-ion batteries.

Table 1. 1 Conductivity of fluoro-organic lithium salts dissolved in the mixed solvent of propylene carbonate and dimethoxy ethane (1/2 by volume) at 25°C. The concentration of lithium salts is 0.1 mol dm^{-3}.

Lithium Salt	Conductivity (mS cm^{-1})	Molecular Weight
$(C_2F_5)_2P(=O)OLi$	0.6	308
CF_3CO_2Li	0.4	120
$(CF_3CO)_2NLi$	0.8	215
CF_3SO_3Li	2.3	156
CH_3SO_3Li	Virtually insoluble	102
$C_4F_9SO_3Li$	2.3	306
$C_6F_5SO_3Li$	1.1	254
$C_6H_5SO_3Li$	0.1-0.2(ca.0.02 mol dm^{-3})	164
$C_8F_{17}SO_3Li$	1.9	506
$(CF_3SO_2)_2NLi$	4.0	287
$(C_2F_5SO_2)_2NLi$	3.8	387
$(C_4F_9SO_2)(CF_3SO_2)NLi$	3.5	437
$(FSO_2C_6F_4)(CF_3SO_2)NLi$	3.0	347
$(C_8F_{17}SO_2)(CF_3SO_2)NLi$	3.2	637
$(CF_3CH_2OSO_2)_2NLi$	3.0	347
$(CF_3CF_2CH_2OSO_2)_2NLi$	3.0	447
$(HCF_2CF_2CH_2OSO_2)_2NLi$	2.9	411
$((CF_3)_2CHOSO_2)_2NLi$	3.1	483
$(CF_3SO_2)_3CLi$	3.6	418
$(CF_3CH_2OSO_2)_3CLi$	2.9	508
LiTFPB*	2.7	870
$LiPF_6$	4.4	152

* LiTFPB : $LiB[3,5\text{-}(CF_3)_2C_6H_4]_4$ (Lithium tetrakis(3,5-bis(trifluoromethyl) phenyl)borate)

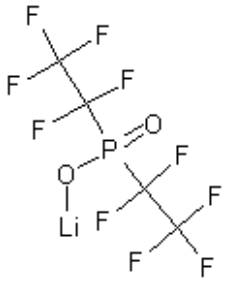

(a) $(C_2F_5)_2P(=O)OLi$
Lithium
bis(pentafluoroethyl)phosphate

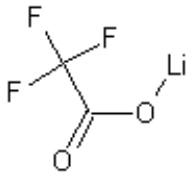

(b) CF_3CO_2Li
Lithium trifluoroacetate

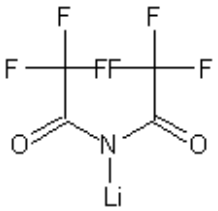

(c) $(CF_3CO)_2NLi$
Lithium bis(trifluoroacetyl)imide
or lithium bistrifluoroacetamide

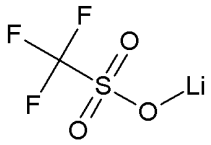

(d) CF_3SO_3Li
Lithium trifluoromethanesulfonate

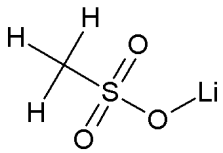

(e) CH_3SO_3Li
Lithium methanesulfonate

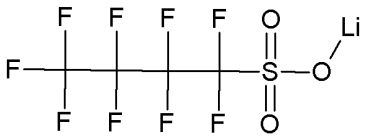

(f) $C_4F_9SO_3Li$
Lithium nonafluorobutanesulfonate

Figure 1. 1 Lewis structures of lithium salts examined in Table 1. 1.

The ionic conductivity of electrolyte depends on the concentration of ions and their mobility [15-17]. Free or associated ions are the electrical current carriers in the electrolyte solutions, which is simply the product of the concentration of lithium salts and the degree of disassociation, i.e.,

ionic conductivity $\propto \sum$(number of charge on an ion $\times$ the degree of disassociation $\times$ the concentration of a lithium salt $\times$ mobility of an ion) (1).

According to equation (1), when the solubility of a lithium salt together with the degree of dissociation is high, an ionic conductivity of the electrolyte solution is high. When the size of an ion is small, the mobility is high because the mobility depends on ionic radius and viscosity of electrolyte [15-17]. Small ionic species is easier to move in viscous liquid than large ionic species. However, a small ion tends to hardly dissolve in aprotic solvents.

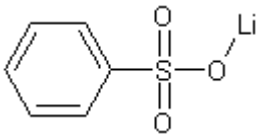

(a) $C_6H_5SO_3Li$
Lithium benzenesulfonate

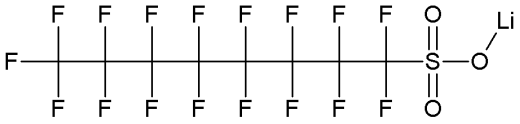

(b) $C_8F_{17}SO_3Li$
Lithium perfluorooctanesulfonate

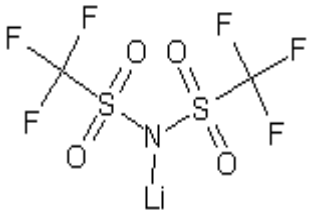

(c) $(CF_3SO_2)_2NLi$
Lithium
bis(trifluoromethanesulfonyl)imide

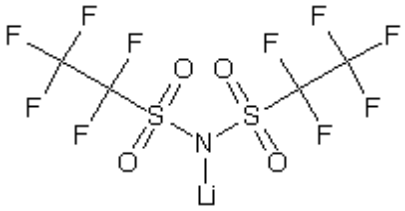

(d) $(C_2F_5SO_2)_2NLi$
Lithium
bis(pentafluoroethylsulfonyl)imide

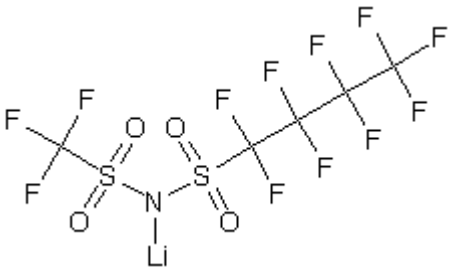

(e) $(C_4F_9SO_2)(CF_3SO_2)NLi$
Lithium (nonafluorobutylsulfonyl)
(trifluoromethylsulfonyl)imide

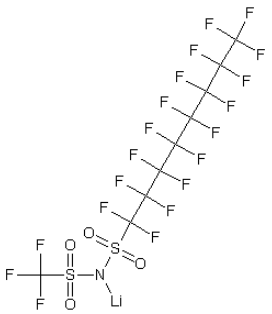

(f) $(C_8F_{17}SO_2)$ $(CF_3SO_2)NLi$
Lithium
(perfluorooctylsulfonyl)(trifluoromethylsulfonyl)
imide

Figure 1. 2 Lewis structures of lithium salts examined in Table 1. 1.

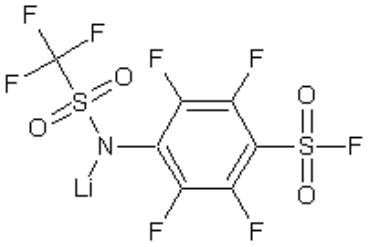

(a) （$FSO_2C_6F_4$）(CF_3SO_2)NLi
Lithium (4-fluorosulfonyl-2,3,5,6-tetrafluorophenyl) (trifluoromethylsulfonyl)imide

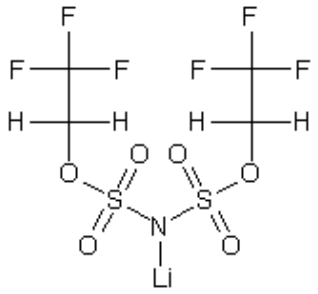

(b) （$CF_3CH_2OSO_2)_2NLi$
Lithium bis(2,2,2-trifluoroetho
sulfonyl)imide

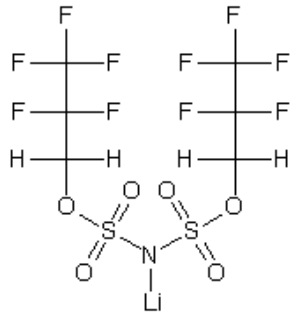

(c) （$CF_3CF_2CH_2OSO_2)_2NLi$
Lithium bis(2,2,3,3,3-pentafluoro propoxysulfonyl)imide

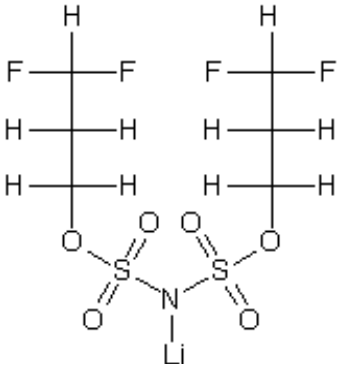

(d) （$HCF_2CF_2CH_2OSO_2)_2NLi$
Lithium bis(2,2,3,3-tetrafluorop
sulfonyl)imide

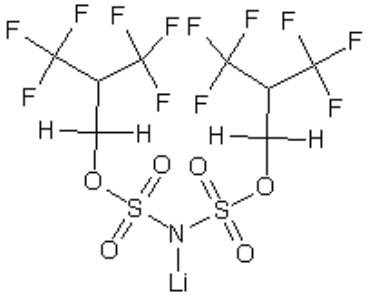

(e) $((CF_3)_2CHOSO_2)_2NLi$
Lithium bis(2,2,2,2',2',2'-hexafluoroisopopoxy-sulfonyl)imide

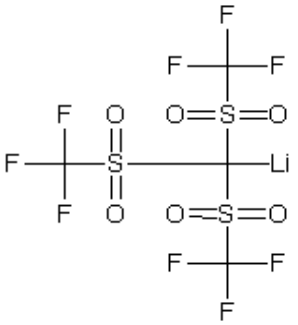

(f) $(CF_3SO_2)_3CLi$
Lithium tris(trifluoromethylsulfonyl)methide

Figure 1. 3 Lewis structures of lithium salts examined in Table 1. 1.

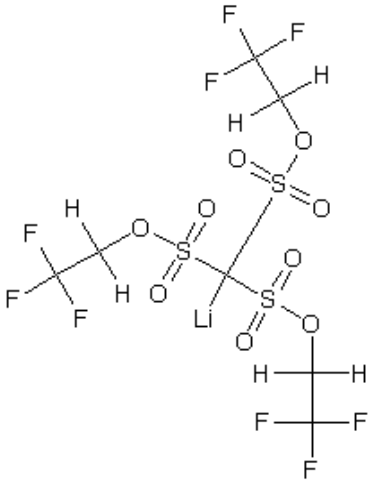

(a) $(CF_3CH_2OSO_2)_3CLi$
Lithium tris(2,2,2-trifluoroethoxysulfonyl)methide

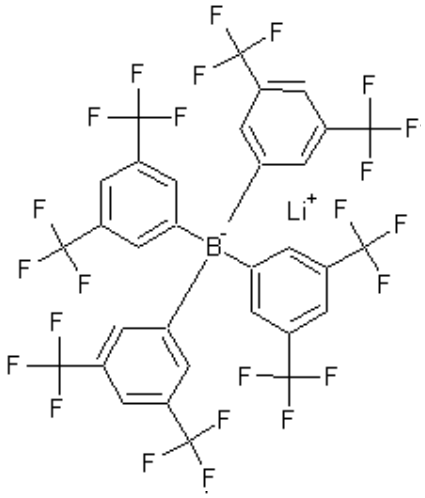

(b) LiTFPB: $(LiB[3,5\text{-}(CF_3)_2C_6H_4]_4)$
Lithium tetrakis(3,5-bis(trifluoromethyl)phenyl)borate

Figure 1. 4 Lewis structures of lithium salts examined in Table 1. 1.

Because lithium salts are main concerns, the number of charge on a cation is +1, i.e., the monovalent lithium ion of Li^+. The above arguments are only applied to counter anions and resulting lithium salts. Again, there seem to be three factors affecting ionic conductivity under consideration, i.e., the concentration of a lithium salt, the degree of dissociation, and the mobility of a lithium and counter ion.

Ue and Mori [18] report the ionic conductivity of some lithium salts in organic solvents. In general, the ionic conductivity decreases as the size of a counter ion increases, i.e.,

$$LiPF_6 \text{ and } LiAsF_6 > LiClO_4, (CF_3SO_2)_2NLi > LiBF_4 > CF_3SO_3Li > C_4F_9SO_3Li \quad (2).$$

Some of lithium fluoro-organic salts show the size effect of counter anions, but some of them are not. Anomalous behaviors of fluoro-organic lithium salts with respect to the size effect in Table 1. 1 are specifically discussed in details.

1. 3. 2 Electronic effects of fluorine substitution upon ionic conductivity

The effect of the number of (CF_3SO_2) and (CF_3CO) in lithium salt upon conductivity. --- As stated above, small ion is easy to move in an electrolyte solution, which is a beneficial effect on ionic mobility. Ionic conductivity also depends on the degree of dissociation of a lithium salt. When the degree of dissociation of a lithium salt consisting of a large anion is high enough to compensate low mobility due to a large anion, conductivity may be high.

The conductivities of $(CF_3SO_2)_2NLi$ and CF_3SO_3Li electrolyte are listed in Table 1. 1 to be 4 and 2.3 mS cm^{-1}, respectively, while $(CF_3CO)_2NLi$ and CF_3CO_2Li show 0.8 and 0.4 mS cm^{-1}, respectively, i.e.,

$(CF_3SO_2)_2$NLi (4 mS cm^{-1}) > **(CF_3SO_2)**OLi (2.3 mS cm^{-1}) (3)

and **$(CF_3CO)_2$**NLi (0.8 mS cm^{-1}) > **(CF_3CO)**OLi (0.4 mS cm^{-1}) (4).

Lithium salts, $(CF_3SO_2)_2NLi$ with two electron-withdrawing CF_3SO_2- groups shows twice as high as ion conductivity of CF_3SO_3Li [=$(CF_3SO_2)OLi$], which contains only one electron-withdrawing CF_3SO_2- functional group. Lithium salts, $(CF_3CO)_2NLi$ with two electron-withdrawing CF_3CO-groups also shows twice as high as ion conductivity of $(CF_3CO)OLi$ [=CF_3CO_2Li], which contains only one electron-withdrawing CF_3CO-functional group. When an ionic radius becomes larger, mobility becomes smaller. However, the electron density on the surface of an anion becomes smaller and consequently the electrostatic interaction between an ion pair becomes weaker. When the number of electron-withdrawing functional groups, CF_3SO_2 or CF_3CO, increases from one to two, the degree of dissociation is expected to increase due to this effect. Figure 1. 5 illustrates how electrons are delocalized in $(CF_3CO)_2N^-$, $CF_3CO_2^-$, $(CF_3SO_2)_2N^-$, and $CF_3SO_3^-$ anions. An anion of $(CF_3SO_2)_2N^-$ with two CF_3SO_2-groups has five resonance structures while an anion of $CF_3SO_3^-$ with one CF_3SO_2-group has only three resonance structures. The resonance structure of $(CF_3SO_2)_2N^-$ anion is considered to be an origin of the stability of the anion and also it affects the degree of dissociation.

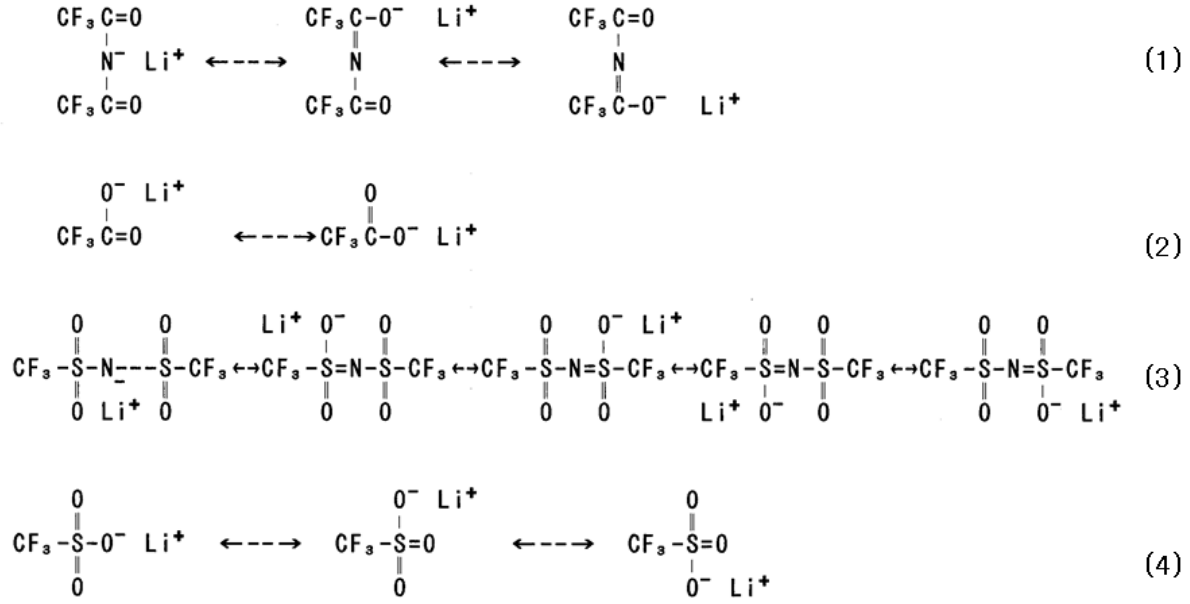

Figure 1. 5 The electron delocalization on $(CF_3CO)_2N^-$, $CF_3CO_2^-$, $(CF_3SO_2)_2N^-$, and $CF_3SO_3^-$ anions.

The effect of SO_2 and CO group in lithium salt upon conductivity.--- The structural effect of SO_2- and CO-group on conductivity is discussed. As seen in Table 1. 1, the conductivities of CF_3SO_3Li, CF_3CO_2Li, and $(C_2F_5)_2POOLi$ in PC/DME is 2.3, 0.4, and 0.6 mS cm^{-1}, respectively. A compound of CF_3SO_3Li with SO_2-group shows higher conductivity than CF_3CO_2Li with CO-group and $(C_2F_5)_2POOLi$ with PO-group; i.e.,

$(CF_3\mathbf{SO_2})OLi$ (2.3 mS cm^{-1}) > $(C_2F_5)_2\mathbf{PO}OLi$ (0.6 mS cm^{-1}) > $(CF_3\mathbf{CO})OLi$ (0.4 mS cm^{-1}) (5).

A lithium salt of $(CF_3SO_2)_3CLi$ with three CF_3SO_2-groups shows 3.6 mS cm^{-1}, which is higher conductivity than that of $(CF_3SO_2)OLi$ with one CF_3SO_2-group, but is smaller than $(CF_3SO_2)_2NLi$ with two CF_3SO_2-groups, i.e,

$\mathbf{(CF_3SO_2)_2}NLi$ (4.0 mS cm^{-1}) > $\mathbf{(CF_3SO_2)_3}CLi$ (3.6 mS cm^{-1}) > $\mathbf{(CF_3SO_2)}OLi$ (2.3 mS cm^{-1}) (6).

The observations indicate that the conductivity of a lithium salt depends not only on the degree of dissociation but also on ionic mobility. In other words, the electronic structures of fluoro-organic anions play a crucial role on the dissociation of lithium salts, exemplified by the results that the conductivity of **$(CF_3SO_2)_3$**CLi and **$(CF_3SO_2)_2$**NLi are high in spite of bulky anions.

The effect of carbon chain length of fluoroalkyl group in lithium salt upon conductivity.--- The effect of length of carbon chain in fluoro-alkyl groups is discussed in terms of ionic mobility and the dissociation of a lithium salt. The conductivity observed is a following order;

CF_3 SO_3Li (2.3 mS cm^{-1}), **C_4F_9**SO_3Li (2.3 mS cm^{-1}) > **C_8F_{17}**SO_3Li (1.9 mS cm^{-1}) (7)

and

(**CF_3**$SO_2)_2$NLi (4.0 mS cm^{-1}) > (CF_3SO_2)(**C_4F_9**SO_2)NLi (3.5 mS cm^{-1}) > (CF_3SO_2)(**C_8F_{17}**SO_2)NLi (3.2 mS cm^{-1}) (8).

The results can be explained by the difference in the molecular weight or the size of an anion affecting the mobility of an anion. It should be noted that imide type lithium salts, such as (CF_3SO_2)($C_4F_9SO_2$)NLi and (CF_3SO_2)($C_8F_{17}SO_2$)NLi, show higher conductivity than CF_3SO_3Li in spite of bulky anions they have. When the conductivities of imide salts are compared, $(CF_3CH_2OSO_2)_2$NLi (3.0 mS cm^{-1}), $(CF_3CF_2CH_2OSO_2)_2$NLi (3.0 mS cm^{-1}), $(HCF_2CF_2CH_2OSO_2)_2$NLi (2.9 mS cm^{-1}) and $((CF_3)_2CHOSO_2)_2$NLi (3.1 mS cm^{-1}) show higher conductivities than CF_3SO_3Li (2.3 mS cm^{-1}). This can also be explained in terms of ion dissociation as has already discussed for $(CF_3SO_2)_2$NLi.

Anomalous conductivity of lithium tetrakis(3,5-bis(trifluoromethyl)phenyl)borate (LiTFPB).--- Among lithium salts examined and listed in Table 1. 1, LiTFPB shows anomalous behaviors. As clearly seen in Table 1. 1, LiTFPB has the largest molecular weight among the samples examined, indicating the most bulky anion.

Table 1. 2 Conductivity of 0.02 mol dm^{-3} fluoro-organic lithium salts in CH_2Cl_2 at 25°C.

Lithium Salt	Conductivity ($mS\ cm^{-1}$)
LiTFPB	0.82
$(CF_3SO_2)_2NLi$ *	0.0007
$LiPF_6$ *	0.0001

*)Virtually insoluble in CH_2Cl_2.

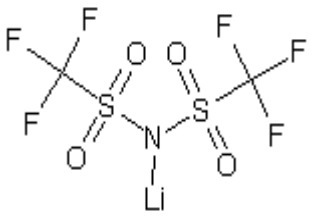

(a) $(CF_3SO_2)_2NLi$
Lithium bis(trifluoromethanesulfonyl)imide

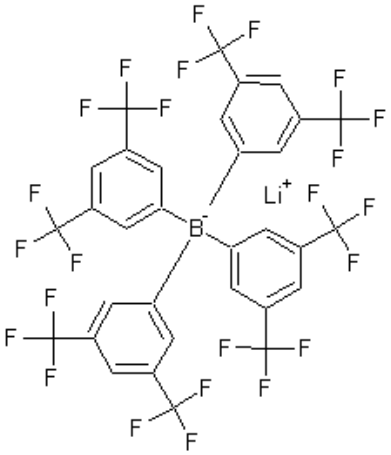

(b) LiTFPB: $(LiB[3,5\text{-}(CF_3)_2C_6H_4]_4)$
Lithium tetrakis(3,5-bis(trifluoromethyl)phenyl)borate

Figure 1. 6 Lewis structures of $(CF_3SO_2)_2NLi$ and LiTFPB examined in Table 1. 2.

The mobility of such a bulky anion is expected to be the smallest value among the samples. However, LiTFPB shows a conductivity of 2.7 mS cm^{-1}, which is higher than CF_3SO_3Li (2.3 mS cm^{-1}). A lithium salt of CF_3SO_3Li is currently used in some of lithium batteries. Although a reason why the conductivity of LiTFPB shows such a high value is not known, it is evident that the dissociation of lithium salts plays a crucial role on conductivity. The longer distance between an anion and cation in LiTFPB would presumably give higher dissociation [6] compared with CF_3SO_3Li due to an electrostatic effect forming an ion pair.

Lithium salts are normally insoluble in a nonpolar solvent. However, LiTFPB shows a unique character such that it dissolves in a nonpolar solvent, e.g., CH_2Cl_2. Table 1. 2 shows the conductivities of LiTFPB, $(CF_3SO_2)_2NLi$, and $LiPF_6$ in CH_2Cl_2. Of these, $(CF_3SO_2)_2NLi$ and $LiPF_6$ are virtually insoluble in CH_2Cl_2. LiTFPB in CH_2Cl_2（0.02 mol dm^{-3}）shows a conductivity of 0.82 mS cm^{-1}, which is almost the same conductivity as 0.1 mole dm^{-3} $(CF_3CO)_2NLi$ in PC/DME (1/2 by volume) as seen in Table.1. 1. A solvent of CH_2Cl_2 is one of the non-flammable solvents, so that a clear understanding of the anomalous conductivity of LiTFPB in CH_2Cl_2 may give an insight into a safe electrolyte solution for advanced lithium-ion batteries. The high conductivity of LiTFPB in CH_2Cl_2 may be derived from the "lipophilicity" of a bulky TFPB anion in CH_2Cl_2 solvent [7]. "Lipophilicity" means the capability to dissolve in nonpolar solvents, such as benzene, CCl_4, CH_2Cl_2, or more generally, fats, oils, etc. In general, lipophilic compounds tend to dissolve in other lipophilic compounds. "Lipophilicity" is a new factor affecting solubility and conductivity, which have learnt from LiTFPB in CH_2Cl_2.

1. 4 Summary

In this chapter, the results of preliminary examinations on the conductivity of fluoro-organic lithium salts in PC/DME (1/2 by volume) have been described. Totally 27 samples have been prepared and examined, which include CH_3SO_3Li, $C_6H_5SO_3Li$, and $LiPF_6$ used as reference samples, and factors affecting the conductivity of an electrolyte solution containing a fluoro-organic lithium salt are discussed in terms of the concentration of free ions, the dissociation of a lithium salt, and the mobility of each ion.

The size effect of anions upon conductivity is always observed. Bulky anions are difficult to move in a viscous liquid, which affects the mobility of an anion, so that there seem to be no merit to use fluoro-organic anions, although many fluoro-organic anions can be prepared and examined. However, the electronic effect of fluoro-organic groups upon conductivity is clearly observed and it is positive, which compensates the negative effect derived from bulkiness of an anion. This clearly indicates that the electronic structures of fluoro-organic lithium salts are

important in developing new fluoro-organic lithium salts for advanced lithium-ion batteries, as will be described in Chapters 2 and 3.

References

[1] C. Glaize and S. Genies, Lithium Batteries and Other Electrochemical Storage Systems, Wiley-ISTE (2013).

[2] K. Matsuda, Z. Takehara, and Z. Ogumi, Editors, Denchi Binran (Handbook of Battery) 3rd Ed., p. 121-124 and p. 279, Maruzen Pub. Co. Ltd., Tokyo, Japan (2001).

[3] G. A. Nazri and G. Pistioa, Ediors, Lithium Batteries Science and Technology, Springer Science-Business Media, LLC (2009).

[4] Kagaku Binran (Chemistry hand book) II 2nd Ed., p. 809, Maruzen Pub. Co. Ltd., Tokyo, Japan (1975).

[5] pp. 122-123 and p. 278 in ref. 2.

[6] J. Yamaki, *Netsu Sokutei*, **30**, 3 (2003).

[7] T. R. Jow, K. Xu, O. Borodin, and M. Ue, Electrolytes for Lithium and Lithium-Ion Batteries (Modern Aspects of Electrochemistry), Springer Science+Business Media LLC (2014).

[8] D. Aurbach, Y. Talyosefa, B. Markovskya, E. Markevicha, E. Zinigrada, L. Asrafa, J. S. Gnanaraja, H. Kim, *Electrochimica Acta*, **50**, 247 (2004).

[9] J. Nie, T. Sonoda, and H. Kobayashi, *J. Fluorine Chemistry*, **87**, 45 (1998).

[10] M. Becke-Goehring, E. Fluck, A. Failli, and T. Moeller, *Inorg. Chem. Synthesis*, **8**, 105 (1966).

[11] V. R. Koch, L. A. Dominey, J. L. Goldman, and M. E. Lamgmure, *J. Power Sources*, **20**, 287 (1987).

[12] L. A. Dominey, J. L. Goldman, V. R. Koch, and C. Nanjundiah, p. 56 in Proceedings of the Symposium on Rechargeable Lithium Batteries, Vol. **90-5,** The Electrochemical Society (1990).

[13] L. A. Dominey, V. R. Koch, and T. J. Blakley, *Electrochim. Acta*, **37**, 1551 (1992)

[14] V. R. Koch, L. A. Dominey, C. Nanjundiah, and M. J. Ondrechen, *J. Electrochem. Soc.*, **143,** 798 (1996).

[15] K. J. Vetter, Electrochemical Kinetics; Theoretical and Experimental Aspects, Academic Press, New York (1967).

[16] J. O. Bockris and A. K. N. Reddy, Modern Electrochemistry, Plenum Press, New York (1973).

[17] R. A. Robinson and R. H. Stokes, Electrolyte Solutions, Dover Publications, Inc., New York (2002).

[18] M. Ue and S. Mori, *J. Electrochem. Soc*., **142**, 2577 (1995).

[19] K. Fujiki, M. Kashiwagi, H. Miyamoto, A. Sonoda, J. Ichikawa, H. Kobayashi, and T. Sonoda, *J. Fluorine Chem.*, **57**, 307 (1992).

Chapter 2

Electrochemical Stability of Fluoro-Organic Lithium Salts for Lithium Batteries

2. 1 Introduction

In Chapter 1, the ionic conductivity of fluoro-organic lithium salts dissolved in polar aprotic solvents was described and an electronic effect of fluorine substitution upon conductivity was discussed. A series of trials described herein is intended to perform high-voltage high-capacity lithium-ion batteries, i.e., high-energy density batteries. A lithium-ion battery consists of a negative and positive electrode separated by a diaphragm with an electrolyte solution. High ionic conductivity of an electrolyte solution reduces an ohmic drop, meaning that lithium ions and anions effectively carry charging or discharging currents between the positive and negative electrodes. Therefore, high ionic conductivity is one of the necessary conditions of electrolytes for lithium-ion batteries, as has already been discussed in Chapter 1.

In lithium-ion batteries, an electrolyte solution is always exposed to the positive and negative electrodes. A positive electrode is highly oxidative and a negative electrode is highly reductive. Consequently, an electrolyte solution should be resistant to the oxidation and reduction due to the positive and negative electrodes, respectively. In electrochemistry, the width of the potential range in which the electrolyte solution remains inert is called “potential window” or “electrochemical window”. The potential window is restricted by the potentials of cathodic and anodic electrochemical processes, which depends on the electrode material, the electrolyte solution, and the level of impurities. The potential window of an electrolyte solution cannot be predicted, so that a voltammetric technique is usually applied to the determination of the potential window. However, there is no exact definition for the current density defining the potential limits of the electrochemical window. When an electrolyte solution remains inert

at higher anodic potentials, it is resistant to oxidation. The electrolyte solution is called an oxidation-resistant electrolyte. Some of common lithium salts dissolved in propylene carbonate (PC) have already been measured by a voltammetric method [1] and shown that $LiPF_6$ is the most resistant to oxidation among lithium salts they examined, i.e.,

$$LiPF_6 > LiBF_4 > CF_3SO_3Li > LiClO_4 \qquad (1).$$

In other words, removing an electron from a ClO_4^- anion is easier than that from a PF_6^- anion. It seems to relate to the electronic structures of anions.

In recent years, computational methods can be applied to the calculation of the electronic structures of molecules [2-5]. An elementary step of the oxidation of an anion of certain chemical species is a process to pick up an electron from an anion and that of reduction is to put an electron. Therefore, if the electronic structures of lithium salts were known, the electrochemical windows of electrolyte solution of lithium salts in polar aprotic solvents can be estimated through the verified one-to-one correspondence of theoretical and experimental parameters. The theoretical parameters selected are the energy levels of the highest occupied molecular orbital, known as the HOMO, and the lowest unoccupied molecular orbital, known as the LUMO. The empirical parameters selected are the onset potentials at which anodic or cathodic currents exceed a limit in an appropriate experimental condition.

In this chapter, fluoro-organic lithium salts are described in terms of stability of electrolytes against oxidation from both theoretical and empirical bases. Discussions as to whether or not the HOMO can be used as effective parameters in considering the electrochemical window of an electrolyte solution consisting of organic solvents, additives, and lithium salts, are given in order to guide a plan to design appropriate electrolytes for lithium and lithium-ion batteries [6-11].

2. 2 Computational methods

In order to calculate the HOMO energies of given lithium salts, mainly fluoro-organic lithium salts, a molecular orbital package of MOPAC Ver.6 [12-13], currently MOPAC 2009, is used on the personal computers or workstations of EWS

SPARC-station 1+ (Sun Microsystems; currently Oracle Co., Ltd., USA). A software of MOPAC (Molecular Orbital Package) is the semi-empirical MO calculation methods including the MNDO (Modified Neglect of Differential Overlap) method and PM3 (Parameterized Model number 3). PM3 has been adopted a function of core repulsion [12, 15]. MNDO is devised by Dewar [14], which is less restrictive than the MINDO (the Modified Intermediate Neglect of Differential Overlap) family, such as MINDO-1, MINDO-2, and MINDO-3. The initial structures of anions under considerations are modified by a Dleiding II force field method using POLYGRAF which is a structure-building software for a MOPAC calculation.

For imide and methide anions, the HOMO energy levels are calculated by the MNDO and PM3 methods using MOPAC (Ver. 6) and also by the DFT (B3LYP/6-31G*//HF/3-21G*) method on SPARTAN V 5.0. "B3LYP/6-31G*//HF/3-21G*" is that the initial coordinates of the anion structures are optimized by a HF(Hartree-Fock) level *ab-initio* MO method of HF/3-21G* and the HOMO energy levels of the optimized structures are calculated by DFT(density functional theory) of B3LYP/6-31G* level. Spartan V 5.0 of Wavefunction, Inc. is the software for a molecular orbital calculation. Gaussian 09 is also used for a DFT calculation [16, 17].

2. 3 Experimental

2. 3. 1 Materials

Lithium tetraphenylborate ($LiBPh_4$) is obtained from Tomiyama Pure Chemical Ind., Co. Ltd., Japan, as $LiBPh_4$・3DME, i.e., three 1,2-dimethoxyethanes (DME) solvated or mixed with $LiBPh_4$. In preparing $LiBPh_4$ in propylene carbonate (PC), DME was removed from $LiBPh_4$・3DME under vacuum at 110℃, and $LiBPh_4$ is dissolved in PC. Fluoro-organic lithium salts used are the same as those described in Section 1. 2. 1. PC (over 99.5% purity, H_2O below 50 ppm) or 1,3-dioxolane (Diox, 99.9% purity, H_2O below 30 ppm) is used as the solvent. The concentration of 0.6 or 0.1 mol dm^{-3} of a lithium salt dissolved in PC or Diox is

used for electrochemical measurements.

2. 3. 2 Electrochemical measurements

In order to examine the electrochemical windows of several electrolytes, the voltammetry of a platinum electrode is performed at room temperature of 18-28°C. The platinum electrode used as a working electrode is a wire of 0.3 mm in diameter and 50 mm in length. The active electrode area is 0.2 cm^2. The counter electrode 21 mm wide and 30 mm long is lithium metal foil 0.2 mm thick. The platinum wire is wrapped with a polyethylene separator and partially heat-sealed to fix a separator on the Pt wire. The platinum electrode with a separator is hold by the folding lithium foil. The cell potential is scanned at a rate of 50 mV s^{-1} by a potentiostat (HA-501, HOKUTO DENKO Co. Ltd., Japan) connected to a function generator (HB-104, HOKUTO DENKO CO. Ltd.). The potential at which anodic current density reaches 0.5 mA cm^{-2} is defined as the oxidation potential of an electrolyte solution.

2. 4 Results and discussion

2. 4. 1 HOMO energy to estimate oxidation stability

HOMO energy levels of $LiBPh_4$ and its derivatives.--- In order to examine whether or not the HOMO energy of a lithium salt is correlated with the oxidation potential of an electrolyte solution containing the lithium salt, $LiBPh_4$ (Ph = C_6H_5) and its derivatives are selected and examined. The selection is performed in such a way that Horowitz group [18] has already reported on the oxidation potential of an electrolyte solution containing $LiBPh_4$ and its derivatives. The HOMO energy is calculated by the semi-empirical methods. Therefore, a treatment may be verified by illustrating one-to-one correspondence between the HOMO energy and the oxidation potential for a series of $LiBPh_4$-based salts in electrolyte solutions.

Table 2. 1 shows the HOMO energy calculated by the MNDO method and the oxidation potentials measured by Horowitz et al. [18] for $LiBPh_4$ and its derivatives

Table 2. 1 HOMO energy calculated by a MNDO method and oxidation potential for a series of tetra-aryl borate anions.

Anion	Caluculated value of HOMO energy (eV)	Oxidation potential by Horowitz [18] (V vs. Li/Li^+)
BPh_4^- :($B(C_6H_5)_4^-$)	-5.31(-----)	3.53(-----)
$BPh_3(Ph\text{-}F\text{-}4)^-$	-5.44(-0.13)	3.56(+0.03)
$B(Ph\text{-}F\text{-}4)_4^-$	-5.82(-0.51)	3.68(+0.15)
$B(C_6F_5)_4^-$	-7.86(-2.55)**	4.40(+0.87)
$BPh_3(Ph\text{-}CF_3\text{-}4)^-$	-5.65(-0.34)	-----
$B(Ph\text{-}CF_3\text{-}4)_4^-$	-6.87(-1.56)	4.06(+0.53)
$B(Ph\text{-}CF_3\text{-}3)_4^-$	-6.52(-1.21)	4.06(+0.53)
$B(Ph\text{-}CF_3\text{-}2)_4^-$	-----	3.84(+0.31)
$BPh_3(Ph\text{-}(CF_3)_2\text{-}3,5)^-$	-5.70(-0.39)	-----
$B(Ph\text{-}(CF_3)_2\text{-}3,5)_4^-$ (TFPB)*	-6.87(-1.56)**	-----

*) LiTFPB: $LiB[3,5\text{-}(CF_3)_2C_6H_4]_4$ (Lithium tetrakis(3,5-bis(trifluoromethyl)phenyl)borate
**) expected value from other anions (7.86=0.51×4+5.31, 6.87=0.39×4+5.31)

in an organic electrolyte. The HOMO energy of $BPh_3(Ph\text{-}F\text{-}4)^-$ is 0.13 eV lower than that of BPh_4^- and that of $B(Ph\text{-}F\text{-}4)_4^-$ is 0.51 eV lower than that of BPh_4^-, indicative of the effect of fluoride atoms upon the HOMO energy, where Ph-F-4 is a 4-fluoro-substituted phenyl group. The oxidation potential for $B(Ph\text{-}F\text{-}4)_4^-$ increases by 0.13 eV per one 4-fluoro-substituent, i.e., the value is almost the same as one fluoro substitution effect of ca. 0.13 eV for $BPh_3(Ph\text{-}F\text{-}4)^-$. If the effect of fluorine substitution on the HOMO energy is assumed to be linear for any kind of fluoro-substituent, the HOMO energy of $B(C_6F_5)_4^-$ is expected to be -7.86 eV, i.e., $-7.86 = -5.31 - 4 \times 5 \times 0.13$, which is 2.55 eV lower than that of BPh_4^-(-5.31 eV). Table 2. 1 shows that the effect of the 4-CF_3 group for the stabilization is 3 times stronger than that of the 4-F substituent for the improvement of the oxidation stability of the borate ions, where $Ph\text{-}CF_3\text{-}4$ is 4-trifluoromethylphenyl. The MO-calculation gives 1.56 eV decrease in the HOMO energy of $B(Ph\text{-}CF_3\text{-}4)_4^-$ compared with that of BPh_4^-. The value is 1.15 times higher than that estimated

from the value of $BPh_3(Ph\text{-}CF_3\text{-}4)^-$. Similarly, the value of TFPB, substituted with four $Ph\text{-}(CF_3)_2\text{-}3,5$ groups, is calculated to be -6.87 eV, which is higher than 1.56 eV of the estimated value calculated from -0.39 eV of $BPh_3(Ph\text{-}(CF_3)_2\text{-}3,5)$.

Correlation between HOMO energy levels and oxidation potentials.--- Figure 2. 1 shows the plots of the HOMO energy against the oxidation potential. The HOMO energy is calculated by the MNDO method and the oxidation potential is given by Horowitz et al. [18]. As clearly seen in Figure 2. 1, the calculated HOMO energy levels and the oxidation potentials are correlated well. A TFPB anion shows the highest oxidation potential among the BPh_4^- derivatives as shown in Table 2. 1, because TFPB has eight CF_3 substitution.

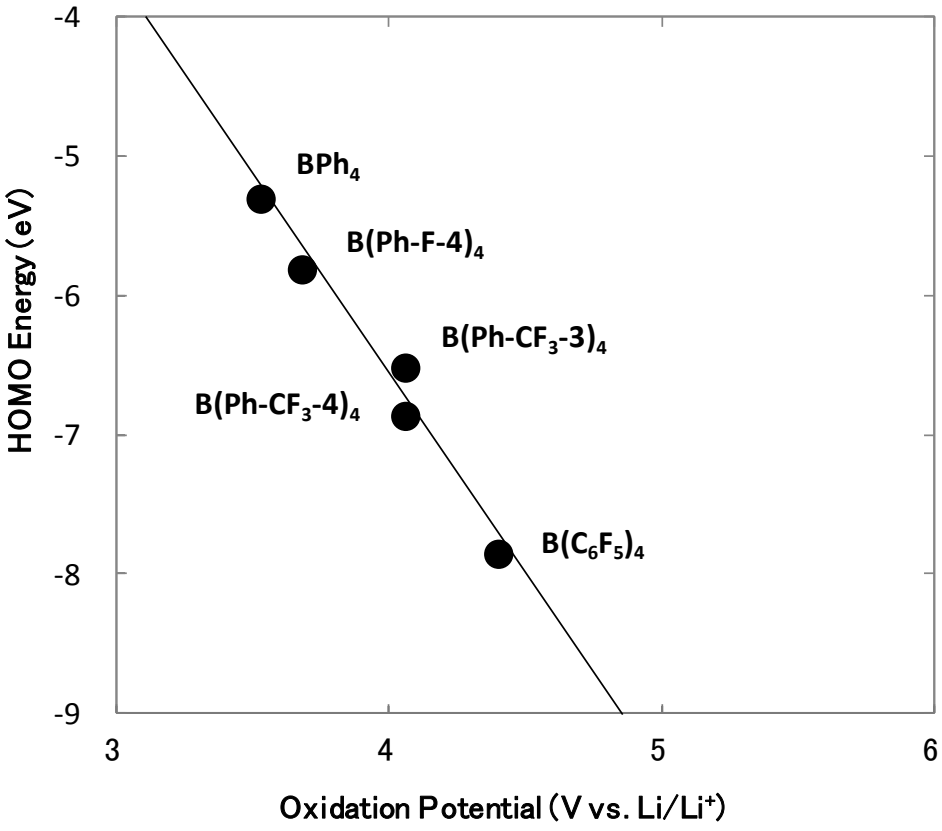

Figure 2. 1 Relation between the HOMO energy calculated by a MNDO method and the oxidation potential observed for a series of tetra-aryl borate anions.

Measurement of the oxidation potential of TFPB anion. --- Figure 2. 2 shows the voltammetric results of electrolyte solutions containing $LiBPh_4$. Solvents are Diox in Fig. 2. 2(a) and (b) and PC in (c). Because $LiBPh_4$•3DME is dissolved in Diox, electrolyte (a) contains 0.6 mol dm^{-3} of $LiBPh_4$ and 1.8 mol dm^{-3} of DME. Similarly, electrolyte (b) contains 0.3 mol dm^{-3} DME in addition to 0.1 mol dm^{-3} of $LiBPh_4$. The oxidation potentials of these electrolytes are 3.65 and 3.55 V, which agree with Horowitz's value of 3.53 V. Electrolyte (c) in Fig. 2. 2 does not contain both Diox and DME. The oxidation potential of electrolyte (c) is observed to be 3.73 V, which is slightly higher than those of electrolytes containing Diox and DME. Thus the oxidation potential of BPh_4^- anion is determined to be 3.73 V.

The result on the oxidation potential measurements of 0.1 mol dm^{-3} LiTFPB in PC is shown in Fig. 2. 3. The result on $LiBPh_4$ is also given in the figure. As seen in Fig. 2. 3, the oxidation potential shifts by 1.24 V when eight hydrogen atoms are substituted by eight CF_3 groups in $LiBPh_4$. The oxidation potential of LiTFPB

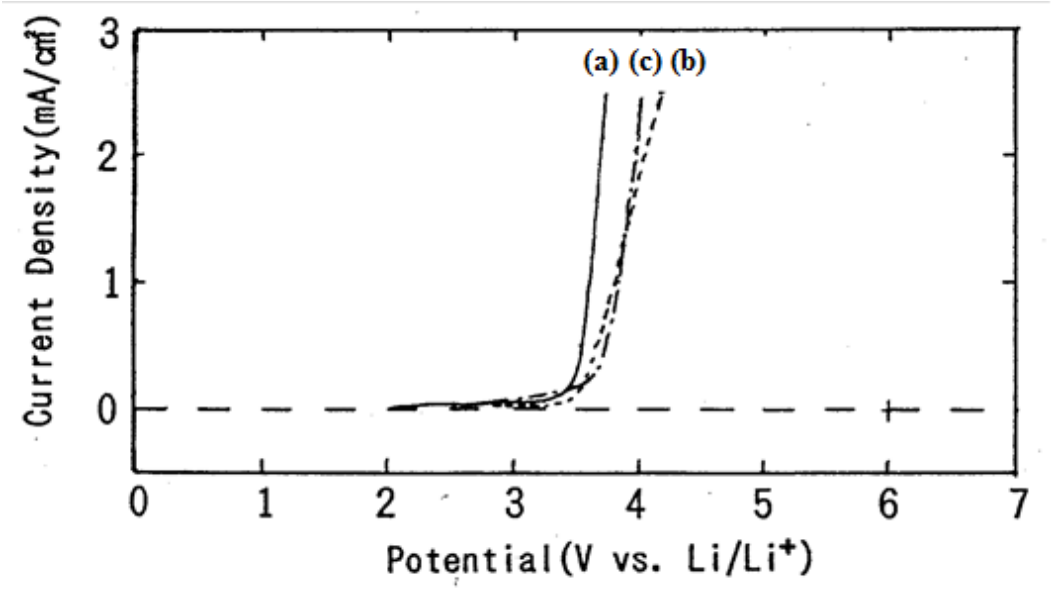

Figure 2. 2 Voltammetric signals of a platinum wire electrode examined at an anodic scan rate of 50 mV s^{-1} in (a) 0.6 mol dm^{-3} $LiBPh_4$ and 1.8 mol dm^{-3} DME in 1,3-Dioxolane, (b) 0.1 mol dm^{-3} $LiBPh_4$ and 0.3 mol dm^{-3} DME in 1,3-Dioxolane, and (c) 0.1 mol dm^{-3} $LiBPh_4$ in PC.

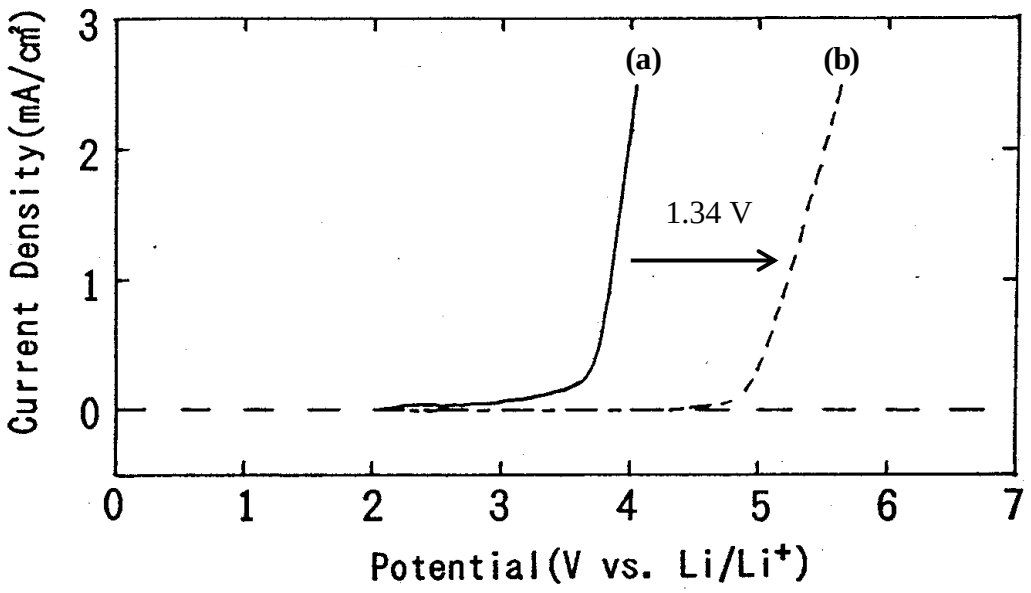

Figure 2. 3 Voltammetric signals of a platinum wire electrode examined at an anodic scan rate of 50 mV s^{-1} in (a) 0.1 mol dm^{-3} $LiBPh_4$ / PC and (b) 0.1 mol dm^{-3} LiTFPB / PC.

determined in PC is 5.07 V vs. Li/Li^+ which is 1.34 V higher than that of $LiBPh_4$. A TFPB anion shows the highest oxidation potential among tetraarylborate anions examined.

As has been described above, it is obvious that the multiple substitution with strong electron-withdrawing CF_3 groups stabilize the TFPB anion in teams of an oxidation-resistant electrolyte;

$BPh_4^- > BPh_3(Ph\text{-}(CF_3)_2\text{-}3,5)^- > \underline{BPh_3(Ph\text{-}(CF_3)_2\text{-}3,5)_4^- (TFPB^-)}$ (2)

-5.31 -5.70 $\underline{-6.87\ eV}$ (HOMO by MNDO)

$BPh_4^- < B(C_6F_5)_4^- < \underline{TFPB^-}$ (3)

+3.73 +4.40 $+\underline{5.07\ V}$ (vs. Li/Li^+)

2. 4. 2 Alkyl chain effect on the oxidation potentials of RSO_3^- anions

Alkyl chain effect of $C_nH_{2n+1}SO_3^-$ and $C_nF_{2n+1}SO_3^-$ anions on HOMO.---In a previous

section, it has been shown that the HOMO energy well reflects on the oxidation potential of $LiBPh_4$ and its relatives. In order to examine whether or not the treatment can be extended to other systems, a series of trials has been undertaken.

Figure 2. 4 shows the HOMO energy calculated for a series of $C_nH_{2n+1}SO_3^-$ anions. As seen in Fig. 2. 4, the HOMO energy is independent of the number of carbon atoms n in C_nH_{2n+1}. In other words, alkyl group C_nH_{2n+1} does not affect the HOMO energy of the $C_nH_{2n+1}SO_3^-$ anion, suggesting that the oxidation potential of a $C_nH_{2n+1}SO_3^-$ anion is almost the same among these anions. When the hydrogen atoms in a $C_nH_{2n+1}SO_3^-$ anion are substituted by fluorine atoms, a series of $C_nF_{2n+1}SO_3^-$ anions can be constructed and then the HOMO energy of each anion is calculated. Results are shown in Fig. 2. 5. The effect of fluorine substitution

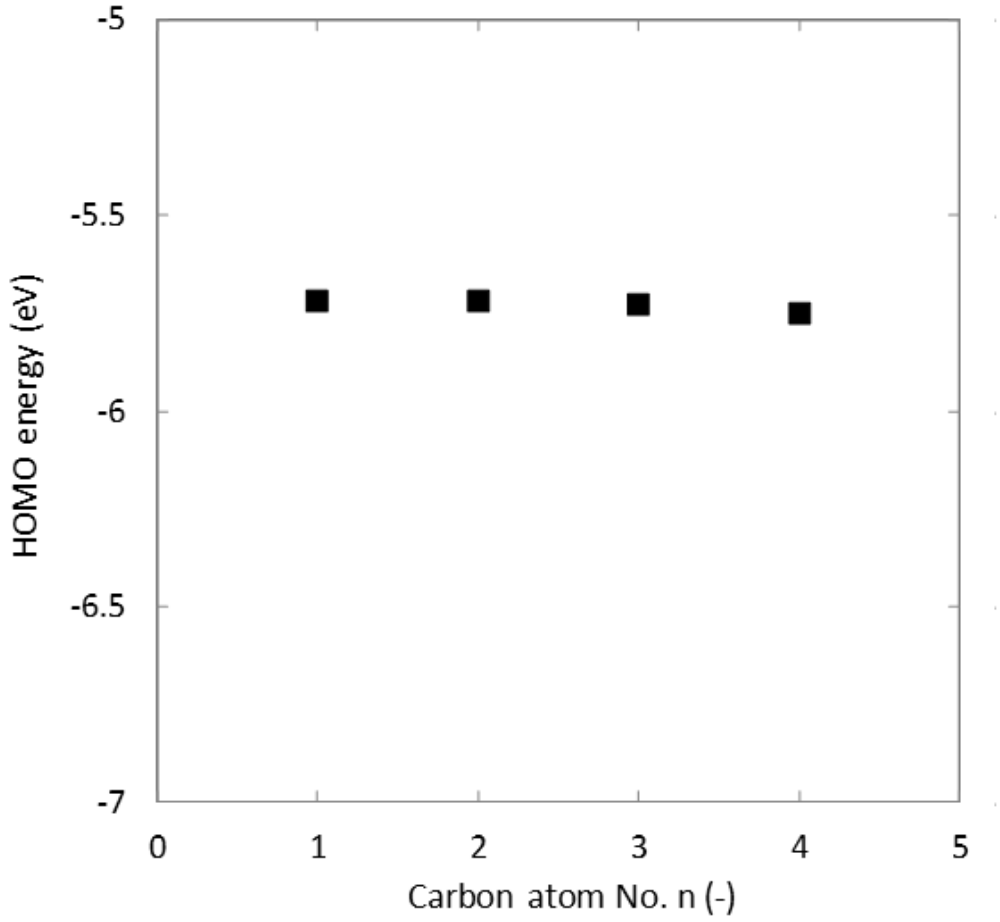

Figure 2. 4 HOMO energy calculated by a MNDO method for $C_nH_{2n+1}SO_3^-$ (n = 1, 2, 3, and 4).

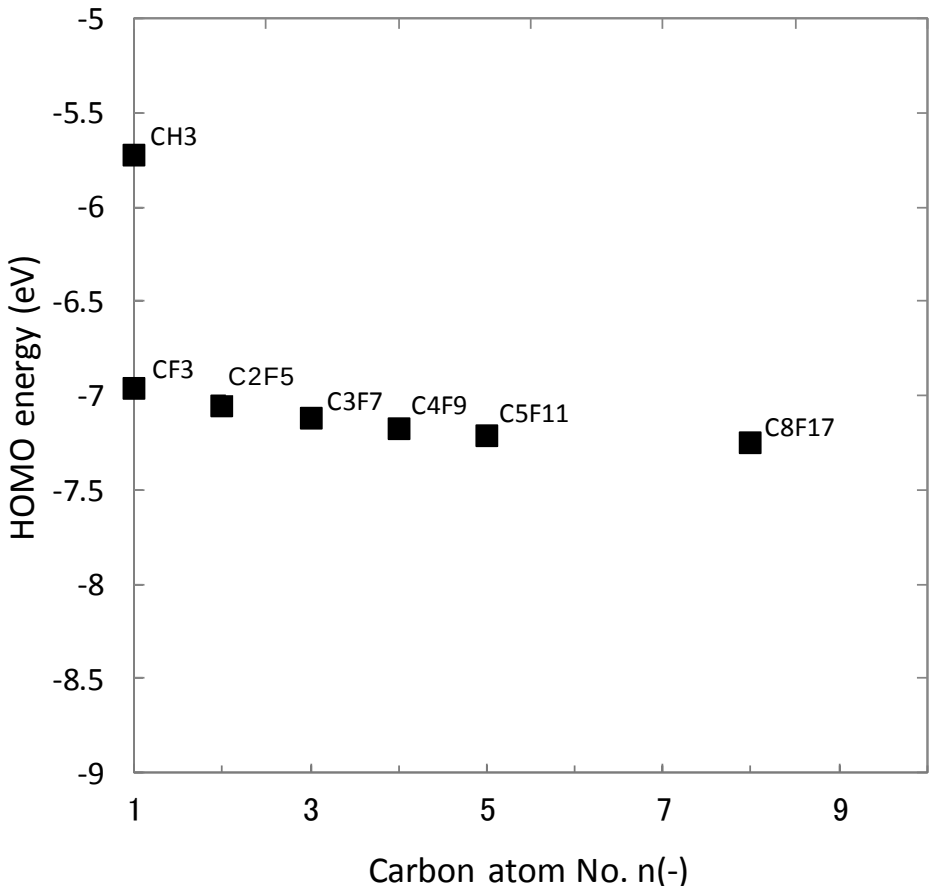

Figure 2. 5 HOMO energy calculated by a MNDO method for $C_nF_{2n+1}SO_3^-$ (n = 1, 2, 3, 4, 5, and 8).

on the HOMO energy is remarkable from $CH_3SO_3^-$ to $CF_3SO_3^-$, i.e., -5.72 to -6.96 eV. The alkyl length in $C_nF_{2n+1}SO_3^-$ anions with fluorine atoms affects obviously their HOMO energy levels, unlike the case of $C_nH_{2n+1}SO_3^-$ anions. When the number of carbon atoms in a $C_nF_{2n+1}SO_3^-$ anion increases, the HOMO energy decreases, suggesting that the oxidation potential shifts towards an anodic direction, i.e., more stable against oxidation, in an order of

$$\underset{-5.72}{CH_3SO_3^-} > \underset{-6.96}{CF_3SO_3^-} > \underset{-7.18}{C_4F_9SO_3^-} > \underset{-7.25\ eV}{C_8F_{17}SO_3^-} \qquad (4).$$

Fluorine atom number effect of $C_nH_mF_lSO_3^-$ anions on HOMO energy levels.--- In order to examine an effect of the number of fluorine atoms in a $C_nH_mF_lSO_3^-$ anion upon the HOMO energy, $C_nH_mF_lSO_3^-$ anions are constructed and the HOMO energy of each anion is calculated. Results are shown in Fig. 2. 6. As seen in the figure, when the number of fluorine atoms in $C_nH_mF_lSO_3^-$ anions increases, the HOMO energy shifts toward low energy. The HOMO energy of a $C_4F_9SO_3^-$ anion is the lowest among $C_2F_5SO_3^-$, $CF_3CF_2CH_2CH_2SO_3^-$, $CF_3CF_2CH_2CH_2SO_3^-$, and other same kinds of anions examined in Fig. 2. 6. An anion of $C_2F_5SO_3^-$ with two carbon atoms shows lower HOMO energy level compared with $CF_3CF_2CH_2CH_2SO_3^-$ with four carbon atoms, indicating that both of number of fluorine atoms and their position are important to decrease HOMO energy. A fluorine atom is more effective to decrease the HOMO energy of an anion when its position is close to a center of SO_3^- anion.

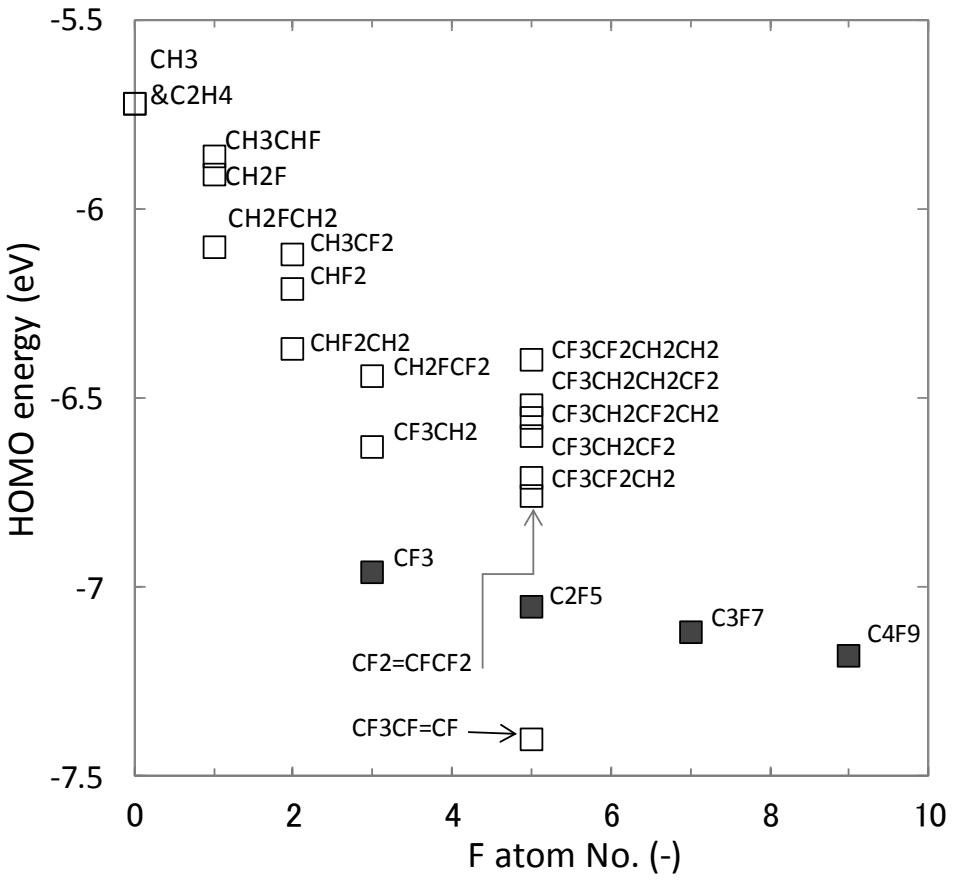

Figure 2. 6 HOMO energy calculated by a MNDO method for a series of $C_nH_mF_lSO_3^-$.

C=C double bond effect of $C_nH_mF_lSO_3^-$ anions on HOMO energy levels.--- In order to explore more effective way to shift the HOMO energy, a C=C double bond is introduced to the same kind of anions. Results are also shown in Fig. 2. 6. A $CF_3CF=CFSO_3^-$ anion having a C=C double bond shows lower HOMO energy than that of a $C_2F_5SO_3^-$ anion having only C–C single bonds. As seen in Fig. 2. 6, a $CF_2=CFCF_2SO_3^-$ anion shows the lowest HOMO energy among the anions examined, suggesting that a $CF_2=CFCF_2SO_3Li$ electrolyte is the most oxidation-resistant electrolyte. The effects of alkyl group and alkylene group on HOMO energy level are examined. $C_nF_{2n+1}SO_3^-$ anions with long fluoro-alkyl group and $C_nH_mF_lSO_3^-$ anions with specific structure, such as $CF_2=CFCF_2SO_3^-$, show lower HOMO energy when the number of fluorine atoms increases, suggesting that they show high electrochemical oxidation potentials.

Measurement of oxidation potential of a $C_nF_{2n+1}SO_3^-$ anion.---The oxidation potentials of lithium salts ($C_nF_{2n+1}SO_3Li$, n = 1, 4, and 8) are measured by a voltammetric method. Figure 2. 7 shows the experimental results on $C_nF_{2n+1}SO_3Li$ where n = 1, 4, and 8. The electrolyte is 0.1 mol dm^{-3} $C_nF_{2n+1}SO_3Li$

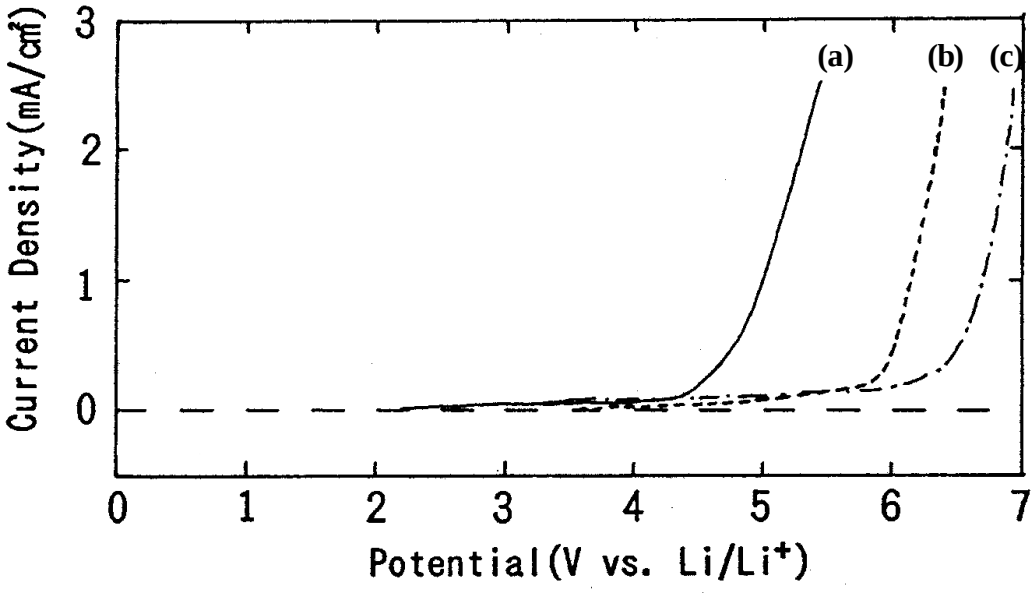

Figure 2. 7 Voltammetric signals of a platinum wire electrode examined at an anodic scan rate of 50 mV s^{-1} in (a) 0.1 mol dm^{-3} CF_3SO_3Li / PC, (b) 0.1 mol dm^{-3} $C_4F_9SO_3Li$ / PC, and (c) 0.1 mol dm^{-3} $C_8F_{17}SO_3Li$ / PC.

dissolved in PC. The potential of a Pt electrode is scanned at a rate of 50 mV s^{-1} and the oxidation potential at which the current reaches 0.5 mA cm^{-2} is determined. As clearly seen in Fig. 2. 7, the oxidation potential of $C_nF_{2n+1}SO_3Li$ dramatically shifts towards an anodic direction when n increases from 1 to 8 via 4 in $C_nF_{2n+1}SO_3Li$, i.e,

$$\underset{+4.8}{CF_3SO_3^-} < \underset{+6.0}{C_4F_9SO_3^-} < \underset{+6.5\ V\ (vs.\ Li/Li^+)}{C_8F_{17}SO_3^-} \quad (5).$$

The oxidation potential of a $RfSO_3Li$ salt shows higher value, when the number of fluorine atoms is increased, as has been expected by a HOMO energy calculation.

Correlation between oxidation potentials and HOMO for $C_nF_{2n+1}SO_3^-$.---Table 2. 2 summarizes the HOMO energy and the oxidation potentials of $C_nF_{2n+1}SO_3^-$ anions where n = 1, 4, and 8.

The HOMO energy levels of the $C_nF_{2n+1}SO_3^-$ anions are correlated with the oxidation potentials measured for their lithium salts in Fig. 2. 7 and Table 2. 2. The $C_nF_{2n+1}SO_3^-$ anions show higher oxidation potentials with decreasing HOMO energy levels. The latter two anions, $C_4F_9SO_3^-$ and $C_8F_{17}SO_3^-$, show a remarkable increase in oxidation potential, which is due to the steric barrier caused by the length of fluoro alkyl group.

Table 2. 2 HOMO energy calculated and the oxidation potential observed for $C_nF_{2n+1}SO_3$ anions (n = 1, 4, and 8) in PC

Lithium salt anion	Caluculated value of HOMO energy (eV)	Oxidation potential (V vs. Li/Li+)
$CF_3SO_3^-$	-6.96	4.8
$C_4F_9SO_3^-$	-7.18	6.0
$C_8F_{17}SO_3^-$	-7.25	6.5

2. 4. 3 An effect of the number of CF_3SO_2 group upon oxidation potential

Figure 2. 8 shows the voltammetric curves of 0.1 mol dm^{-3} CF_3SO_3Li, $(CF_3SO_2)_2NLi$, or $(CF_3SO_2)_3CLi$ dissolved in PC. All lithium salts contain the CF_3SO_2 group. The oxidation potential determined for CF_3SO_3Li, $(CF_3SO_2)_2NLi$ or $(CF_3SO_2)_3CLi$ is 4.8, 5.2, or 5.3 V, respectively. Table 2. 3 shows the HOMO energy and oxidation potential for each $(CF_3SO_2)_nXLi$ where n = 1 for X = O, n = 2 for X = N, or n = 3 for X = C. In Table 2. 3, the HOMO energy obtained by four different computational methods is given. Although the values vary when different methods are applied, an order of the HOMO energy is the same, i.e.,

$$CF_3SO_3^- > (CF_3SO_2)_2N^- > (CF_3SO_2)_3C^- \quad (6),$$

which is correlated with the oxidation potential, i.e.,

$$\underset{+4.8}{(CF_3SO_2)O^-} < \underset{+5.2}{(CF_3SO_2)_2N^-} < \underset{+5.3\ V\ (vs.\ Li/Li^+)}{(CF_3SO_2)_3C^-} \quad (7).$$

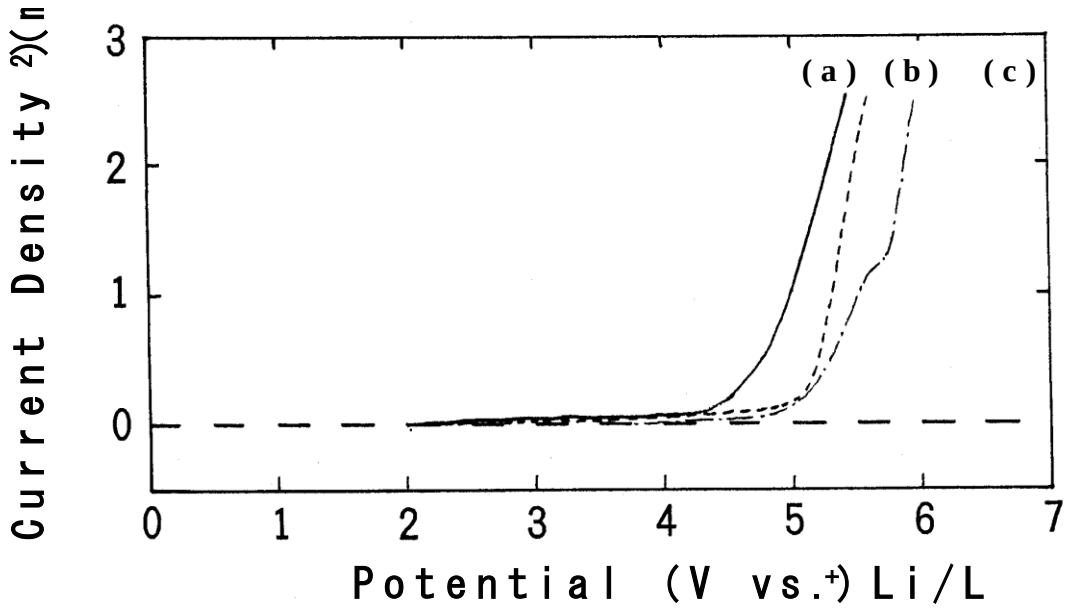

Figure 2. 8 Voltammetric signals of a platinum wire electrode examined at a rate of 50 mV s^{-1} in (a) 0.1 mol dm^{-3} CF_3SO_3Li / PC, (b) 0.1 mol dm^{-3} $(CF_3SO_2)_2NLi$ / PC, and (c) 0.1 mol dm^{-3} $(CF_3SO_2)_3CLi$ / PC.

Table 2. 3 HOMO energy calculated by several methods and the oxidation potential determined by a voltammetric method for CF_3SO_3Li, $(CF_3SO_2)_2NLi$, and $(CF_3SO_2)_3CLi$. The oxidation potential is measured in 0.1 mol dm^{-3} lithium salt dissolved in PC as shown in Fig. 2. 8.

Lithium salt	Caluculated HOMO energy levels of anions (eV)				Oxidation potential (V vs. Li/Li+)*
	MNDO	PM3	HF/3-21G*	B3LYP/6-31G*// HF/3-21G*	
CF_3SO_3Li	-6.96	-6.39	-6.41	-1.98	4.8
$(CF_3SO_2)_2NLi$	-7.17	-7.18	-7.61	-3.32	5.2
$(CF_3SO_2)_3CLi$	-7.25	-8.15	-8.00	-3.78	5.3

The $(CF_3SO_2)_nXLi$ electrolyte solutions show lower HOMO energy levels when the number of $RfSO_2$ group is increased, suggesting high electrochemical oxidation potentials.

2. 4. 4 An effect of the length of fluoro-alkyl chain in imide salts on the oxidation potentials

Figure 2. 9 shows the voltammetric examinations to determine the oxidation potentials of three imide salts. A lithium salt of $(CF_3SO_2)_2NLi$ shows the oxidation potential of +5.2 V vs. Li/Li^+. When CF_3SO_2 is substituted to $C_4F_9SO_2$ or $C_8F_{17}SO_2$, the oxidation potential shifts to an anodic direction by about 1 V, i.e., +5.9 V vs. Li/Li^+ of the oxidation potential for $(C_4F_9SO_2)(CF_3SO_2)NLi$ or +6.0 V vs. Li/Li^+ for $(C_8F_{17}SO_2)(CF_3SO_2)NLi$. As seen in Fig. 2. 9, the effect of introducing long fluoro-alkyl chain to imide salts is remarkable, which is consistent with the previous observation described in section 2. 4. 2.

Other types of imide electrolytes are also examined. Table 2. 4 shows the HOMO energy calculated for $(C\underline{F_3}CH_2OSO_2)_2NLi$, $(H\underline{CF_2}\underline{CF_2}CH_2OSO_2)_2NLi$, $(\underline{CF_3}\underline{CF_2}CH_2OSO_2)_2NLi$, or $((CF_3)_2CHOSO_2)_2NLi$, by three different computational methods. When the number of fluorine atoms increases in the imide ester salts, the HOMO energy decreases regardless of computational methods used, suggesting

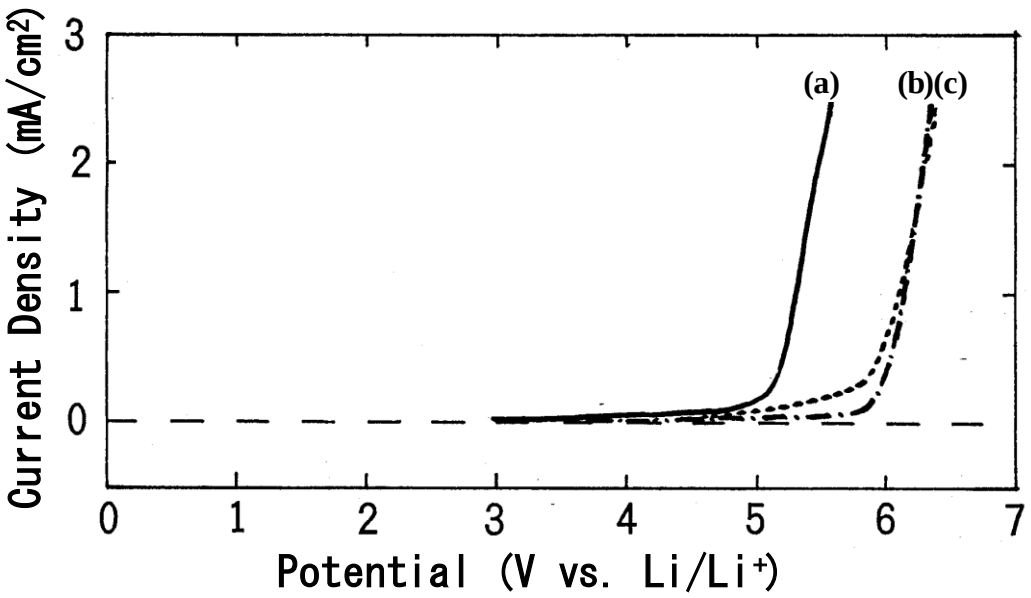

Figure 2. 9 Voltammetric signals of a platinum wire electrode examined at a rate of 50 mV s^{-1} in (a) 0.1 mol dm^{-3} $(CF_3SO_2)_2NLi$ / PC, (b) 0.1 mol dm^{-3} $(C_4F_9SO_2)(CF_3SO_2)NLi$ / PC, and (c) 0.1 mol dm^{-3} $(C_8F_{17}SO_2)(CF_3SO_2)NLi$ / PC. The oxidation potential determined is (a) 5.2, (b) 5.9, or (c) 6.0 V.

Table 2. 4 HOMO energy calculated by several methods for new imide anions of $(RfOSO_2)_2N^-$, in which Rf is a fluoro-alkyl group.

Anion	Caluculated HOMO energy levels of anions		
	PM3	HF/3-21G*	B3LYP/6-31G*// HF/3-21G*
$(CF_3CH_2OSO_2)_2N^-$	-6.89	-7.32	-3.13
$(HCF_2CF_2CH_2OSO_2)_2N^-$	-6.63	-7.33	-3.27
$(CF_3CF_2CH_2OSO_2)_2N^-$	-6.95	-7.63	-3.4
$((CF_3)_2CHOSO_2)_2N^-$	-7.29	-8.03	-3.84

the possibility of new imide ester salts highly stable to oxidation. In order to evaluate the oxidation potentials of imide ester salts, voltammetric examinations are carried out. Figures 2. 10 shows the voltammetric results on $(CF_3CH_2OSO_2)_2NLi$ and $(CF_3CH_2CH_2OSO_2)_2NLi$. The result on $(CF_3SO_2)_2NLi$ is also shown in Figure

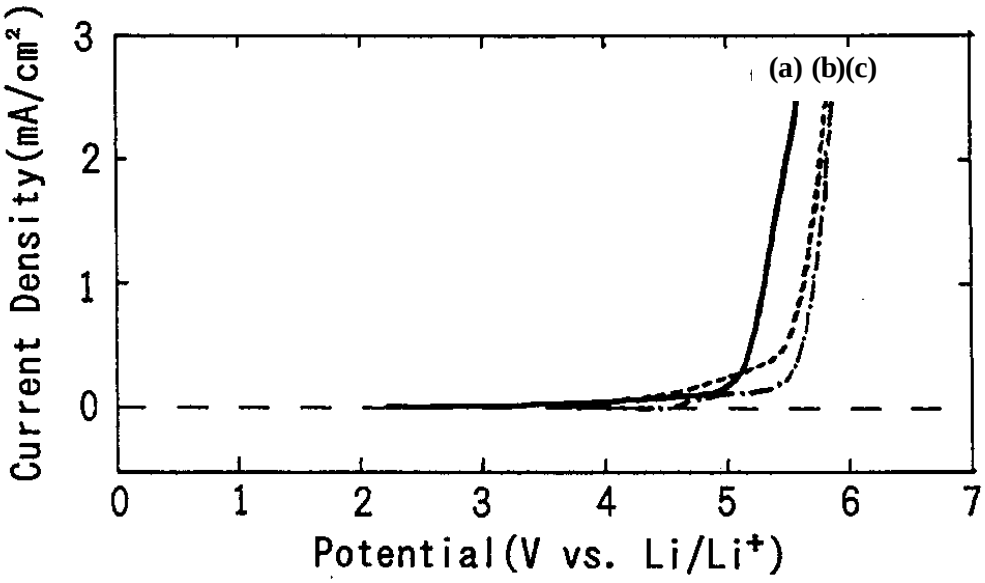

Figure 2. 10 Voltammetric signals of a platinum wire electrode examined at a rate of 50 mV s^{-1} in (a) 0.1 mol dm^{-3} $(CF_3SO_2)_2NLi$ / PC, (b) 0.1 mol dm^{-3} $(CF_3CH_2OSO_2)_2NLi$ / PC, and (c)0.1 mol dm^{-3} $(CF_3CF_2CH_2OSO_2)_2NLi$ / PC. The oxidation potential determined is (a) 5.2, (b) 5.4, or (c) 5.6 V.

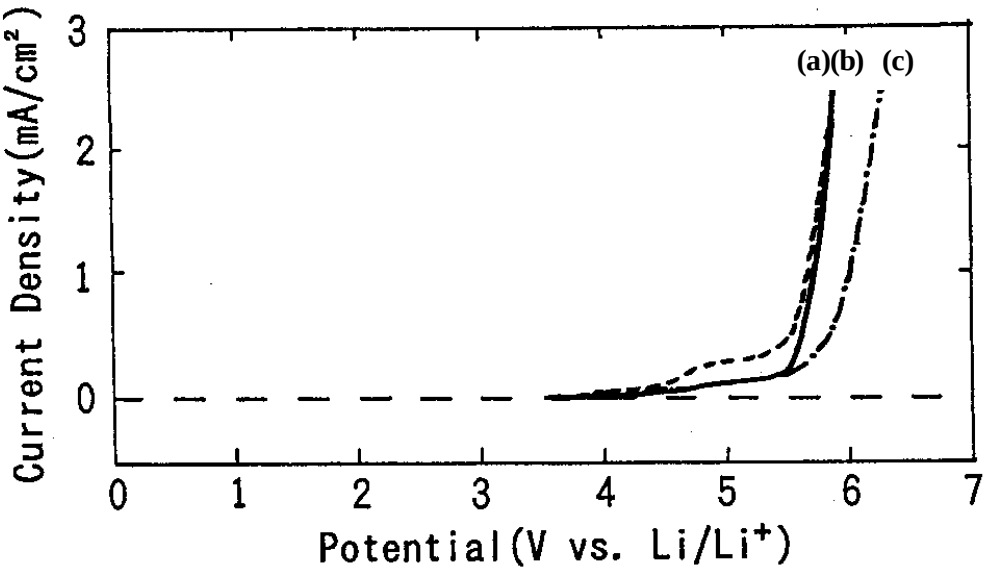

Figure 2. 11 Voltammetric signals of a platinum wire electrode examined at a rate of 50 mV s^{-1} in (a) 0.1 mol dm^{-3} $(HCF_2CF_2CH_2OSO_2)_2NLi$ / PC, (b) 0.1 mol dm^{-3} $(CF_3CF_2CH_2OSO_2)_2NLi$ / PC, and (c) 0.1 mol dm^{-3} $(CF_3)_2CHOSO_2)_2NLi$ / PC. The oxidation potential determined at anodic current density of 0.5 mA cm^{-2} is (a) 5.5, (b) 5.6, or (c) 5.8 V.

2. 10 by comparison. As seen in the Figure 2. 10, $(CF_3CH_2OSO_2)_2NLi$ and $(CF_3CH_2CH_2OSO_2)_2NLi$ are more stable to oxidation than $(CF_3SO_2)_2NLi$, although each lithium salt contains 6 fluorine atoms. Figure 2. 11 shows the branched ester imide salt of $((CF_3)_2CHOSO_2)_2NLi$ together with $(HCF_2CF_2CH_2OSO_2)_2NLi$ and $(CF_3CF_2CH_2OSO_2)_2NLi$. The branched ester imide salt of $((CF_3)_2CHOSO_2)_2NLi$ is extraordinarily stable to oxidation among imide salts. This is better illustrated in Figure 2. 12.

Lithium salts of $(CF_3CH_2OSO_2)_2NLi$, $(HCF_2CF_2CH_2OSO_2)_2NLi$, and $(CF_3CF_2CH_2OSO_2)_2NLi$ respectively contain 6, 8, and 10 fluorine atoms and show +5.4, +5.5, and +5.6 V vs. Li/Li^+ of oxidation potential, so that the oxidation potential linearly increases as the number of fluorine atoms increases. Specifically it increases by 0.1 V when two fluorine atoms are added in lithium salts, which correspond to a decrease in the HOMO energy as shown in Table 2. 4.

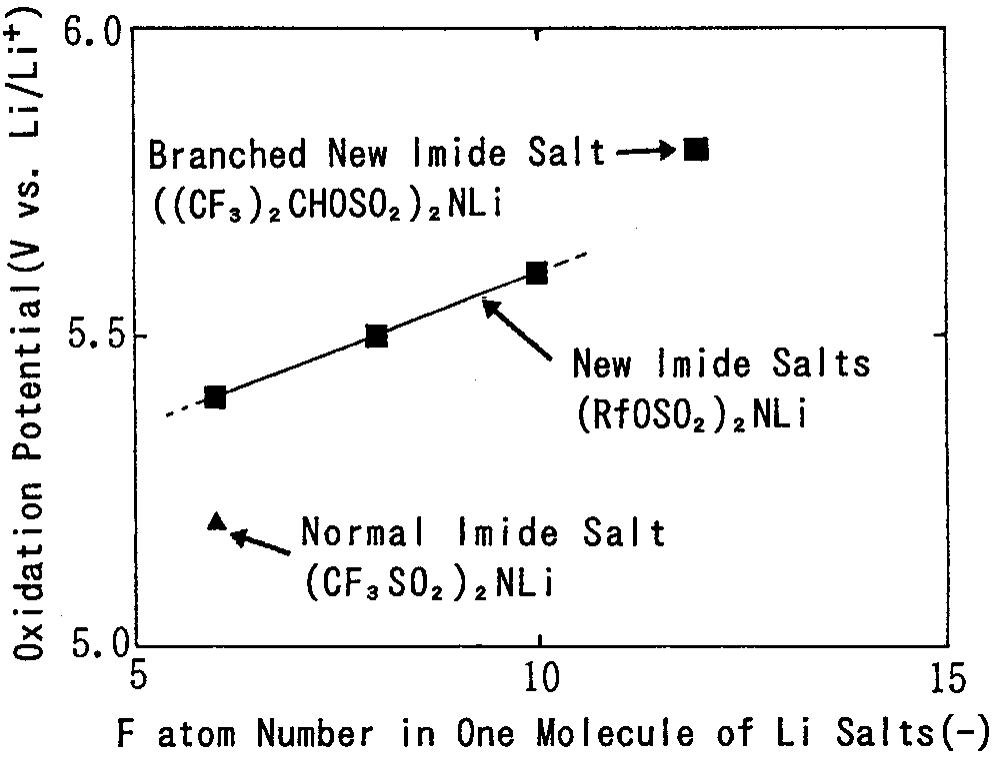

Figure 2. 12 An effect of fluorine substitution in a lithium imide salt upon the oxidation potential determined by a voltammetric method at 25°C.

A branched imide ester salt $((CF_3)_2CHOSO_2)_2NLi$ shows the highest oxidation potential of 5.8 V among the imide ester salts examined. The oxidation potential is higher than the expected value of 5.7 V in Fig. 2. 12. The remarkably higher oxidation potential of an imide anion with branched $(CF_3)_2CHO$ group is due to the electron-withdrawing ability of branched imide ester compared with the linear structure of $HCF_2CF_2CH_2O$ group with the same fluorine atom number.

2. 4. 5 Corrosion of aluminum current feeder in fluoro-organic lithium salts electrolyte

Aluminum foil is usually used as the current feeder of a positive electrode in lithium-ion batteries. An aluminum current feeder should be stable over 4.3 V vs. Li/Li^+ in an electrolyte solution for lithium-ion batteries, because the charge-end voltage is normally 4.2 V for current lithium-ion batteries. Krause et al. [19] reported that aluminum was corroded in the $(CF_3SO_2)_2NLi$ / PC solution at 4.2 V vs.

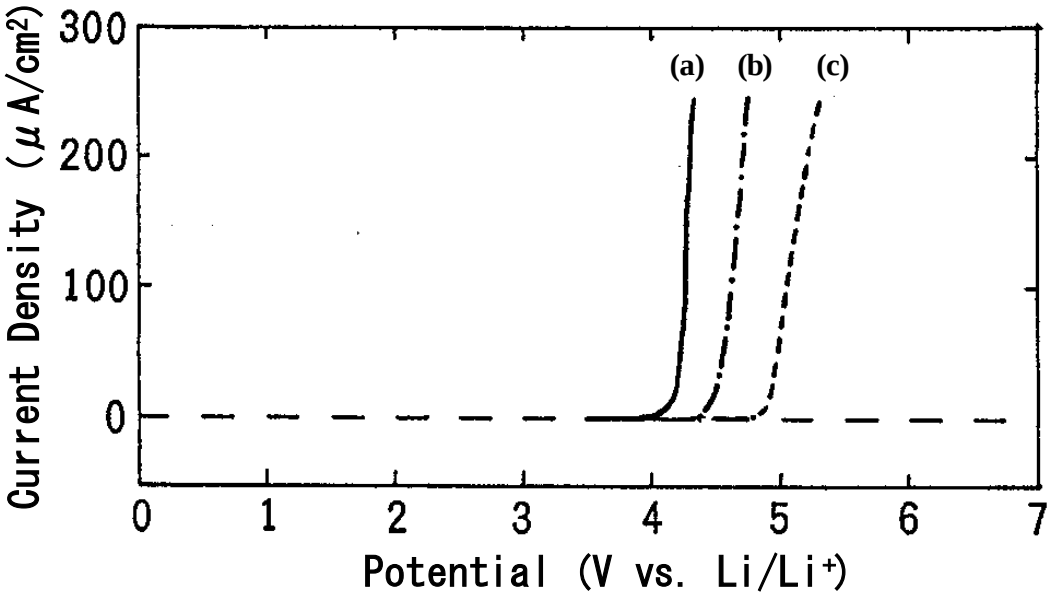

Figure 2. 13 Voltammetry of an aluminum electrode 0.1 mm thick examined at a rate of 5 mV s^{-1} at 25°C in (a) 0.1 mol dm^{-3} $(CF_3SO_2)_2NLi$ / PC, (b) 0.1 mol dm^{-3} $((CF_3)_2CHOSO_2)_2NLi$ / PC, and (c) 0.1 mol dm^{-3} $(C_4F_9SO_2)(CF_3SO_2)NLi$ / PC. Aluminum dissolution potential is determined to be (a) 4.0, (b) 4.3, and (c) 4.8 V. Electrode area of aluminum is 1.0 cm^2.

Li/Li^+. Structure-modified fluoro-organic lithium salts should be satisfied against the aluminum corrosion above 4.3 V vs. Li/Li^+. Therefore, aluminum corrosion is examined by a voltammetric method. Because an aluminum oxide layer protects aluminum dissolution from the aluminum current feeder at the first scan, the data obtained at the second scan is used for aluminum stability tests. Results are shown in Figure 2. 13. The electrode used is a 1.0-cm^2 aluminum plate 0.1 mm thick. As seen in Fig. 2. 13, aluminum dissolves in the $(CF_3SO_2)_2NLi$ electrolyte at ca. 4.0 V vs. Li/Li^+, which is consistent with the previous result [19]. However, aluminum does not dissolve in $(C_4F_9SO_2)(CF_3SO_2)NLi$ and $((CF_3)_2CHOSO_2)_2NLi$ electrolytes at 4.3 V vs. Li/Li^+. The new ester-type imide salt, $((CF_3)_2CHOSO_2)_2NLi$ does not dissolve the aluminum current feeder up to 4.8 V.

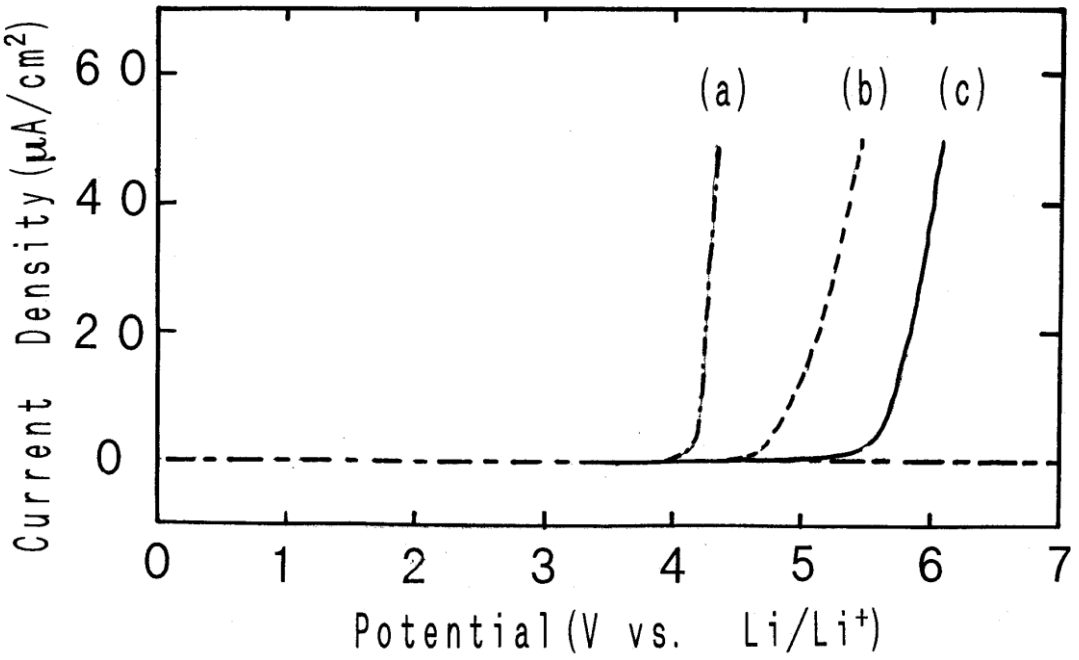

Figure 2. 14 Voltammetry of an aluminum electrode 0.1 mm thick examined at a rate of 5 mV s^{-1} at 25°C in (a) 0.1 mol dm^{-3} $(CF_3SO_2)_2NLi$ / PC, (b) 0.1 mol dm^{-3} $(CF_3SO_2)_3CLi$ / PC, and (c) 0.1 mol dm^{-3} $(CF_3CH_2OSO_2)_3CLi$ / PC. Aluminum dissolution potential is determined to be (a) 4.0, (b) 4.6, and (c) 5.5 V. Electrode area of aluminum is 1.0 cm^2. Methide type salts, $(CF_3SO_2)_3CLi$ and $(CF_3CH_2OSO_2)_3CLi$, show higher aluminum dissolution potential than $(CF_3SO_2)_2NLi$.

The onset potential of aluminum dissolution is 4.0 V vs. Li/Li^+ for $(CF_3SO_2)_2NLi$, 4.3 V for $(CF_3)_2CHOSO_2)_2NLi$, or 4.8 V $(C_4F_9SO_2)(CF_3SO_2)NLi$, which correlate with the oxidation potential of 5.3 V for $(CF_3SO_2)_2NLi$, 5.8 V for $(CF_3)_2CHOSO_2)_2NLi$, or 5.9 V for $(C_4F_9SO_2)(CF_3SO_2)NLi$. This may be due to the bulkiness of fluoro-organic anions. In order to assess an effect of bulkiness and oxidation potentials upon the aluminum corrosion potentials, $(CF_3SO_2)_3CLi$ and $(CF_3CH_2OSO_2)_3CLi$ are examined and the results are shown in Fig. 2. 14. Lithium salts of $(CF_3SO_2)_3CLi$ and $(CF_3CH_2OSO_2)_3CLi$ show the higher aluminum dissolution potentials 4.6 V and 5.5V vs. Li/Li^+ respectively than imide salts in PC electrolyte solution. Figure 2. 15 shows the relation between the electrochemical

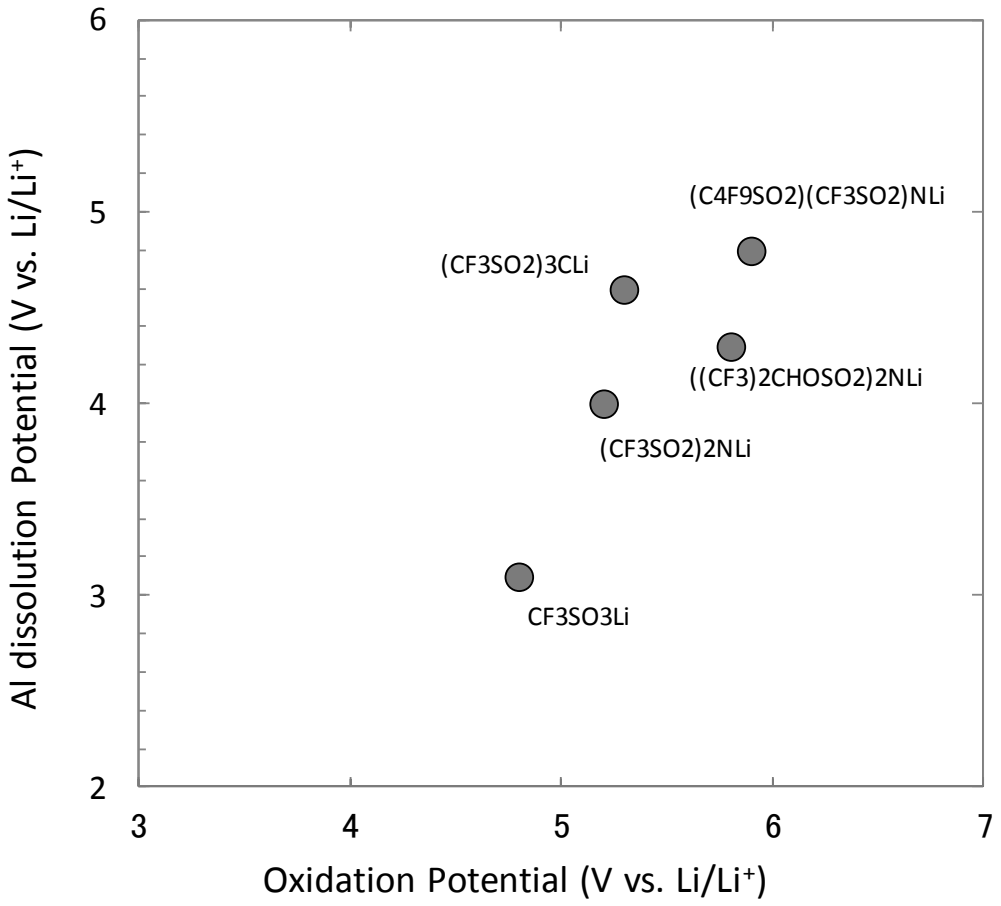

Figure 2. 15 The dissolution potential of an aluminum electrode versus the oxidation potential determined using a platinum electrode in fluoro-organic lithium salts dissolved in PC. The dissolution potential is the same as the corrosion potential of aluminum.

oxidation potentials and aluminum dissolution potentials of different types of lithium imide salts. The lithium salts with high oxidation potentials tend to show high aluminum dissolution potentials. Especially an imide salt with a long fluoroalkyl group, such as $(C_4F_9SO_2)(CF_3SO_2)NLi$, and a methide salt with three $RfSO_2$ substitute, such as $(CF_3SO_2)_3CLi$, show higher dissolution potentials. This suggests that aluminum dissolution via soluble species of $[(CF_3SO_2)_3C]_3Al$ or $[(C_4F_9SO_2)(CF_3SO_2)N]_3Al$ is difficult or very slow because of their bulkiness. Schmitz et al. [20] report that the different type of bulky di-lithium salts, such as a $(CF_3SO_2)NSO_2CF_2SO_2C(SO_2CF_3)_2^{2-}$ anion, suppress the aluminum dissolution. Schmitz et al. also report that a $(CF_3SO_2)NSO_2CF_2SO_2N(SO_2CF_3)^{2-}$ anion shows gradual dissolution in voltage up to 5 V vs. Li/Li^+. A $(CF_3SO_2)NSO_2CF_2SO_2C(SO_2CF_3)_2^{2-}$ anion with a methide structure suppresses aluminum dissolution and a $(CF_3SO_2)NSO_2CF_2SO_2N(SO_2CF_3)^{2-}$ anion with short chain imide structure ($-CF_2SO_2N(SO_2CF_3)$) shows aluminum dissolution.

As seen in Fig. 2. 15, imide salts having longer fluoro-alkyl groups or methide salts with three $RfSO_2$ substitutes show higher aluminum dissolution potentials, i.e.,

$$\underset{4.0}{(CF_3SO_2)_2NLi} < \underset{4.3}{((CF_3)_2CHOSO_2)_2NLi} < \underset{4.8\ V\ (vs.\ Li/Li^+)}{(C_4F_9SO_2)(CF_3SO_2)NLi} \quad (8),$$

$$\text{and } \underset{4.6}{(CF_3SO_2)_3CLi} < \underset{5.5\ V\ (vs.\ Li/Li^+)}{(CF_3CH_2OSO_2)_3CLi} \quad (9)$$

2. 5 Summary

In this chapter, the electrochemical stability against oxidation for fluoro-organic lithium salts in polar aprotic solvents is examined in both theoretical and empirical bases. The theoretical parameter selected is the HOMO energy calculated by the computational methods for a series of fluoro-organic lithium salts and the empirical parameter is the oxidation potential determined by a voltammetric method with respect to a lithium electrode. One-to-one correspondence between the HOMO energy and oxidation potential has been shown for a series of

fluoro-organic lithium salts.

According to the results, $BPh_3(Ph\text{-}(CF_3)_2\text{-}3,5)_4^-$ ($TFPB^-$) shows the highest oxidation potential of 5.07 V vs. Li/Li^+ among the same class of lithium salts based on borates, whose oxidation potentials are below 4 V vs. Li/Li^+. The oxidation potential higher than 5.07 V vs. Li/Li^+ for $TFPB^-$ is observed for $C_4F_9SO_3^-$ and $C_8F_{17}SO_3^-$ to be 6.0 and 6.5 V vs. Li/Li^+, respectively. Imide salts are more stable against oxidation than CF_3SO_3Li. Especially, the branched imide ester salt of $((CF_3)_2CHOSO_2)_2NLi$ and imide salt with long fluoro alkyl group $(C_4F_9SO_2)(CF_3SO_2)NLi$ show the higher oxidation potential of ca. 6.0 V vs. Li/Li^+ than $(CF_3SO_2)_2NLi$ (4.0 V vs. Li/Li^+). Both $((CF_3)_2CHOSO_2)_2NLi$ and $(C_4F_9SO_2)(CF_3SO_2)NLi$ also show high aluminum dissolution potentials over 4.3 V.

As has been shown in this chapter, an application of the computational methods to calculate the HOMO energy is an effective way to explore the oxidation-resistant electrolytes for advanced lithium-ion batteries.

References

[1] N. Koshiba, T. Ikehata, and K. Takata, *National Technical Report*, **37**, 64 (1991).

[2] F. Jensen, "Introduction to Computational Chemistry" Second Edition, John Wiley & Sons, Chichester (2007).

[3] C. J. Cramer, "Essentials of Computational Chemistry" Second Edition, John Wiley & Sons, Chichester (2005).

[4] A. Szabo and N. S. Ostlund, "Modern quantum chemistry: introduction to advanced electronic structure theory" Dover Publications INC. NY (1986)

[5] R. G. Parr and W. Yang, "Density-Functional Theory of Atoms and Molecules" Oxford Science (1989).

[6] M. Ue, A. Murakami, and S. Nakamura, *J. Electrochem. Soc.*, **149**, A1572 (2002).

[7] X. Wang, E. Yasukawa, and S. Mori, *J. Electrochem. Soc.*, **146**, 3992 (1999).

[8] H. Yamaguchi, H. Takahashi, M. Kato, and J. Arai, *J. Electrochem. Soc.*, **150**, A312 (2003).

[9] V. R. Koch, L. A. Dominey, and C. Nanjundiah, *J. Electrochem. Soc*., **143**, 798 (1996).

[10] K. Tasaki, K. Kanda, T. Kobayashi, S. Nakamura, and M. Ue, *J. Electrochem. Soc*., **153**, A2192 (2006).

[11] J. Barthel, R. Buestrich, H. J. Gores, M. Schmidt, and M. Wuhr, *J. Electrochem. Soc*., **144**, 3866 (1997).

[12] J. J. P. Stewart, *QCPE Bull.*, **9**,10 (1989)

[13] K. Nishida, *JCPE NEWS letter*, **3**, 10 (1991).

[14] M. J. S. Dewar and W. Thiel, *J. Am. Chem. Soc.,* **99**, 4899 (1977).

[15] J. J. P. Stewart, *J. Mol. Mod.*, **10**, 155 (2004).

[16] D. Young, p. 342 in Computational Chemistry, John Wiley & Sons, Inc., NY (2001).

[17] Gaussian 92-94 (currently Gaussian 09, Revision D.01), M. J. Frisch, G. W. Trucks, H. B. Schlegel, G. E. Scuseria, M. A. Robb, J. R. Cheeseman, G. Scalmani, V. Barone, B. Mennucci, G. A. Petersson, H. Nakatsuji, M. Caricato, X. Li, H. P. Hratchian, A. F. Izmaylov, J. Bloino, G. Zheng, J. L. Sonnenberg, M. Hada, M. Ehara, K. Toyota, R. Fukuda, J. Hasegawa, M. Ishida, T. Nakajima, Y. Honda, O. Kitao, H. Nakai, T. Vreven, J. A. Montgomery, Jr., J. E. Peralta, F. Ogliaro, M. Bearpark, J. J. Heyd, E. Brothers, K. N. Kudin, V. N. Staroverov, R. Kobayashi, J. Normand, K. Raghavachari, A. Rendell, J. C. Burant, S. S. Iyengar, J. Tomasi, M. Cossi, N. Rega, J. M. Millam, M. Klene, J. E. Knox, J. B. Cross, V. Bakken, C. Adamo, J. Jaramillo, R. Gomperts, R. E. Stratmann, O. Yazyev, A. J. Austin, R. Cammi, C. Pomelli, J. W. Ochterski, R. L. Martin, K. Morokuma, V. G. Zakrzewski, G. A. Voth, P. Salvador, J. J. Dannenberg, S. Dapprich, A. D. Daniels, Ö. Farkas, J. B. Foresman, J. V. Ortiz, J. Cioslowski, and D. J. Fox, Gaussian, Inc., Wallingford CT, 2009.

[18] H. H. Horowitz, J. I. Haberman, L. P. Kleman, G. H. Newman, E. L. Stogryn and T. A. Whitney, p. 131 in Proceedings of the Symposium on Lithium Batteries, **Vol. 81-4**, The Electrochemical Society (1981).

[19] L. J. Krause, W. Lamanna, J. Summerfield, M. Engle, G. Korba, and R. Loch, *J. Power Sources*, **68**, 320 (1997).

[20] P. Murmann, R. Schmitz, S. Nowak, H. Gores, N. Ignatiev, P. Sartori, S.

Passerini, M. Winter, and R. W. Schmitz, *J. Electrochem. Soc*., **160**, A535 (2013).

Chapter 3

Evaluation of Fluoro-Organic Lithium Salts in Lithium-ion Batteries

3. 1 Introduction

In previous chapters, conductivity and stability of lithium fluoro-organic salts against an electrochemical oxidation in polar aprotic solvents have been described. Among fluoro-organic lithium salts examined in chapters 1 and 2, $(C_2F_5SO_2)_2NLi$, $(CF_3)_2CHOSO_2)_2NLi$, and $(C_4F_9SO_2)(CF_3SO_2)NLi$ are compatible with $LiPF_6$ currently used in lithium-ion batteries. Although aluminum corrosion is one of the problems in applying the imide salts to lithium-ion batteries, $(CF_3)_2CHOSO_2)_2NLi$ and $(C_4F_9SO_2)(CF_3SO_2)NLi$ show that the onset potential at which aluminum dissolution occurs is more than 4.3 V with respect to a lithium electrode. In order to assure that $(C_2F_5SO_2)_2NLi$, $(CF_3)_2CHOSO_2)_2NLi$ and $(C_4F_9SO_2)(CF_3SO_2)NLi$ can be used in lithium-ion batteries, prototype batteries consisting of the $LiCoO_2$-positive and graphite-negative electrodes separated by a porous membrane containing the electrolyte under consideration are fabricated and examined in terms of rate capability, cycle, and storage tests.

In this chapter, the property of $(C_2F_5SO_2)_2NLi$, $(CF_3)_2CHOSO_2)_2NLi$ and $(C_4F_9SO_2)(CF_3SO_2)NLi$ superior to $LiPF_6$ is shown and discussed in terms of the formation of effective solid electrolyte interface (SEI) based on the results on the X-ray photoelectron spectroscopy (XPS) analysis on the graphite-negative electrodes together with the battery performance.

3. 2 Experimental

3. 2. 1 Electrolytes and electrode materials

Lithium hexafluorophosphate $LiPF_6$ is obtained from STELLA CHEMIFA Co.

Ltd., Japan. $(C_2F_5SO_2)_2NLi$ is obtained from Sumitomo 3M Co. Ltd., Japan. Other imide salts of $((CF_3)_2CHOSO_2)_2NLi$ and $(C_4F_9SO_2)(CF_3SO_2)NLi$ are obtained from Central Glass, Co., Ltd., Japan. $LiPF_6$ is used as received. The other lithium salts are dried under vacuum at 130°C for 3 h, and then cooled to room temperature overnight. The dried lithium salts in glass bottles are stored in an argon-filled dry box before use.

Battery grade ethylene carbonate (EC) and methyl ethyl carbonate (MEC) are obtained from Ube Industries, Ltd., Japan. EC and MEC are mixed in the volume ratio of 1 to 2 in an argon-filled dry box. The concentration of each lithium salt is 1.0 mol dm^{-3} in the mixed solvent.

3. 2. 2 Prototype batteries

The electrode materials selected in fabricating the prototype batteries are an artificial graphite of mesocarbon microbeads, abbreviated MCMB hereafter, and $LiCoO_2$. Both materials are widely used in current lithium-ion batteries. The negative electrode consists of 90 weight percent (wt%) MCMB and 10 wt% polyvinylidene difluoride (PVdF) coated on both sides of copper foil. The positive electrode consists of 90 wt% $LiCoO_2$, 6 wt% conductive carbon, and 4 wt% PVdF coated on both sides of aluminum foil. The separator used is a polyethylene microporous membrane 25 μm thick obtained from Toray Battery Separator Film Co. Ltd., Japan. Cell hardware used in fabricating prototype batteries is a cylindrical 14500 battery (14 mm diameter and 50 mm height), which is known as AA size as shown in Figure 3. 1. Positive and negative electrodes separated by two sheets of a microporous membrane are wound up into a bobbin and inserted into a 14500 can. After the electrode tab from the positive electrode is welded to a cap on the top and the tab from the negative electrode is welded to a center at the bottom of the can, the electrolyte is injected into the electrode bobbin inside the can. Finally, the can is tightly sealed with the cap by crimp-seal. After pre-charging, the batteries are open-circuited and stored at 60°C overnight in a temperature-controlled oven (Yamato Scientific Co. Ltd., Japan), so-called an aging process.

Figure 3. 1 A photograph of prototype 14500 lithium-ion battery. The battery is also called AA size battery, which is 14 mm in diameter and 50 mm height.

The 600-mAh 14500 batteries are designed, fabricated, and examined in voltage ranging from 2.75 to 4.1 V. The electrolyte was 1.0 mol dm^{-3} lithium salt dissolved in ethylene carbonate (EC) / methyl ethyl carbonate (MEC) (1 / 2 by volume). The lithium salts examined are $LiPF_6$, $(C_2F_5SO_2)_2NLi$, $(C_4F_9SO_2)(CF_3SO_2)NLi$, and $(CF_3)_2CHOSO_2)_2NLi$. When $(C_2F_5SO_2)_2NLi$ is examined in the batteries, 0.05 mol dm^{-3} $LiPF_6$ is added into the electrolyte as a stabilizer, as will be discussed in the results and discussion section

3. 2. 3 Testing procedures

Battery cyclers used are TOSCAT 3000 charge-discharge system (TOYO SYSTEM Co., Ltd., Japan). The battery is charged at constant current until the terminal voltage reached charge-end voltage and then kept at that voltage, so-called constant-current and constant-voltage mode (CCCV). Figure 3. 2 illustrates how the terminal voltage and current are recorded as a function of time during charge and discharge in a CCCV mode. Specifically the batteries are charged at 1.0 C-rate until the terminal voltage reached 4.1 V and then charged at constant voltage of 4.1 V for 2.5 h on charge at 23 ± 2°C. After charging, the batteries are discharged at

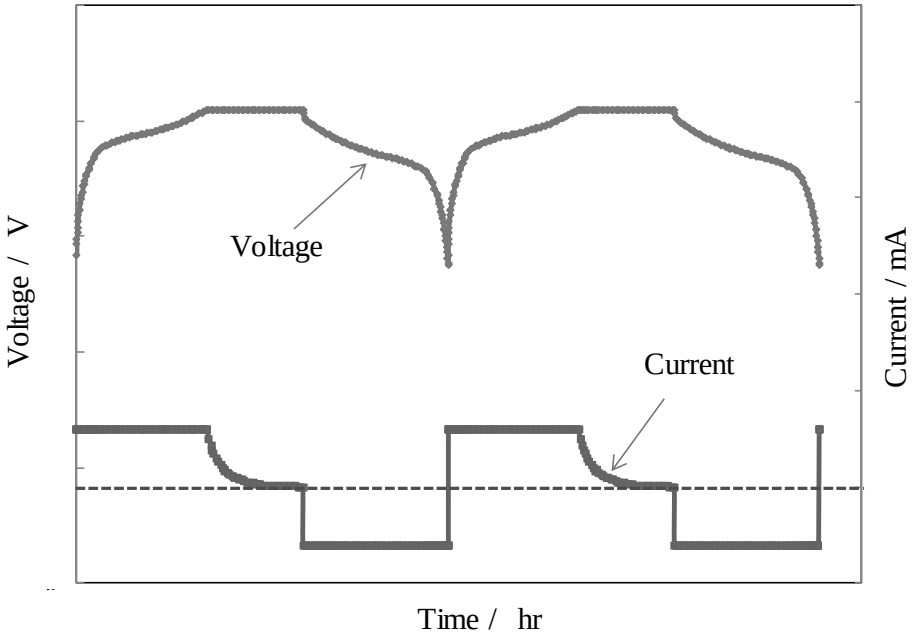

Figure 3. 2 Typical charge and discharge curves of a lithium-ion battery. A lithium-ion battery is usually charged at constant current until the terminal voltage reaches charge-end voltage and then charged at constant voltage, so-called constant-current and constant-voltage charging (CCCV) mode.

0.2 C-rate until the terminal voltage reached 2.75 V to determine the nominal capacity of a battery designed. Because the nominal capacity designed is 600 mAh, 0.2, 1.0, or 2.0 C-rate corresponds to the current of 120, 600, or 1200 mA, respectively. Rate capability tests of the batteries are performed at 0.2, 1.0, and 2.0 C-rate after charging at 1.0 C-rate in the CCCV mode.

Cycle tests are continuously performed for 200 cycles. Charging condition is the same as that for rate capability tests and discharging condition is the constant-current discharge at 1.0 C-rate to 2.75 V.

3. 2. 4 Storage tests

In order to examine the increase in an internal resistance of the battery during storage at an elevated temperature, fully charged batteries were stored in a

temperature-controlled oven, Yamato Scientific Co. Ltd., Japan, at 60°C for 20 days, and the impedance of batteries before and after the storage was measured at 25°C by a 1-kHz impedance meter (Type 4263B, Hewlett-Packard Co. Ltd., USA).

3. 2. 5 Analysis on graphite-negative electrodes by X-ray photoelectron spectroscopy

After the 200-cycle tests of lithium-ion batteries, the batteries in a discharged state are disassembled in an argon-filled glove box. The negative electrode is cut into ca. 4 cm^2-piece and washed with a solvent of methyl ethyl carbonate twice. The negative-electrode piece is dried under vacuum for 15 h at room temperature. The sample taken from the negative electrode is placed on a sample folder in an argon atmosphere and transferred to a chamber for X-ray photoelectron spectroscopy (XPS) under an argon stream. XPS is also called electron spectroscopy for chemical analysis (ESCA). The samples are analyzed using ESCA Lab Mark 2 Surface Analysis System (VG Systems Co. Ltd., Germany; currently Thermo Fisher Scientific Inc., USA) with Mg-Kα radiation (1253.6 eV, 12 kV-10 mA). A C1s signal at 285 eV is used to compensate the charge-up effect. The other sets of experimental conditions are given in results and discussion section.

3. 3 Results and discussion

3. 3. 1 Performance of prototype 14500 batteries

Rate capability.--- Figure 3. 3 shows the discharge curves of two batteries examined at 0.2 C (120 mA), 1.0 C (600 mA), and 2.0 C (1200 mA) rate. The batteries are identical with each other except the electrolyte. One contains 1M $LiPF_6$ EC/MEC (1/2 by volume) and the other contains 1M $(C_2F_5SO_2)_2NLi$ in EC/MEC (1/2 by volume). In other words, lithium salts are different between two batteries, so that these batteries are abbreviated $LiPF_6$, $(C_2F_5SO_2)_2NLi$, or more generally lithium salt battery hereafter to distinguish the batteries. As clearly seen in Fig. 3. 3, the discharge capacity is observed to be 600 mAh for both $LiPF_6$ and $(C_2F_5SO_2)_2NLi$

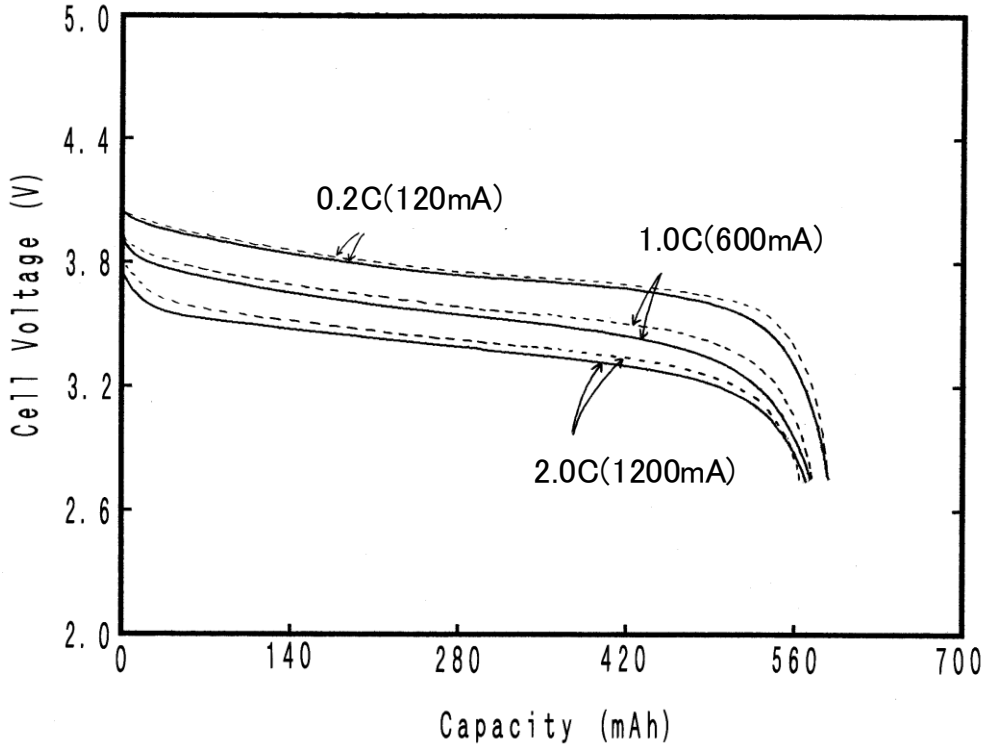

Figure 3. 3 Discharge curves of prototype14500 lithium-ion batteries consisting of $LiCoO_2$ and graphite. The electrolyte is 1.0 mol dm^{-3} $(C_2F_5SO_2)_2NLi$ (solid curves) or $LiPF_6$ (dashed) dissolved in EC/MEC (1/2 by volume). The batteries are charged in a constant-current (600 mA) constant-voltage (4.1 V) mode for 2.5 h and discharged at current ranging from 120 to 1200 mA until the terminal voltage reaches 2.75 V.

batteries examined at 0.2 C-rate, indicating that the 600 mAh 14500 batteries are properly designed and fabricated. However, the operating voltage of $(C_2F_5SO_2)_2NLi$-battery is slightly lower than that of $LiPF_6$-battery. When the discharge current is increased from 0.2 to 1 or 2 C rate, the difference in operating voltage between two batteries becomes apparent while the discharge capacity determined at 2.75 V is the same. Table 3. 1 summarizes the discharge capacity of these batteries at 0.2, 1.0, and 2.0 C rate. As clearly seen in Fig. 3. 3 combined with Table 3. 1, the discharge capacity observed at 0.2, 1.0 and 2.0 C rate is the same between two batteries. The difference is the operating voltage. An imide electrolyte of 1.0 M $(C_2F_5SO_2)_2NLi$ EC/MEC (1/2 by volume) shows the

Table 3. 1 Performance of prototype 14500 lithium-ion batteries consisting of $LiCoO_2$ and graphite. Electrolytes are 1.0 mol dm^{-3} lithium salts dissolved in EC/MEC (1/2 by volume). The batteries are charged in a constant-current (600 mA) constant-voltage (4.1 V) mode for 2.5 h and discharged at 120 - 1200 mA to 2.75 V.

	Capacity in mAh at 25℃		
	0.2C (120mA)	1.0C (600mA)	2.0C (1200mA)
$LiPF_6$	590 (100)	577 (97.8)	567 (96.1)
$(C_2F_5SO_2)_2NLi$	589 (100)	575 (97.6)	571 (96.9)
$(C_2F_5SO_2)_2NLi^*$	592 (100)	576 (97.2)	573 (96.8)
$(C_4F_9SO_2)(CF_3SO_2)NLi$	592 (100)	571 (96.4)	566 (95.6)
$((CF_3)_2CHSO_2)_2NLi$	599 (100)	580 (96.8)	573 (95.7)

* contains 0.05 mol dm^{-3} $LiPF_6$

conductivity of 6.5 mS cm^{-1} while that of 1.0 M $LiPF_6$ in the same mixed solvents shows 9.5 mS cm^{-1}, which correspond to 155 Ω cm for $(C_2F_5SO_2)_2NLi$ and 105 Ω cm for $LiPF_6$. Therefore, the difference in operating voltage between two batteries is derived from an ohmic drop due to the resistivity of the electrolyte.

Cycle performance.--- The cycle performance of the batteries with the imide electrolyte is evaluated. Figure 3. 4 shows the rechargeable capacity as a function of cycle number for four types of lithium-ion batteries examined at 1 C rate for 200 cycles. As seen in Figure 3. 4, $(C_2F_5SO_2)_2NLi$ battery containing 0.05 M $LiPF_6$ is better than a $LiPF_6$ battery in terms of capacity retention. Specifically, the $LiPF_6$ battery shows the discharge capacity of 492 mAh at 200th cycle while the first discharge capacity is 577 mAh, so that the capacity retention after 200 cycles is calculated to be 85%. Similarly, the capacity retention of $(C_2F_5SO_2)_2NLi$ battery after 200 cycles is calculated to be 87%, i.e., 509 mAh at 200th cycle versus 576 mAh at an initial cycle. The capacity of the $(C_2F_5SO_2)_2NLi$ battery after 200 cycles is 17 mAh larger than that of the $LiPF_6$ battery. The $(C_4F_9SO_2)(CF_3SO_2)NLi$ battery shows lower capacity than $(C_2F_5SO_2)_2NLi$-battery, when the batteries are examined at 1.0 C (600 mA) rate, as seen in Table 3. 1.

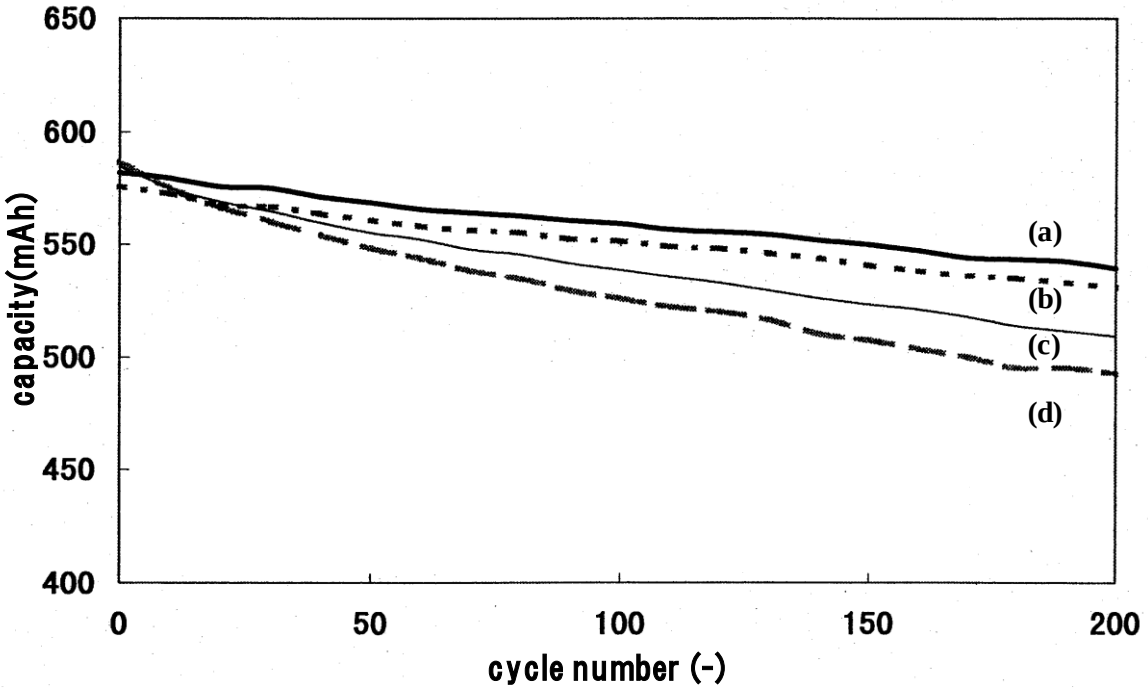

Figure 3. 4 Discharge capacities as a function of cycle number for the prototype 14500 lithium-ion batteries consisting of $LiCoO_2$ and graphite. The electrolyte is 1.0 mol dm^{-3} lithium salt dissolved in EC/MEC (1/2 by volume); (a) $((CF_3)_2CHOSO_2)_2NLi$, (b) $(C_4F_9SO_2)$ $(C_2F_5SO_2)NLi$, (c) $(C_2F_5SO_2)_2NLi$, or (d) $LiPF_6$. The batteries are charged in a constant-current (600 mA) constant-voltage (4.1 V) mode for 2.5 h and discharged at 600 mA to 2.75 V.

Capacity retention of the $(C_4F_9SO_2)(CF_3SO_2)NLi$ battery, however, is better than that of the $(C_2F_5SO_2)_2NLi$-battery. The $(C_4F_9SO_2)(CF_3SO_2)NLi$ battery shows the capacity of 531 mAh after 200 cycles, i.e., 92% capacity retention after 200 cycles. The capacity of $(C_4F_9SO_2)(CF_3SO_2)NLi$ battery after 200 cycles is 38 mAh larger than that of $LiPF_6$ battery, despite of lower capacity at an initial cycle. The $((CF_3)_2CHOSO_2)_2NLi$ battery shows the best cycle performance among four batteries examined, i.e., 93% capacity retention of 540 mAh after 200 cycles, which is 48 mAh larger capacity than that of $LiPF_6$ battery.

As has been described above, fluoro-organic lithium salts show better capacity retention than $LiPF_6$ currently used in lithium-ion batteries. The results are

summarized in a descending order of

$$((CF_3)_2CHOSO_2)_2NLi > (C_4F_9SO_2)(CF_3SO_2)NLi > (C_2F_5SO_2)_2NLi > LiPF_6 \quad (1),$$
$$93\% \qquad 92\% \qquad 87\% \qquad 84\%$$

in which a number in percents is the capacity retention calculated from the capacity at 200th cycle and that in an initial cycles. All batteries containing lithium imide salts show better cycle performance than $LiPF_6$-battery.

Increase in impedance during storage. --- The impedance increase of the batteries with imide is also measured to evaluate the battery stability at high temperature. The results are shown in Table 3. 2. The initial impedance of the battery with $(C_2F_5SO_2)_2NLi$ salts is 0.119-0.120 Ω. This value is a little higher than that of $LiPF_6$ because of conductivity difference. The impedance increase ratio of the imide battery after 20 days storage at 60°C is smaller than that of $LiPF_6$ battery because of the better stability of the imide [$(C_2F_5SO_2)_2NLi$: 13% (0.135 Ω), $LiPF_6$: 22% (0.141 Ω). The $(C_2F_5SO_2)_2NLi$ battery with 1.0 mol dm^{-3} imide and 0.05 mol dm^{-3} $LiPF_6$ shows only 9% (0.130 Ω) of impedance increase.

Table 3. 2 Change in impedance of prototype 14500 lithium-ion batteries consisting of $LiCoO_2$ and graphite during the storage at 60°C for 20 days. The electrolyte is 1.0 mol dm^{-3} $(C_2F_5SO_2)_2NLi$ or $LiPF_6$ dissolved in EC/MEC (1/2 by volume). Batteries were fully charged to 4.1 V and then stored.

Li Salt	Conductivity ($mS\ cm^{-1}$)	Cell Impedance (Ω; at 1 kHz)	
		Before Storage	After Storage
$LiPF_6$	9.5	0.116(100%)	0.141(+22%)
$(C_2F_5SO_2)_2NLi$	6.5	0.120(100%)	0.135(+13%)
$(C_2F_5SO_2)_2NLi$+0.05 mol dm^{-3} $LiPF_6$	6.6	0.119(100%)	0.130(+9%)

3. 3. 2 Factor affecting the capacity retention of lithium imide salt batteries

As has been described in a previous section, the property of lithium imide salt batteries is superior to $LiPF_6$ lithium-ion batteries in terms of capacity retention. The lithium-ion batteries consist of $LiCoO_2$-positive and graphite-negative electrodes. The operating voltage of a $LiCoO_2$-positive electrode ranges from 3.8 to 4.2 V with respect to a lithium electrode and that of a graphite-negative electrode is 0 to 0.3 V vs. Li/Li^+. The real situation of a 600-mAh 14500 battery is that the $LiCoO_2$-positive electrode and the graphite-negative electrode are separated by a diaphragm 25 μm thick with the electrolyte. The electrolyte is exposed to an oxidative condition at the $LiCoO_2$-positive electrode and also to a reductive condition at the graphite-negative electrode. The operating voltage of the graphite-negative electrode is very close to a lithium metal electrode, so that any chemical species is potentially reduced at that voltage. For example, hydrogen gas is known as a reductive gas in chemistry. However, when H_2 is contacted to lithium or lithium-graphite intercalation compounds, H_2 is electrochemically reduced to LiH, i.e.,

$H_2 + 2e^- \rightarrow 2H^-$ (2) and $2Li \rightarrow 2Li^+ + 2e^-$ (3),

giving an overall reaction of $2Li + H_2 \rightarrow 2LiH$ [1]. Lithium is the strongest reducing agent among chemical species, so that any electrolyte potentially or thermodynamically reacts with lithium or lithium-graphite intercalation compounds. However, the real reactivity of lithium or lithium-graphite intercalation electrode is determined by the reaction products formed at an electrode/electrolyte interface. If the reaction product of LiH does not dissolve in an electrolyte, a passive film of LiH protects the corrosion because LiH is the electric insulator of an ionic crystal, and if LiH is a lithium-ion conductor, a lithium metal covered with a LiH-passive layer does not react with H_2 or other chemical species anymore while the function of a lithium metal of storing and producing electrons and lithium ions does not damage. Such an ideal interface to protect corrosion and consequently an active material is called solid electrolyte interface (SEI), which is an important concept in considering

lithium and lithium-ion batteries.

The graphite-negative electrode/electrolyte interface in $LiPF_6$ lithium-ion batteries is discussed in terms of the formation of SEI by Aurbach et al. [2-4], Yoshida et al. [5], Honbou et al.[6], Naoi et al.[7], and so forth. Although the reaction mechanisms are still debatable subjects among researchers, there seem to be general agreements that the electrolytes react with lithium and lithium-graphite intercalation compounds.

Ethylene carbonate (EC) is a main solvent used in current lithium-ion batteries. EC is electrochemically reduced on the graphite-negative electrode producing solid products and a gas of ethane, i.e.,

$$2\ EC + 2e^- + 2\ Li^+ \rightarrow (-CH_2OCO_2Li)_2 + C_2H_4 \uparrow \qquad (4)$$ and

$$EC + 2e^- + 2Li^+ \rightarrow Li_2CO_3 + C_2H_4 \uparrow \qquad (5).$$

Because EC is a viscous liquid above room temperature or a solid below room temperature, dimethyl carbonate (DMC) or diethyl carbonate (DEC) is used to reduce viscosity and consequently increase conductivity. DMC and DEC are also electrochemically reduced on the negative electrode, i.e.,

$$DMC + e^- + Li^+ \rightarrow CH_3OCO_2Li + CH_3\bullet \qquad (6),$$

in which $CH_3\bullet$ will generate CH_4 by picking up H or combine each other producing C_2H_6, and

$$DMC + e^- + Li^+ \rightarrow CH_3OLi + CH_3CO_2\bullet \qquad (7),$$

in which $CH_3CO_2\bullet$ will generate CH_3CO_2H or CH_3CO_2Li.

Similarly, DEC is electrochemically reduced in a fashion;

$$DEC + e^- + Li^+ \rightarrow CH_3CH_2OCO_2Li + CH_3CH_2\bullet \qquad (8),$$

in which $CH_3CH_2\bullet$ will generate C_2H_6 by picking up H, and

$$DEC + e^- + Li^+ \rightarrow CH_3CH_2OLi + CH_3CH_2CO_2\bullet \qquad (9),$$

in which $CH_3CH_2CO_2\bullet$ will generate $CH_3CH_2CO_2H$ or $CH_3CH_2CO_2Li$.

Lithium hexafluorophosphate ($LiPF_6$) commonly used in lithium-ion batteries is also electrochemically reduced on the graphite-negative electrode and chemically decomposed with H_2O producing HF in a complicated manner. The decomposition reactions of $LiPF_6$ and related compounds, such as POF_3, have been reported by Momota [8], i.e.,

$$LiPF_6 + n\ e^- + n\ Li^+ \rightarrow LiF + PF_5 \qquad (10).$$

PF_5 is highly reactive, so that PF_5 reacts with H_2O producing POF_3 and HF, i.e.,

$$PF_5 + H_2O \rightarrow POF_3 + 2HF \qquad (11),$$

$$POF_3 + H_2O \rightarrow H[OPOF_2] + HF \qquad (12),$$

$$H[OPOF_2] + H_2O \rightarrow H_2[O_2POF] + HF \qquad (13), \text{ and}$$

$$H_2[O_2POF] + H_2O \rightarrow H_3[PO_4] + HF \qquad (14).$$

These acids further react with basic lithium salts, such as LiOH, Li_2CO_3, etc., to form LiF, Li_3PO_4, Li_2PFO_3, and $LiPF_2O_2$. Among these intermediate compounds, POF_3 is electrochemically reactive, i.e.,

$$POF_3 + 2x\ Li^+ (Li\ salts) + 2x\ e^- \rightarrow Li_xPOF_{3-x} + x\ LiF \quad (15).$$

Hydrogen fluoride in eqs. (11) to (14) is a strong acid, which catalyzes the decomposition of esters, such as EC, DMC, and DEC, and decomposes some of positive-electrode materials, such as $LiMn_2O_4$, $LiNiO_2$, $LiCoO_2$, or more generally $LiCo_xNi_{1-x}O_2$, producing Mn^{2+}, Co^{2+}, or Ni^{2+} in an electrolyte through a disproportionation reaction of Mn^{3+}, Ni^{3+}, or Co^{3+}. In addition to such reactions, HF reacts with lithium salts, i.e.,

$$HF + ROCO_2Li \rightarrow LiF + ROCO_2H \quad (16),$$

$$2HF + Li_2CO_3 \rightarrow 2LiF + H_2CO_3\ (or\ 2LiF + CO_2 + H_2O) \quad (17),$$

$$2HF + Li_2O \rightarrow 2LiF + H_2O \quad (18),\ and$$

$$2HF + LiOH \rightarrow 2LiF + H_2O \quad (19).$$

Water molecules are initially contaminated in spite of careful dehydration of every component used in lithium-ion batteries, which are consumed by reactions (11) to (14) producing HF and also by the reactions of

$$2\ ROCO_2Li + H_2O \rightarrow Li_2CO_3 + 2\ ROH + CO_2\uparrow \quad (20)$$

$$and\ 2\ H_2O + 2\ Li^+ + 2e^- \rightarrow 2\ LiOH + H_2\uparrow\ (or\ 2\ Li_2O + 2\ H_2\uparrow) \quad (21).$$

The other reactions seem to involve are

$$Li_2CO_3 \rightarrow Li_2O + CO_2 \uparrow \quad (22)$$

$$\text{and } 2LiOH \rightarrow Li_2O + H_2 \uparrow \quad (23).$$

Among chemical species in a solid state, $(-CH_2OCO_2Li)_2$, CH_3OCO_2Li, $CH_3CH_2OCO_2Li$, CH_3OLi, CH_3CH_2OLi, Li_2CO_3, LiOH, Li_2O, LiF, (POF_3,) $LiPF_2O_2$, and Li_3PO_4 are identified. However, which chemical species is responsible for SEI is not known at present.

As have been described above, the reactions associated with $LiPF_6$ lithium-ion batteries are so complicated to give a rational explanation on the reaction mechanism of a graphite-negative electrode and to properly describe the cell chemistries inside $LiPF_6$ lithium-ion batteries. It should be noted here that reactions from (10) to (15) producing the acids are characteristic of a $LiPF_6$-based electrolyte, which are not involved in an imide salt electrolyte. According to the results described in a previous section, all batteries containing lithium imide salts show better cycle performance than $LiPF_6$-battery. This may be due to the formation of SEI derived from the reduction products of lithium imide salts. In order to examine whether or not this is true, XPS examinations on the graphite-negative electrodes after 200 cycles in lithium imide batteries are carried out.

3. 3. 3 XPS examinations on the graphite-negative electrodes

Table 3. 3 shows analytical results on the surface of graphite-negative electrode. The atomic percent (at%) of carbon, fluorine, lithium, sulfur, nitrogen, and oxygen on the surface analyzed by XPS are given. Of these, nitrogen and sulfur are derived from the imide salt, so that the imide salt on the surface is calculated based on the atomic percent of nitrogen in Table 3. 3 and summarized in Table 3. 4. For $(C_2F_5SO_2)_2NLi$, for example, 2.1 at% of nitrogen is listed in Table 3. 3, which is derived from $(C_2F_5SO_2)_2NLi$, meaning that other components should be 4.2 at% sulfur, 8.4 at% oxygen, 2.1 at% lithium, 21 at% fluorine, and 8.4 at% carbon. The estimated value of 4.2 at% sulfur roughly agrees with the observed

Table 3. 3 The atomic percent on the graphite surface analyzed by XPS after the cycle tests of prototype 14500 lithium-ion batteries consisting of $LiCoO_2$ and graphite.

Salt used in the battery	C	F	Li	S	N	O
$LiPF_6$	33.0	19.6	10.7	0.0	0.0	32.6
$(C_2F_5SO_2)_2NLi$	33.1	27.7	9.2	5.2	2.1	22.4
$(C_4F_9SO_2)(CF_3SO_2)NLi$	28.8	32.8	10.9	3.2	1.5	20.7
$((CF_3)_2CHSO_2)_2NLi$	26.5	32.8	7.3	6.5	2.4	24.3

Table 3. 4 The atomic percent calculated by assuming that nitrogen atoms in Table 3. 3 is derived from the corresponding imide salt.

Salt used in the battery	C	F	Li	S	N	O	Total
$(C_2F_5SO_2)_2NLi$	8.4	21.0	2.1	4.2	2.1	8.4	46.2
$(C_4F_9SO_2)(CF_3SO_2)NLi$	15.0	18.0	1.5	3.0	1.5	6.0	45.0
$((CF_3)_2CHOSO_2)_2NLi$	14.4	28.8	2.4	4.8	2.4	14.4	67.2

value 5.2 at% in Table 3. 3. This suggests that 46.2 at% in Table 3. 3 is derived from $(C_2F_5SO_2)_2NLi$. Other imide salts are also examined and summarized in Table 3. 4. Graphite-negative electrode surface is covered by corresponding imide salt or its relatives in atomic percent ranging from 45 to 67 at%.

According to the cycle tests described in section 3. 3. 1, lithium-ion batteries having an imide electrolyte show superior properties to that having $LiPF_6$. This may be explained in terms of “solid electrolyte interface”. The surface layer derived from imide salts may suppress the electrolyte decomposition on the graphite-negative electrode. Figure 3. 5 shows the surface layer models for the graphite-negative electrode cycled in $LiPF_6$. $LiPF_6$ and its related compounds cover only 30 at% on the graphite-negative electrode surface from the calculation based on 3.8 at% phosphorous (not shown in the table). The imide salts and its related compounds cover 45-67 at% on the surface from the calculation based on 1.5-2.4 at% nitrogen in Table 3. 3 as have been discussed above. An imide anion reacts with a graphite-negative electrode to form LiF on the surface as shown in Figure 3. 5. Figure 3. 6 shows the initial surface layer models on the graphite-

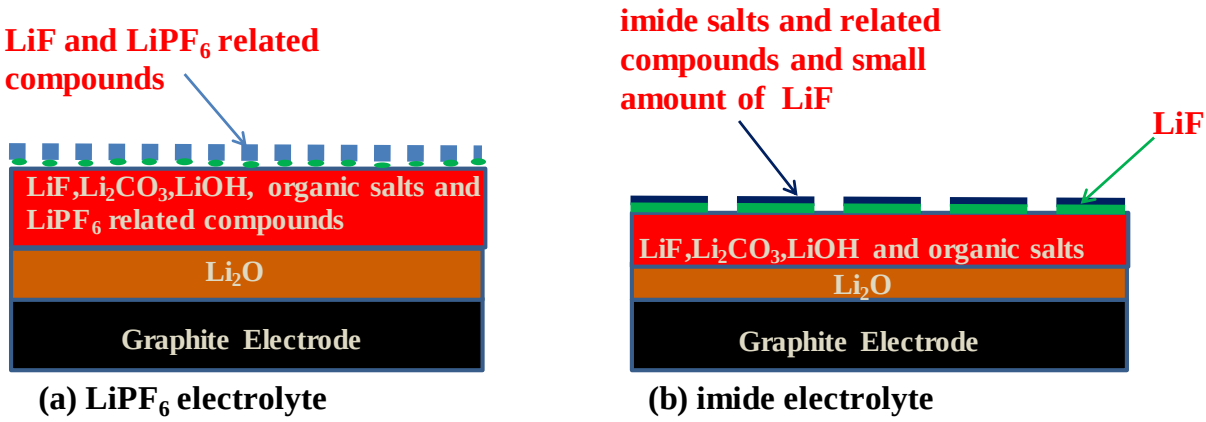

Figure 3. 5 Surface layer models on the graphite-negative electrodes cycled in (a) $LiPF_6$ and (b) imide salt to explain cycle performance in Fig. 3. 4 combined with XPS results. An imide anion reacts with negative electrode to form LiF and some other products derived from an imide salt.

negative electrode in a (a) $LiPF_6$ and (b) imide electrolyte in order to explain the XPS analysis, cycle performance, and reported reaction of $LiPF_6$. The imide electrolyte forms LiF under imide anion as shown in Figure 3. 6. Lithium fluoride is formed by the reaction of imide and graphite-negative electrode. The $LiPF_6$ electrolyte forms LiF by reactions (3) to (7) in smaller coverage of $LiPF_6$ or its related compounds than that of imide or its related compounds. For $LiPF_6$ electrolyte, the decomposition products come from reactions (8) − (12). The decomposition product of HF forms LiF with lithium salts such as Li_2CO_3 and LiOH. In this case, lithium fluorite is porous, because molar equivalent density of LiF (Formula weight; 25.9 g mol^{-1}, density: 2.64 g cm^{-3}) and Li_2CO_3 (Formula weight 73.8 g mol^{-1}, density: 2.11 g cm^{-3}) are 0.102 and 0.057 mol cm^{-3}, respectively, i.e., 0.102 = 2.64 / 25.9 and 0.057 = 2.11 / 73.8 × 2. An amount of 0.057 mol cm^{-3} Li_2CO_3 forms 0.057 mol cm^{-3} of LiF. When Li_2CO_3 is converted to LiF forming "the solid electrolyte" without volume change, a SEI of Li_2CO_3 component forms 0.057 mol cm^{-3} of LiF, indicating that the porosity of LiF layer is 45%, because the nonporous LiF is 0.102 mol cm^{-3}. A porous LiF layer is not effective "solid electrolyte interface" to protect a reaction of the electrolyte on the graphite-negative electrode.

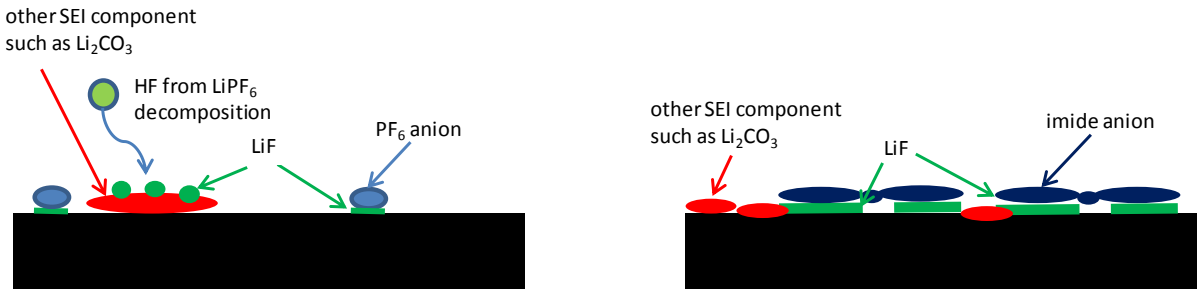

(a) $LiPF_6$ electrolyte **(b) imide electrolyte**

Figure 3. 6 Initial surface layer models grown on the graphite-negative electrode in (a) $LiPF_6$ and (b) imide.

This is more clear for $((CF_3)_2CHOSO_2)_2NLi$-battery. As seen in Table 3. 4, 28.8 at% F are detected as the imide salts or its relatives on the surface, which is almost the same as that observed 32.8 at% F in Table 3. 3. Total amount of imide-ester $((CF_3)_2CHOSO_2)_2NLi$ is calculated to be 67 at% as seen in Table 3. 4, while that for $LiPF_6$ is only 30 at%. The same arguments have been done by Naoi et al. [7]. They show the model on the surface of lithium that is covered with the adsorption layer of anion for the $(C_2F_5SO_2)_2NLi$ electrolyte. Ghimbeu et al. [9] have examined several types of graphite electrode material in the LiTFSI electrolyte, in which the decomposition products (LiF,-SOx) on the graphite-negative electrode are detected by XPS.

In order to examine why the imide electrolyte affects cycle performance, detailed examinations are carried out by XPS. Table 3. 5 shows the detailed analytical results on F1s XPS signals. When the imide salts are used in batteries, the graphite-negative electrode surface is mainly covered with organic fluorine compounds derived from imide salts, i.e., 25-32 at% identified by the signals at 687-688 eV. Conversely, when $LiPF_6$ is used in batteries, the surface is mainly covered with the $LiPF_6$-related compounds excluding LiF, i.e., 14.0 at% identified at 686 eV and fluoro-organic compounds including PVdF, i.e., 5.6 at% identified at 687-688 eV. Lithium fluorite is formed from $LiPF_6$ by equations (7) – (12). Lithium fluorite is also formed from imide salts, because the amount of LiF determined from the signals at 685 eV is almost the same as that from $LiPF_6$.

Table 3. 5 The detailed fluorine atomic percent on the graphite electrode surface by F1s XPS peak analysis. Total atomic percent of fluorine is the same as that in Table 3. 2.

Salt used in the battery	685 eV (LiF)	686 eV ($LiPF_6$ and related)	687-688 eV (imide salt and related or PVDF)	Total
$LiPF_6$	1.3	12.7	5.6	19.6
$(C_2F_5SO_2)_2NLi$	1.2	1.0	25.5	27.7
$(C_4F_9SO_2)(CF_3SO_2)NLi$	1.3	0.0	31.5	32.8
$((CF_3)_2CHOSO_2)_2NLi$	0.9	0.0	31.9	32.8

*Graphite negative electrode after cycle test.

Naoi et al. [7] also recognize LiF under the adsorbed or imide salts layer on a lithium electrode for a $(C_2F_5SO_2)_2NLi$ PC electrolyte. Yamaki et al. [10] report the SEI growth on the graphite-negative electrode from 0.03 up to 0.5 μm during storage at 40°C. Yamachi et al. [11] also report the XPS results after cycle tests, in which they state that the SEI growth during charge discharge is accelerated by the change in volume of the graphite-negative electrode. Nie et al. [12] have examined the SEI formation in six different types of lithium salts in ethylene carbonate (EC). They report the surface film is smooth and uniform for the electrodes cycled in $LiPF_6$, LiBOB, LiTFSI, and LiFSI electrolytes, while the film is grainy for $LiBF_4$ and LiDFOB because of high amount of LiF in the film. Peres et al. [13] have reported that the amount of inorganic species (phosphates / fluorophosphates) increases, whereas carbonate species disappear for cycling at 85°C compared to 60°C, and the positive-electrode interface layer is much thinner than the SEI formed at the negative electrode side. Andersson et al. [14] have reported the SEI derived from $LiPF_6$ electrolyte includes LiF particle on the graphite-negative electrode. Lithium fluoride is formed not only directly from $LiPF_6$ but also HF in the electrolyte for $LiPF_6$ electrolyte. For the imide electrolytes, LiF is formed by the reaction between the graphite-negative electrode and imide anions.

As have been discussed above, it is suggested that inorganic or stable organic SEI layer, maybe high-density compounds with low solvent diffusion, is effective to protect the negative electrode from the electrolyte attack. Ideally, a SEI layer is

durable for the volume change of graphite-negative electrodes with low resistance. The imide salts described here seem to be provided continuous and high-density LiF protective layers on the graphite-negative electrode than $LiPF_6$.

3. 4 Summary

In this chapter, the lithium imide salts of $(C_2F_5SO_2)_2NLi$, $(CF_3)_2CHOSO_2)_2NLi$ and $(C_4F_9SO_2)(CF_3SO_2)NLi$ have been examined in prototype 14500 lithium-ion batteries consisting of the $LiCoO_2$-positive and graphite-negative electrodes. The results have been compared with $LiPF_6$ batteries. Although the internal resistance is slightly higher than that of $LiPF_6$ battery, cycle performance of these batteries are superior to $LiPF_6$ batteries. Among these batteries, $((CF_3)_2CHOSO_2)_2NLi$ battery shows the best performance in terms of capacity retention and a possible mechanism is discussed in terms of the formation of an effective solid electrolyte interface.

References

[1] M. Pourbaix, Atlas of Electrochemical Equilibria in Aqueous Solutions, Pergamon Press, New York, 1966.

[2] D. Aurbach, A. Zaban, Y. Ein-Eli, I. Weissman, O. Chusid, B. Markovsky, M. Levi, E. Levi, A. Schechter, and E. Granot, *J. Power Sources,* **68**, 91 (1997).

[3] D. Aurbach, Y. Ein-Eli, B. Markovsky, A. Zaban, S. Luski, Y. Carmeli, and H. Yamin, *J. Electrochem. Soc*., **142**, 2882 (1995).

[4] D. Aurbach, B. Markovsky, I. Weissman, E. Levi, and Y. Ein-Eli, *Electrochim. Acta,* **45,** 67 (1999).

[5] H. Yoshida, T. Fukunaga, T. Hazama, M. Terasaki, M. Mizutani, M. Yamachi, *J. Power Sources*, **68**, 311 (1997).

[6] H. Honbou, Y. Muranaka, and F. Kita, *Denki Kagaku (currentry Electrochemistry, Tokyo, Japan)*, **69**, 686 (2001).

[7] K. Naoi, M. Mori, Y. Naruoka, W. M. Lamanna, and R. Atanasoski, *J. Electrochem. Soc*., **146**, 462 (1999).

[8] K. Momota, *Denchi Gijyutsu* (*Battery Technology*), **8,** 108 (1996).

[9] C. M. Ghimbeu, C. Decaux, P. Brender, M. Dahbi, D. Lemordant, E. R. Pinero, M. Anouti, F Beguin, and C. V. Guterl, *J. Electrochem. Soc*., **160**, A1907 (2013).

[10] T. Yoshida, M. Takahashi, S. Morikawa, C. Ihara, H. Katsukawa, T. Shiratsuchi, and J. Yamaki, *J. Electrochem. Soc*., **153**, A576 (2006).

[11] T. Wada T. Aoki, T. Sasaki, H. Wada, T. Murata, and M. Yamachi, GS Technical Report, **63**, 18 (2004).

[12] M. Nie and B. L. Lucht, *J. Electrochem. Soc*., **161,** A1001 (2014).

[13] L. Bodenes, R. Dedryvere, H. Martinez, F. Fischer, C. Tessier, and J. Peres, *J. Electrochem. Soc*., **159,** A1739 (2012).

[14] A. M. Andersson and K. Edstrom, *J. Electrochem. Soc*., **148**, A1100 (2001).

Chapter 4

Fluoro-Organic Lithium Salts Based on $LiPF_6$

4. 1 Introduction

As have been described in previous chapters, computational methods have been successfully introduced to explore fluoro-organic lithium salts for lithium-ion batteries. Some of them are examined in prototype lithium-ion batteries consisting of $LiCoO_2$-positive and graphite-negative electrodes and shown that the imide salts, especially $((CF_3)_2CHOSO_2)_2NLi$, show better battery performance than $LiPF_6$.

$LiPF_6$ is widely used in an electrolyte solution for a lithium-ion battery because of high solubility and conductivity. However, $LiPF_6$ dissolved in a polar aprotic solvent is difficult to handle even in a laboratory, because $LiPF_6$ is easily decomposed generating HF in a solution even when a trace of water is contaminated in a solution. Generated HF behaves like a catalyst, reactant, and free acid, as has been discussed in Chapter 3. Therefore, $LiPF_6$ is carefully handled in a dry atmosphere and all parts including a separator are dehydrated as thoroughly as possible. PF_6^- anion itself is thermally stable in aqueous solutions [1-4] and in quaternary ammonium salts; $(C_2H_5)_3(CH_3)NPF_6$ (Et_3MeNPF_6) and $(C_4H_9)_4NPF_6$ (Bu_4NPF_6). $NaPF_6$ and KPF_6 are also stable in nonaqueous electrolytes. This suggests that the modification of $LiPF_6$ is possible to stabilize PF_6^- anion in polar aprotic solvents even when water contaminates. Because lithium ions are necessary for lithium-ion batteries, a method to modify PF_6^- is intuitively limited to an introduction of P-CF_3 or P-C_2F_5 bonds substituting for P-F bonds in PF_6^-, giving specifically $PF_{6-n}(CF_3)_n^-$ and $PF_{6-n}(C_2F_5)_n^-$.

In this chapter, new fluoro-organic lithium salts of $PF_{6-n}(CF_3)_n^-$ and $PF_{6-n}(C_2F_5)_n^-$ are examined by the computational methods and described in terms of thermal and chemical stability together with dissociation associated with

conductivity. Among fluoro-organic lithium salts based on $LiPF_6$, $LiPF_4(CF_3)_2$ is examined in prototype lithium-ion batteries and shown to be superior to $LiPF_6$.

4. 2 Backgrounds on computational methods

As have been described in previous chapters, computational methods have been advanced in a quite high level during the past 20 years [5]. However, computational errors have been still a debatable subject in theoretical chemistry, especially in calculating bond energies of chemical species by semi-empirical methods, classical Hartree-Fock or recent Gaussian methods. In order to minimize computational errors mainly due to the electron correlation effect, several methods have been proposed in computational chemistry, e.g., *isogyric* and *isodesmic* reactions. Both are not listed in general chemistry. An *isodesmic* reaction is a convenient way to calculate thermochemical properties of a chemical reaction under consideration relative to a reference chemical species. Sastre et al. have reported the pKa calculations of common organic molecules by the isodesmic reaction [6]. A reference chemical species selected in this chapter is $LiPF_6$ and a target chemical species is $LiF_{6-n}(CF_3)_n$ or $LiPF_{6-n}(C_2F_5)_n$.

$LiPF_6$ is supposed to be decomposed to PF_5 and LiF, i.e.,

$$LiPF_6 \rightarrow PF_5 + LiF \qquad (1),$$

and similarly $LiF_{6-n}(CF_3)_n$ to $PF_{5-n}(CF_3)_n$ and LiF, i.e,

$$LiPF_{6-n}(CF_3)_n \rightarrow PF_{5-n}(CF_3)_n + LiF \qquad (2).$$

When one would like to know which lithium salt, $LiPF_6$ or $LiPF_{6-n}(CF_3)_n$, is thermochemically stable, subtracting eq. (2) from eq. (1) gives the following new reaction;

$$LiPF_6 + PF_{5-n}(CF_3)_n + LiF \rightarrow PF_5 + LiF + LiPF_{6-n}(CF_3)_n \qquad (3).$$

In eq. (3), there are (11 – n) P-F single bonds and n P-C single bonds on the left side. On the right side, there are the same number of P-F and P-C bonds as on both sides. A compound of LiF involves in both sides, so that it cancels out calculating the properties for reaction (3). Equation (3) is called *an isodesmic reaction*, in which the number and types of chemical bonds are conserved on both sides of the reaction.

The electronic energies of all species in eq. (3) can be calculated by the computational methods. By applying Gaussian B3LYP/6-31G* calculations, energies at 298 K can be calculated and thermal corrections to energy, enthalpy, and Gibbs free energy are also provided. Therefore, the thermal stability of $LiPF_{6-n}(CF_3)_n$ can be discussed with respect to $LiPF_6$ using *isodesmic reaction* (3) under a framework of chemical thermodynamics. When E and H denote internal energy and enthalpy, all chemical species in eq. (3) can be calculated at any temperature. ΔE and ΔH for reaction (3) are calculated in a usual manner. Specifically, equation (4) is re-written as

$$\underset{E(LiPF_6)}{LiPF_6} + \underset{E(PF_{5-n}(CF_3)_n)}{PF_{5-n}(CF_3)_n} \rightarrow \underset{E(PF_5)}{PF_5} + \underset{E(LiPF_{6-n}(CF_3)_n)}{LiPF_{6-n}(CF_3)_n} \quad (4),$$

where E(X) is a calculated total energy of compound X (X= $LiPF_6$, $PF_{5-n}(CF_3)_n$, PF_5, and $LiPF_{6-n}(CF_3)_n$).

$$\Delta E = E(PF_5) + E(LiPF_{6-n}(CF_3)_n) - E(LiPF_6) - E(PF_{5-n}(CF_3)_n) \quad (5)$$

After thermal correction, the reaction enthalpy ΔH for eq. (3) is calculated from

$$\Delta H = H(PF_5) + H(LiPF_{6-n}(CF_3)_n) - H(LiPF_6) - H(PF_{5-n}(CF_3)_n) \quad (6).$$

When the calculated enthalpy ΔH is negative, reaction (3) is exothermic, which suggests that $LiPF_{6-n}(CF_3)_n$ on the product side is more stable than $LiPF_6$ on the reactant side. Thus, the stability of $LiPF_{6-n}(CF_3)_n$ or $LiPF_{6-n}(C_2F_5)_n$ relative to $LiPF_6$ is evaluated using an *isodesmic reaction* (3) by computational methods.

The ionic conductivity of an electrolyte solution is very difficult to predict by computational methods. It depends on a kind of lithium salts and solvents, solubility, and the degree of dissociation. Although there seems to be impossible to give basic line on estimating the conductivity of a lithium salt in a polar aprotic solvent, the isodesmic reaction may help predict which gives higher conductivity in the same aprotic solvent, $LiPF_6$ or $LiPF_{6-n}(CF_3)_n$.

$LiPF_6$ is supposed to dissociate into Li^+ and PF_6^- in a solvent, i.e.,

$$LiPF_6 \rightarrow Li^+ + PF_6^- \qquad (7),$$

and similarly $LiPF_{6-n}(CF_3)_n$ is supposed to dissociate in the same solvent, i.e,

$$LiPF_{6-n}(CF_3)_n \rightarrow Li^+ + PF_{6-n}(CF_3)_n^- \qquad (8).$$

Subtracting eq. (8) from eq. (7) gives the *isodesmic reaction* of

$$\underset{E(PF_6^-)}{PF_6^-} + \underset{E(LiPF_{6-n}(CF_3)_n)}{LiPF_{6-n}(CF_3)_n} \rightarrow \underset{E(LiPF_6)}{LiPF_6} + \underset{E(PF_{6-n}(CF_3)_n^-)}{PF_{6-n}(CF_3)_n^-} \qquad (9).$$

$$\Delta E = E(LiPF_6) + E(PF_{6-n}(CF_3)_n^-) - E(PF_6^-) - E(LiPF_{6-n}(CF_3)_n) \qquad (10)$$

After thermal correction, the reaction enthalpy ΔH for eq. (9) is calculated from

$$\Delta H = H(LiPF_6) + H(PF_{6-n}(CF_3)_n^-) - H(PF_6^-) - H(PF_{6-n}(CF_3)_n) \qquad (11).$$

When the calculated enthalpy ΔH is negative, the reaction (9) is exothermic, which suggests that $LiPF_{6-n}(CF_3)_n$ on the reactant side is more dissociative than $LiPF_6$ on the product side. More properly, when the thermal correction to Gibbs free energy is possible for each species, the Gibbs free energy change ΔG for eq. (9) is given as

$$\Delta G = G(LiPF_6) + G(PF_{6-n}(CF_3)_n^-) - G(PF_6^-) - G(PF_{6-n}(CF_3)_n) \qquad (12).$$

When the calculated Gibbs free energy change is negative, $LiPF_{6-n}(CF_3)_n$ is better than $LiPF_6$ in terms of ionic dissociation. Thus, the dissociation of $LiPF_{6-n}(CF_3)_n$ or $LiPF_{6-n}(C_2F_5)_n$ relative to $LiPF_6$ is evaluated using the *isodesmic reaction* (9) by the computational methods. The above treatment on the dissociation of a fluoro organic lithium salt is oversimplified, but it is sufficient to give a basic guideline for designing materials research on fluoro organic lithium salts for lithium-ion batteries.

4. 3 Experimental

4. 3. 1 Electrolytes and electrode materials

$LiPF_{6-n}(CF_3)_n$ salts (n = 1, 2, and 3) are obtained from Institute of Organic Chemistry, Ukrainian Academy of Science, Kiev, Ukraine. Yagupolskii et al. report the synthesis of related compound $(C_3F_7)_3PF_2$ and $(C_3F_7)_3PF_3^-K^+$ [7]. Of these, $LiPF_3(CF_3)_3$ contains 1,2-dimethoxyethane (DME) as $LiPF_3(CF_3)_3 \cdot 3DME$. $LiPF_6$ is obtained from STELLA CHEMIFA Corp. Ltd., Japan. Battery grade ethylene carbonate (EC) and methyl ethyl carbonate (MEC) are obtained from Ube Industries, Co. Ltd., Japan. EC and MEC are mixed in the volume ratio of 1 to 2 in an argon-filled glove box. The concentration of each lithium salt is 0.1 mol dm^{-3} in the mixed solvents. The positive and negative electrode materials are the same as described in section 3. 2. 2.

4. 3. 2 Prototype batteries

The prototype 14500 batteries fabricated are the same as used in section 3. 3. 2 except the electrolyte. The 600 mAh batteries are designed, fabricated, and examined in voltage ranging from 2.5 to 4.2 V. The lithium salts examined are $LiPF_6$ and $LiPF_{6-n}(CF_3)_n$ (n = 1, 2, and 3). Testing procedures are the same as described in section 3. 2. 3. The batteries are charged at 60 mA until terminal voltage reaches 4.2 V and then kept at 4.2 V at room temperature totally for 12 h on charge, so-called a CC(60 mA)CV(4.2 V)-charging mode, and the batteries are discharged at 60 mA to 2.75 V. The charge and discharge are repeated for 180

cycles.

4. 3. 3 Storage tests

In order to examine the thermal stability of 0.1 mol dm^{-3} $LiPF_6$ and $LiPF_4(CF_3)_2$ EC/DME (1/2 by volume), both electrolytes are stored at room temperature for 3 years. Each electrolyte is tightly sealed in a 10-ml glass vial by a Teflon-coated rubber plug and stored in an argon-filled dry box for three years at room temperature. After a 3-year storage both electrolytes are visually inspected, such as change in color and the degree of transparency.

Fully charged 14500 batteries are also stored at 60℃ for 20 days in a temperature-controlled oven, and battery impedance at 1 kHz was measured by an impedance meter type 4263B (Hewlett-Packard Co. Ltd., USA).

4. 3. 4 X-Ray photoelectron spectroscopy (XPS)

Measurements and analytical procedures are the same as described in section 3. 2. 5. The other sets of experimental conditions are given in results and discussion section.

4. 4 Results and discussion

4. 4. 1 Thermal stability of $PF_{6-n}(CF_3)_n$ anions

As have been discussed in section 4. 2, the thermal stability of $PF_{6-n}(CF_3)_n^-$ (n = 1, 2, and 3) anions can be examined using an isodesmic reaction (3) by the computational methods. Table 4. 1 summarizes ΔH values calculated from eq. (6). Because all the values for $PF_{6-n}(CF_3)_n^-$ (n = 1, 2, and 3) anions are negative, these anions are more stable than PF_6^- anion;

$\Delta H\ (PF_4(CF_3)_2^-)$; –7.3 > $\Delta H\ (PF_5(CF_3)^-)$; –4.4 > $\Delta H(PF_3(CF_3)_3^-)$; –4.1 > $\Delta H(PF_6^-)$; 0 kcal mol^{-1}

Table 4. 1 Energies calculated for isodesmic reactions together with HOMO energy for $PF_{6-n}(CF_3)_n$ anions calculated by B3LYP/6-31G*. ΔH, ΔG, and HOMO energies relate to the thermal stability, ability to dissociate, and capability in resisting oxidation, respectively.

Li Salt	Energy (kcal mol^{-1})		HOMO Energy
	ΔH	ΔG	of Anion (eV)
$LiPF_6$	0.0	0.0	-4.26
$LiPF_5(CF_3)$	-4.4	-0.5	-3.99
$LiPF_4(CF_3)_2$	-7.3(trans)	-2.1	-4.30
$LiPF_3(CF_3)_3$	-4.1(mer)	-8.6	-3.72

These results imply that $PF_4(CF_3)_2^-$ anion is the most stable species among $PF_{6-n}(CF_3)_n^-$ (n=1, 2, and 3) anions. In order to understand why $PF_4(CF_3)_2^-$ anion is the most stable, an anionic size and conformation of each anion is calculated by DFT method with B3LYP/6-31G* and shown in Figs. 4. 1 and 4. 2. $LiPF_6$ is also shown in both figures for comparison. As clearly seen in Figs. 4. 1 and 4. 2, when P-CF_3 single bond is substituted for P-F bond in the PF_6^- anion, the bond distance of P-F single bond in PF_6^- increases from 1.637 Å to 1.919 Å for a P-CF_3 single bond in $PF_5CF_3^-$, 1.890 Å in $PF_4(CF_3)_2^-$, and 1.939 Å in $PF_3(CF_3)_3^-$. Consequently, the volume of an anion increases from 93 $Å^3$ for PF_6^- anion to 127 $Å^3$ for $PF_5CF_3^-$, 160 $Å^3$ for $PF_4(CF_3)_2^-$, and 193 $Å^3$ for $PF_3(CF_3)_3^-$. In calculating the volume of each anion, the volume inside the boundary face at which an electron density is more than 0.001 electron/$bohr^3$ is calculated by DFT method with B3LYP/6-31G*. Thermal stability of $PF_{6-n}(CF_3)_n^-$ (n=1, 2, and 3) anions compared with PF_6^- anion may be understood in terms of size effect. However, the thermal stability of $PF_4(CF_3)_2^-$ anion cannot be explained in terms of size effect. It may be derived from the symmetry of anionic species. $PF_4(CF_3)_2^-$ anion shows higher symmetry than others as seen in Fig. 4. 1. $PF_4(CF_3)_2^-$ anion shows a good symmetrical structure with two P-CF_3 bond of ca. 1.90 Å. $PF_5(CF_3)^-$ and $PF_3(CF_3)_3^-$ anions do not show symmetrical structures because of one or three P-CF_3 bond.

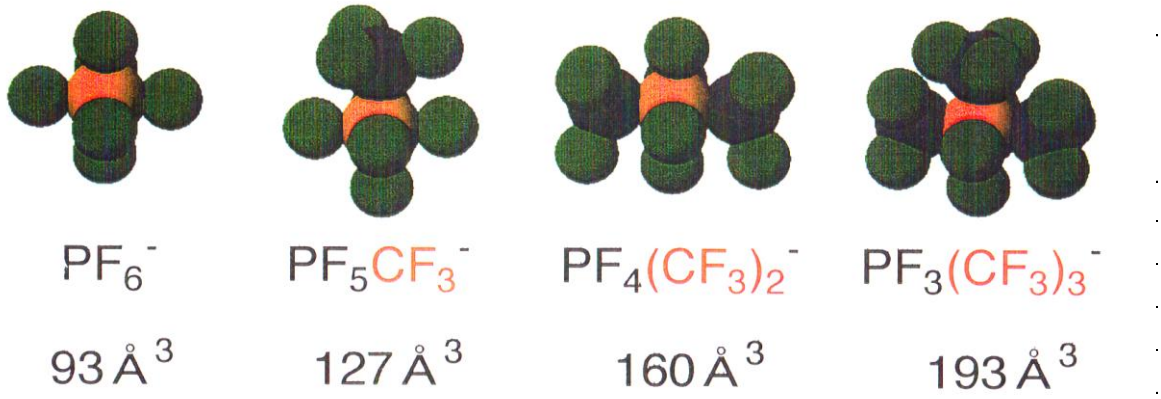

Figure 4. 1 The structures and their sizes for $PF_{6-n}(CF_3)_n$ (n = 1, 2, and 3) anions calculated by DFT calculation using B3LYP/6-31G* on Spaltan V 5. 0.

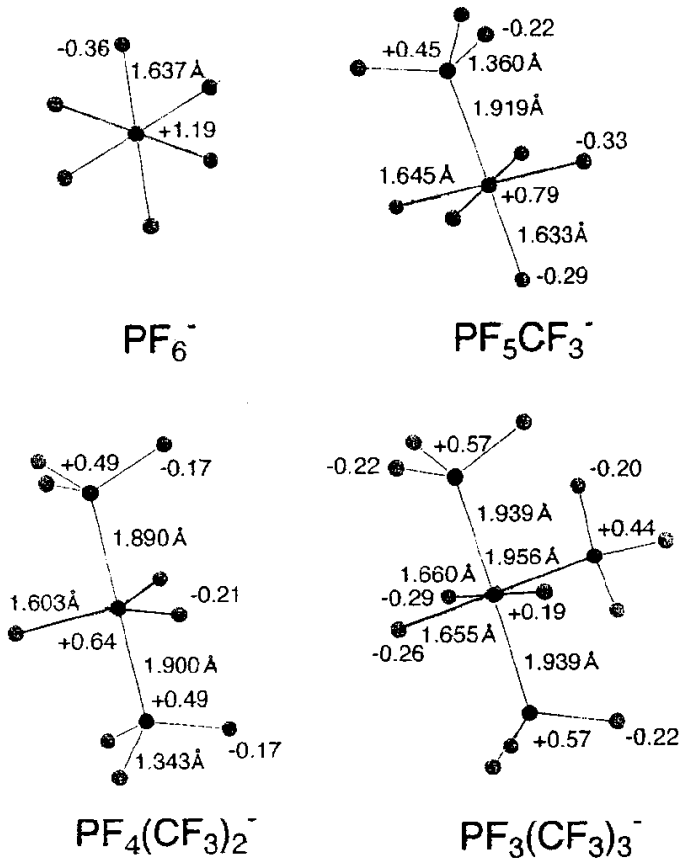

Figure 4. 2 The P-CF_3 and P-F bonds distance of $PF_{6-n}(CF_3)_n$ (n=0-3) anions calculated by DFT using B3LYP/6-31G* on Spaltan V 5. 0. Number given in each atom is formal charge.

In order to ensure the stability of $LiPF_4(CF_3)_2$ electrolyte, the storage or aging tests are carried out. Figure 4. 3 shows a photo after the storage of $LiPF_6$ and $LiPF_4(CF_3)_2$ electrolytes. Freshly prepared electrolytes are colorless, transparent liquid. $LiPF_6$ PC/DME (1/2 by volume) on the left became brown in color after the storage at room temperature for 3 years. $LiPF_4(CF_3)_2$ PC/DME (1/2 by volume) on the right in Fig. 4. 3 remained colorless and transparent liquid even after three-years storage. The result on the storage test is a clear evidence that $PF_4(CF_3)_2^-$ anion is more stable than PF_6^- anion as lithium salt electrolyte.

By using *an isodesmic reaction* (9), the ionic dissociation of $LiPF_{6-n}(CF_3)_n$ is also examined. Results are shown in Table 4. 1. All the values calculated are negative, suggesting that $LiPF_{6-n}(CF_3)_n$ salts (n = 1, 2, and 3) are more dissociative than $LiPF_6$;

$\underline{\Delta G(LiPF_3(CF_3)_3); 8.6}$ > $\Delta G(LiPF_4(CF_3)_2)$; 2.1 > $\Delta G(LiPF_5(CF_3))$; 0.5 > $\Delta G(LiPF_6)$; 0 kcal mol^{-1}

Figure 4. 3 Visual inspection on the stability of $LiPF_4(CF_3)_2$ electrolyte. The $LiPF_4(CF_3)_2$ electrolyte, i.e., 0.1 mol dm^{-3} PC/DME (1/2 by volume) on the right, was stored for 3 years at room temperature. The $LiPF_6$ electrolyte on the left is also stored in the same condition in order to compared to the $LiPF_4(CF_3)_2$ electrolyte.

Table 4. 2 Conductivity measured in 0.1 mol dm^{-3} lithium salt dissolved in PC/DME (1/2 by volume) and the oxidation potential measured by a platinum electrode in 0.1 mol dm^{-3} lithium salt dissolved in PC for $LiPF_{6-n}(CF_3)_n$ at 25°C.

Salt	Conductivity	Oxidation Potential
	(mS cm^{-1})	(V vs. Li/Li^+)
$LiPF_6$	4.4	6.0
Li PF_6+3DME	—	5.3
$LiPF_5(CF_3)$	4.2	6.2
$LiPF_4(CF_3)_2$	3.9	6.2
$LiPF_3(CF_3)_3$+3DME	3.9	5.1

Table 4. 2 shows the conductivity of 0.1 mol dm^{-3} $LiPF_{6-n}(CF_3)_n$ PC/DME (1/2 by volume). The mobility of $PF_{6-n}(CF_3)_n$ anions decreases when n increases from 1 to 3 because of an increase in the volume of an anion as shown in Fig. 4. 1. However, the observed conductivity is 3.9 – 4.2 mS cm^{-1}, which is almost the same level conductivity as 4.4 mS cm^{-1} for a $LiPF_6$ electrolyte. This is due to an increase in the degree of dissociation as is expected.

4. 4. 2 HOMO energy of $PF_{6-n}(CF_3)_n^-$ anions associated with oxidation potentials

The HOMO energy for $LiPF_{6-n}(CF_3)_n$ is already shown in Table 4. 1. Among $LiPF_{6-n}(CF_3)_n$ (n = 1, 2, and 3), $PF_4(CF_3)_2$ anion shows the lowest HOMO energy, which is lower than that of a PF_6^- anion, implying that a $LiPF_4(CF_3)_2$ electrolyte is more stable against oxidation than $LiPF_6$ electrolyte. In order to ensure the stability of $LiPF_4(CF_3)_2$ electrolyte against oxidation, voltammetric examinations are carried out. Experimental methods are the same as those described in section 2. 3. 2. Results are summarized in Table 4. 2. The electrolytes used are 0.1 mol dm^{-3} $LiPF_6$, $LiPF_5(CF_3)$, or $LiPF_4(CF_3)_2$ dissolved in propylene carbonate (PC). $LiPF_3(CF_3)_3$ contains 3DME, so that 0.1 mol dm^{-3} $LiPF_3(CF_3)_3$ dissolved in PC also contains 0.3 mol dm^{-3} DME. In order to examine the effect of DME contaminated

in PC electrolyte upon an oxidation potential, $LiPF_6$ + 3DME is prepared and dissolved in PC. As clearly seen in Table 4. 2, the oxidation potential of 5.1 V vs. Li/Li^+ for $LiPF_3(CF_3)_3$ is due to DME contaminated.

As seen in Table 4. 2, a 0.1 mol dm^{-3} $LiPF_4(CF_3)_2$ PC electrolyte shows almost the same oxidation potential as that of $LiPF_6$ or slightly higher oxidation potential.

4. 4. 3 Comparison between $PF_{6-n}(CF_3)_n^-$ and $PF_{6-n}(C_2F_5)_n^-$ anions

Synthesis and conductivity of $LiPF_4(i\text{-}C_3F_7)_2$ and $LiPF_3(C_2F_5)_3$ have already been reported by Sartori et al. and a Merck research group [8-13]. Merck group reported that $LiPF_6$ electrolyte with 500 ppm water is hydrolyzed to generate HF more than 600 ppm, while LiFAP electrolyte with 1000 ppm water is stable under hydrolysis conditions without generating any HF, which agrees well with the results described in section 4. 4. 1.

In order to examine which anion is more suitable for electrolyte, $P\text{-}CF_3$, $P\text{-}C_2F_5$, or $P\text{-}C_3F_7$ single bond to be substituted for P-F single bond in considering new electrolytes, $PF_{6-n}(C_2F_5)_n^-$ anions are also compared with $PF_{6-n}(CF_3)_n^-$. Li $PF_{6-n}(C_2F_5)_n$ anions are calculated using isodesmic reactions similar to eqs. (4) and (9) in order to compare the results with those for $LiPF_{6-n}(CF_3)_n$. Table 4. 3 shows the results of ΔH calculated for *isodesmic reaction* (4), ΔG for reaction (9), and HOMO energy for $LiPF_4(C_2F_5)_2$ and $LiPF_3(C_2F_5)_3$ anions together with corresponding to $LiPF_4(CF_3)_2$ and $LiPF_3(CF_3)_3$ anions. In order to compare the calculated values properly, a DFT method with GGA(pw91)/DND is applied for the calculation. The generalized gradient corrected (GGA) functional, by Perdew and Wang (PW91) is derived by considering low- and high-density regimes and by enforcing various summation rules. Ciezak et al. [14] reported that the PW91 method was found to be slightly superior to the BLYP/ DND and B3LYP/6-31G** methods. In Table 4. 3, the conductivity ratio of a target lithium salt to $LiPF_6$ is also shown. For $PF_n(CF_3)_{6-n}$ anions, ΔH, ΔG, and HOMO energy are the same order and tendency as already shown in Table 4. 1 calculated by a DFT method with B3LYP/6-31G*.

Table 4. 3 Energies calculated for isodesmic reactions together with HOMO energy calculated by DFT using GGA(pw91)/DND for $PF_{6-n}(CF_3)_n$ and $PF_{6-n}(C_2F_5)_n$ anions. Conductivity ratio is based on the conductivity of $LiPF_6$ electrolyte. Conductivity data for $LiPF_3(C_2F_5)_3$ is taken from refs. 8 and 9.

Li Salt	Conductivity ratio (salt concentration in mol dm^{-3})	Energy (kcal mol^{-1})		HOMO Energy of Anion (eV)
		ΔH	ΔG	
$LiPF_6$	1.00(0.1M)	0.0	0.0	-3.64
trans-$LiPF_4(CF_3)_2$	0.88(0.1M)	-7.0	-5.2	-3.92
mer-$LiPF_3(CF_3)_3$	0.88(0.1M)	-5.0	-9.9	-3.60
trans-$LiPF_4(C_2F_5)_2$	-	-13.4	-8.4	-4.05
mer-$LiPF_3(C_2F_5)_3$	0.82(0.5,0.8M)	-8.3	-10.4	-3.91

As seen in Table 4. 3, $PF_4(C_2F_5)_2^-$ and $PF_4(CF_3)_2^-$ anions are thermally more stable than a $PF_3(CF_3)_3^-$ anion. $PF_{6-n}(C_2F_5)_n^-$ anions give negative values in ΔH and ΔG, suggesting that $PF_{6-n}(C_2F_5)_n^-$ anions are thermally stable and dissociative. The HOMO energy associated with the stability against oxidation is of an order;

$$PF_4(C_2F_5)_2^- < PF_4(CF_3)_2^- \leq PF_3(C_2F_5)_3^- < PF_6^- < PF_3(CF_3)_3^-,$$

implying that $PF_4(C_2F_5)_2^-$ and $PF_4(CF_3)_2^-$ are oxidation-resistant anions compared to PF_6^-.

As have been described above, $PF_{6-n}(CF_3)_n^-$ and $PF_{6-n}(C_2F_5)_n^-$ (n=1 and 2) anions are superior to $LiPF_6$ except conductivity. The conductivity ratio for $LiPF_3(C_2F_5)_3$ is 0.82, meaning 18% lower than that of $LiPF_6$, although $LiPF_3(C_2F_5)_3$ is expected to be highly dissociative by a computational method. This is due to a size effect on conductivity as discussed in section 1. 3. 2. $LiPF_4(CF_3)_2$ shows the conductivity ratio of 0.88, meaning 12% lower than that of $LiPF_6$.

From these results, $LiPF_4(CF_3)_2$ is selected to be the best candidate salt because it shows the highest conductivity, thermal stability, and stability against oxidation among $LiPF_{6-n}(CF_3)_n$ and $LiPF_{6-n}(C_2F_5)_n$ examined.

4. 4. 4 New fluoro-organic lithium salt $LiPF_4(CF_3)_2$ in prototype 14500 batteries

As has been discussed in section 3. 3. 1, any chemical species including a new lithium salt to be introduced to lithium-ion batteries should be examined in prototype batteries consisting of a positive and negative electrode separated by a diaphragm 25-microns thick with an electrolyte, because all chemical species are exposed to severe conditions. In order to examine whether or not a new fluoro organic lithium salt $LiPF_4(CF_3)_2$ can be used in lithium-ion batteries, prototype lithium-ion batteries consisting of a $LiCoO_2$-positive and graphite-negative electrodes with a 0.1 mol dm^{-3} $LiPF_4(CF_3)_2$ EC/MEC (1/2 by volume) electrolyte are fabricated and examined. Figure 4. 4 shows the charge and discharge curves of a prototype 14500 battery operated at 60 mA. To compare the results, a prototype 14500 battery with 0.1 mol dm^{-3} $LiPF_6$ EC/MEC (1/2 by volume) electrolyte is also fabricated and examined, as shown in Fig. 4. 4. Although 600 mAh battery is designed, both batteries cannot deliver 600 mAh electricity due to low concentration of lithium ions. When $LiPF_4(CF_3)_2$-battery is compared to $LiPF_6$-battery, the discharge capacity determined at cutoff voltage of 2.75 V is the same. However, the charging curve of $LiPF_4(CF_3)_2$-battery follows slightly higher voltage than that of $LiPF_6$-battery. Conversely, the discharge curve of $LiPF_4(CF_3)_2$-battery follows lower voltage than that of $LiPF_6$-battery. According to Table 4. 2, the conductivity of a 0.1 mol dm^{-3} $LiPF_4(CF_3)_2$ EC/MEC electrolyte is 3.9 mS cm^{-1} while that of a 0.1 mol dm^{-3} $LiPF_6$ EC/MEC electrolyte is 4.4 mS cm^{-1}. The difference in conductivity reflects upon the polarization in the charge and discharge curves described above. Although $LiPF_4(CF_3)_2$-battery shows poor performance in terms of polarization, capacity retention is better than that of $LiPF_6$-battery, as shown in Figure 4. 5. Capacity retention of $LiPF_4(CF_3)_2$-battery after 150 cycles is 62% based on the initial capacity while that of $LiPF_6$-battery is 46%. The capacity retention difference of each battery is 16% of initial capacity. This cycle retention difference is caused by initial 50 cycles. The $LiPF_6$-battery shows 36% of capacity loss for initial 50 cycles, beside $LiPF_4(CF_3)_2$-battery shows only 20%. The capacity loss difference reached 16% of initial capacity.

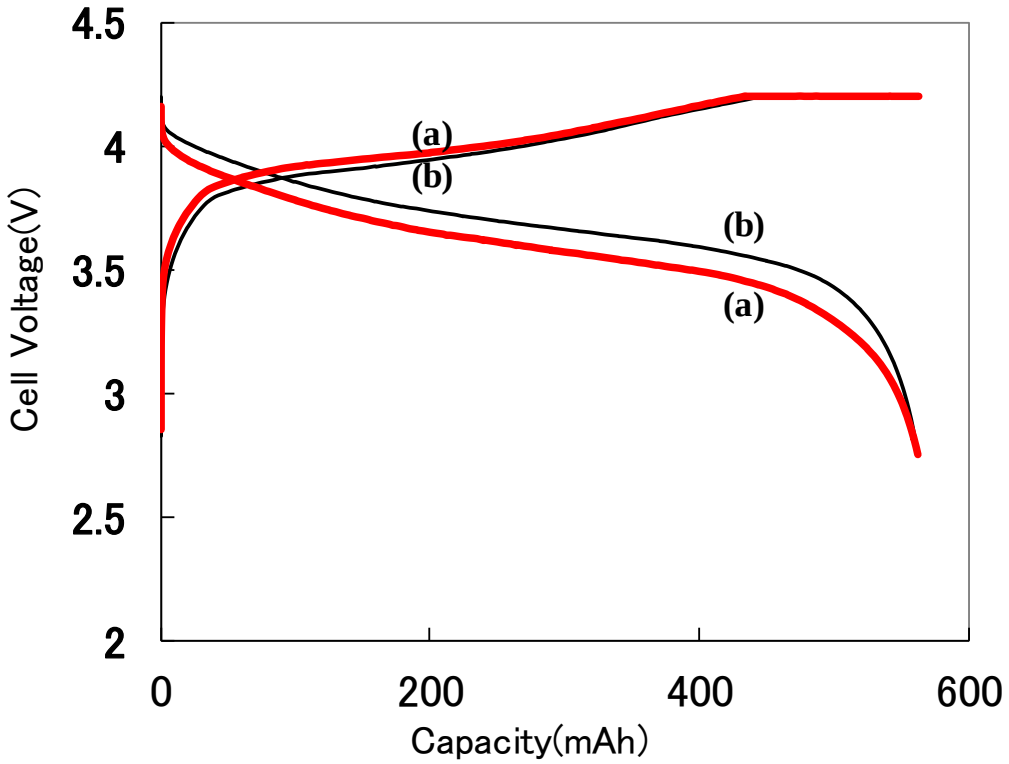

Figure 4. 4 Charge and discharge curves of prototype 14500 lithium-ion batteries consisting of $LiCoO_2$-positive and graphite-negative electrodes. The electrolyte is (a) 0.1 mol dm^{-3} $LiPF_4(CF_3)_2$ dissolved in EC/MEC (1/2 by volume) or (b) 0.1 mol dm^{-3} $LiPF_6$ dissolved in EC/MEC (1/2 by volume). The batteries are charged in a constant-current (60 mA) constant-voltage (4.2 V) charging mode for 12 h and discharged at 60 mA to 2.75 V.

4. 4. 5 Prototype batteries stored at 60°C for 20 days

As discussed in section 4. 4. 1, $LiPF_4(CF_3)_2$ is evaluated as a thermally stable salt than $LiPF_6$ by computational calculation and $LiPF_4(CF_3)_2$ electrolyte shows good stability even for three years storage. In order to ensure the thermal stability of $LiPF_4(CF_3)_2$-battery, the prototype batteries with $LiPF_4(CF_3)_2$ and $LiPF_6$ are stored at 60°C.

Table 4. 4 shows the results on the impedance measurements for $LiPF_4(CF_3)_2$ and $LiPF_6$ prototype batteries before and after the storage at 60°C for 20 days.

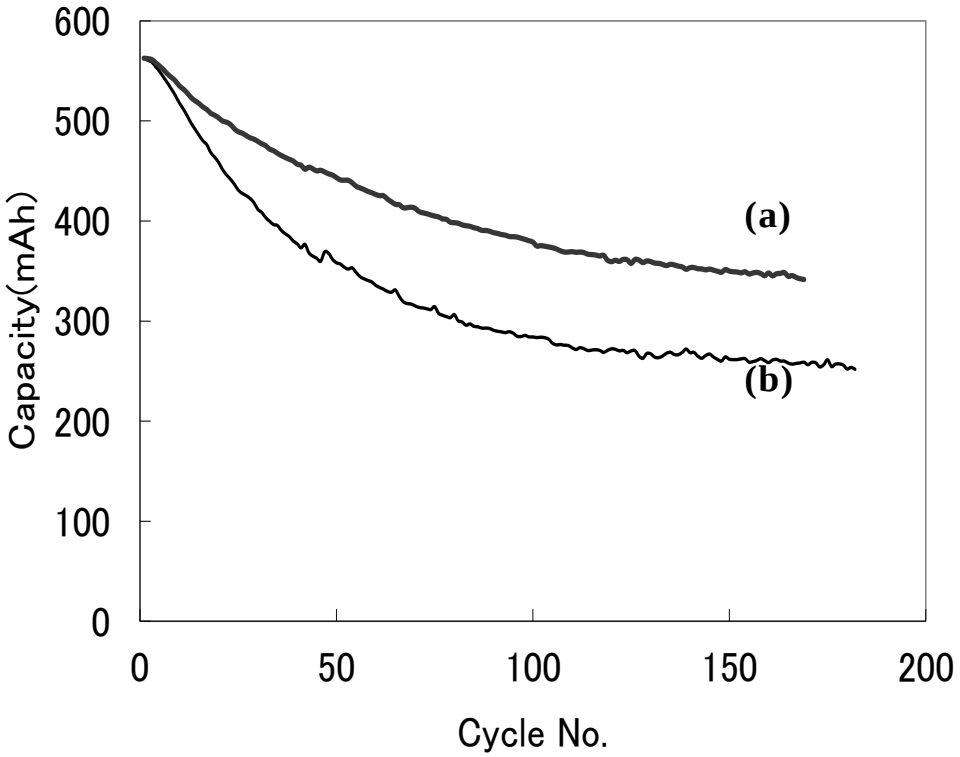

Figure 4. 5 Discharge capacities as a function of cycle number for prototype 14500 lithium-ion batteries consisting of $LiCoO_2$-positive and graphite-negative electrodes. The electrolyte is (a) 0.1 mol dm^{-3} $LiPF_4(CF_3)_2$ dissolved in EC/MEC (1/2 by volume) or (b) 0.1 mol dm^{-3} $LiPF_6$ dissolved in EC/MEC (1/2 by volume). The batteries are charged in a constant-current (60 mA) constant-voltage (4.2 V) charging mode for 12 h and discharged at 60 mA to 2.75 V.

The impedance of $LiPF_4(CF_3)_2$ battery increases from 0.149 to 0.193 Ω, while that of $LiPF_6$ battery increases from 0.147 to 0.207 Ω. The increase in impedance for $LiPF_4(CF_3)_2$ battery is 30%, which is smaller than that for $LiPF_6$ battery, i.e., 41% increase during the storage at 60°C for 20 days. The initial impedance for $LiPF_4(CF_3)_2$ battery, 0.149 Ω, is slightly larger than that for $LiPF_6$ battery, 0.147 Ω, because of the difference in conductivity. After the storage at 60°C for 20 days, the impedance for $LiPF_4(CF_3)_2$ battery, 0.193 Ω, is smaller than that for $LiPF_6$ battery, 0.207 Ω.

Table 4. 4 Change in impedance of prototype 14500 lithium-ion batteries during the storage at 60°C for 20 days. The electrolyte is 0.1 mol dm^{-3} $LiPF_4(CF_3)_2$ or $LiPF_6$ dissolved in EC/MEC (1/2 by volume). Batteries are fully charged to 4.2 V and then stored.

Li Salt	Battery Impedance (Ω; at 1 kHz)	
	Before Storage	After Storage
$LiPF_6$	0.147(100%)	0.207(141%)
$LiPF_4(CF_3)_2$	0.149(100%)	0.193(130%)

4. 4. 6 XPS examinations on the graphite-negative electrodes

Table 4. 5 shows the results of XPS analysis on the graphite-negative electrodes. The analytical results are given in atomic percent (at%) for carbon, fluorine, lithium, phosphorous, and oxygen. Of these, phosphorous and fluorine are primarily derived from $LiPF_4(CF_3)_2$ or $LiPF_6$. In order to examine the analytical results, the atomic percent of phosphorous in Table 4. 5 is assumed to be derived from $LiPF_4(CF_3)_2$ and the amounts of corresponding fluorine and lithium are calculated. In the second column from the right in Table 4. 5, the content of phosphorous is listed to be 0.5 at%. Consequently, the amount of fluorine is calculated to be 5.0 at% based on the formula of $LiPF_4(CF_3)_2$. Similarly, the

Table 4. 5 The atomic percent on the graphite-negative electrode surface examined by XPS after cycle tests on the prototype 14500 lithium-ion batteries consisting of $LiCoO_2$ and graphite. XPS analysis was measured under Mg-Kα 12 kV-10 mA by ESCA LAB Mark 2 (Thermo Fisher Scientific Inc.).

Salt used in the battery	C	F	Li	P	O
1.0 mol dm^{-3} $LiPF_6$	33.0	19.6	10.7	3.8	32.6
0.1 mol dm^{-3} $LiPF_6$	45.7	4.6	14.0	0.6	22.4
0.1 mol dm^{-3} $LiPF_4(CF_3)_2$	43.2	6.0	15.2	0.5	20.7

Table 4. 6 The calculated atomic percent based on the observed phosphorous in Table 4. 5.

Salt used in the battery	C	F	Li	P	O	Total
1.0 mol dm^{-3} $LiPF_6$	0.0	22.8	3.8	3.8	-	30.4
0.1 mol dm^{-3} $LiPF_6$	0.0	3.6	0.6	0.6	-	4.8
0.1 mol dm^{-3} $LiPF_4(CF_3)_2$	1.0	2.0+3.0	0.5	0.5	-	2.0

amounts of lithium and carbon are calculated to be 0.5 at% and 1.0 at%, respectively, as is summarized in Table 4. 6. The calculated value of 5 at% agrees well with the observed value of 6.0 at% in Table 4. 5, because PVdF used as a binder in the graphite-negative electrode contains fluorine detected, indicating that 7.0 at% is derived from the $LiPF_4(CF_3)_2$ salt or its relatives.

Although the amount of lithium is small (ca. 0.5 at%), the amount of $LiPF_6$ or $LiPF_4(CF_3)_2$ is calculated to be 4.8 at% for $LiPF_6$ or 7.0 at% for $LiPF_4(CF_3)_2$ as can be seen in Table 4. 6. The amount of $LiPF_4(CF_3)_2$-related compounds on the graphite-negative electrode is larger than that of $LiPF_6$. The strong F1s peak at 687-688 eV is observed only for a $LiPF_4(CF_3)_2$ surface, suggesting that $LiPF_4(CF_3)_2$ covered on the graphite-negative electrode continuously generates a LiF layer as has already been discussed in section 3. 3. 3. In Table 4. 5, the amount of carbon and oxygen decreases by ca. 2 at%, i.e.,

$LiPF_4(CF_3)_2$: C(43.2 at%), O(20.7 at%)
$LiPF_6$: C(45.7 at%), O(22.4 at%)

Because carbon and oxygen are derived from solvent molecules, this suggests that the surface layer derived from $LiPF_4(CF_3)_2$ suppresses the reaction of solvent molecules on the graphite-negative electrode more effectively than that from $LiPF_6$.

The amount of fluorine, 6.0 at%, for $LiPF_4(CF_3)_2$ in Table 4. 5 is larger than that, 4.6 at%, for $LiPF_6$. Table 4. 7 shows the detailed analysis of F1s XPS signals. The signal at 685 eV is identified as LiF. For $LiPF_6$, LiF is derived from $LiPF_6$ or HF, as has already been discussed in chapter 3. For $LiPF_4(CF_3)_2$, LiF is derived

Table 4. 7 The detailed fluorine atomic percent on the graphite-negative electrode surface analyzed by F1s XPS peak analysis. Total atomic percent of fluorine is the same as that in Table 4. 5.

Salt used in the battery	685 eV (LiF)	686 eV (Other inorganic F)	687-688 eV (Organic F such as C-F of $LiPF_4(CF_3)_2$)	Total
1.0 mol dm^{-3} $LiPF_6$	1.3	18.5	0.0	19.8
0.1 mol dm^{-3} $LiPF_6$	1.4	2.8	0.0	4.2
0.1 mol dm^{-3} $LiPF_4(CF_3)_2$	2.6	1.4	2.1	6.1

mainly from $LiPF_4(CF_3)_2$, because $LiPF_4(CF_3)_2$ is thermally stable, not to generate HF as discussed section 4. 4. 1. Lithium fluorite is a reaction product of $LiPF_4(CF_3)_2$ and graphite-negative electrode. Larger amount of LiF, 2.6 at%, is formed from $LiPF_4(CF_3)_2$, compared to that from $LiPF_6$, 1.4 at%, and it grows on the surface under the $LiPF_4(CF_3)_2$ salt and its related compounds.

$LiPF_4(CF_3)_2$: F(6.0 at%) : (**2.6** at% out of 6.0 at% is LiF)
$LiPF_6$: F(4.6 at%) : (**1.4** at% out of 4.6 at% is LiF)

As have been discussed above, the graphite-negative electrode surface is covered with $LiPF_4(CF_3)_2$ salt and its related compounds, in which a LiF-protective layer on the surface is formed more efficiently than $LiPF_6$ layer. These factors play an important role on the improvement of battery performance. In other words, the fluoro-organic lithium salts are the effective additives to the graphite-negative electrodes in lithium-ion batteries.

4. 5 Summary

In this chapter, possible alternatives to $LiPF_6$ currently used in lithium-ion batteries have been examined by modifying PF_6 anion. The problem in applying $LiPF_6$-based electrolytes is its instability due to decomposition with contaminated water to give HF, which induces several problems in lithium-ion batteries. In

order to solve the problem, the computational methods are applied to materials design based on $LiPF_6$. Specifically, P-CF_3 single bond is introduced to substitute with P-F single bond in PF_6 anion, resulting in $PF_{6-n}(CF_3)_n^-$ anion. A P-CF_3 single bond can be further replaced by a P-C_2F_5 single bond if necessary. The thermal stability of $LiPF_{6-n}(CF_3)_n$ (n = 1, 2, or 3) is evaluated using the isodesmic reaction of

$$LiPF_6 + PF_{5-n}(CF_3)_n \rightarrow PF_5 + LiPF_{6-n}(CF_3)_n,$$

The ability of dissociation is estimated using the isodesmic reaction of

$$PF_6^- + LiPF_{6-n}(CF_3)_n \rightarrow LiPF_6 + PF_{6-n}(CF_3)_n^-.$$

The HOMO energy of each anionic species associated with oxidation stability is also examined by the first-principles calculation in advance of materials preparation and examination.

According to the first-principles calculation, $PF_{6-n}(CF_3)_n^-$ (n = 1, 2, and 3) anions are thermally more stable than PF_6^- anion. Of these, $PF_4(CF_3)_2^-$ anion is calculated to be the most stable, which is evidenced by a fact that the electrolyte containing $LiPF_4(CF_3)_2$ is colorless and transparent liquid even after 3-years storage at room temperature while that containing $LiPF_6$ is brown in color under the same condition. From the data on thermal stability, conductivity, and stability against electrochemical oxidation, $LiPF_4(CF_3)_2$ is selected to be the best material among $LiPF_{6-n}(CF_3)_n$ and $LiPF_{6-n}(C_2F_5)_n$.

Comparative study of $LiPF_4(CF_3)_2$ and $LiPF_6$ in prototype 14500 lithium-ion batteries consisting of $LiCoO_2$ and graphite clearly shows that $LiPF_4(CF_3)_2$ is superior to $LiPF_6$ in terms of the stability of impedance during storage tests at 60°C for 20 days and the capacity retention during charge and discharge cycles.

A possible mechanism on why $LiPF_4(CF_3)_2$ is superior to $LiPF_6$ in prototype lithium-ion batteries is discussed in terms of a solid-electrolyte interface formed on the graphite-negative electrode based on the XPS observations after the cycle tests of both batteries, and it is shown that the lithium salt of $LiPF_4(CF_3)_2$ behaves like an effective additive to the graphite-negative electrodes in lithium-ion batteries in

addition to a superior electrolyte.

References

[1] T. Sonoda, H. Kamizori, S. Ikeda, H. Nagashima, K. Momota, T. Hashimoto, A. Kimura, J. Yamaki, R. Hagiwara, and F. Kita, 2D19 in the extended abstract of The 40th Battery Symposium in Japan, Kyoto, Nov.14-16, 1999.

[2] H. Kamizori, A. Kimura, S. Ikeda, T. Sonoda, J. Yamaki, H. Nagashima, K. Momota, T. Hashimoto, R. Hagiwara, and F. Kita, 2C01 in the extended abstract of The 41st Battery Symposium in Japan, Nagoya, Nov.20-22, 2000.

[3] E. S. Hong, S. Okada, T. Sonoda, S. Gopukumar, and J. Yamaki, *J. Electrochem. Soc.*, **151**, A1836 (2004).

[4] K. Tasaki, K. Kanda, S. Nakamura, and M. Ue, *J. Electrochem. Soc.*, **150**, A1628 (2003).

[5] David Young, "Computational Chemistry", Wiley-Interscience, Appendix A.A.3.2 p 342 (2001).

[6] S. Sastre, R. Casasnovas, F. Munoz, and J. Frau, *Theoretical Chemistry Accounts*, **132,** 1310 (2013).

[7] L. M. Yagupolskii and Yu. L. Yagupolskii, *J. Fluorine Chem.*,**72**, 225 (1995).

[8] P. Sartori, N. Ignat'ev, R. Wenige, U. Heider, and V. Hilarius, AB-160 in the extended abstract of The Electrochem. Soc. Fall Meeting, Boston, Masachusetts, Nov.1-6, 1998.

[9] U. Heider, R. Oestein, and M. Jungnitz, *J. Power Sources,* **81-82**, 119 (1999).

[10] M. Schmidt, U. Heider, A. Kuehner, R. Oesten, M. Jungnitz, N. Ignat'ev, and P. Sartori, *IMLB 1*0, May.28-June.2, Como/Italy, Abs.22 (2000).

[11] M. Schmidt, U. Heider, A. Kuehner, R. Oesten, M. Jungnitz, N. Ignat'ev, and P. Sartori, *J. Power Sources,* **97/98,** 557 (2001).

[12] N. Ignat'ev and P. Sartori, *J. Fluorine Chem.*, **101**, 203 (2000).

[13] N. V. Ignat'ev, U. Welz-Biermann, M. Schmidt, M. Weiden, U. Heider, A. I. Kucherina, and H. Willner, Ab. No.90 in the extended abstract of The 16th Winter Fluorine Conference, Florida, Jan. 12-17, 2002.

[14] J. A. Ciezak, J. B. Lea, and B. S. Hudson, *J. Mol. Struct.: THEOCHEM*, **767,** 23 (2006)

Concluding Remarks

Research described herein has been done to explore new electrolytes for advanced lithium and lithium-ion batteries since the late 1980's at Hitachi Maxell Corporation. The application of lithium and lithium-ion batteries is still expanding throughout the world. Batteries for some applications to safety devices require high reliability and batteries for power devices require high input and output power with the heat-resistant nature. Lithium batteries or lithium-ion batteries at that time or even at present cannot satisfy all the severe requirements imposed by users mainly due to the lack of electrolytes. Lithium hexafluorophosphate $LiPF_6$ is an excellent electrolyte for lithium and lithium-ion batteries because of outstanding stability to oxidation and high ionic conductivity. However, lithium-ion batteries having $LiPF_6$ solutions do not survive when the batteries are operated at high temperature or deteriorate during the operation for long periods at ambient temperature, because $LiPF_6$ is well known as a thermally unstable species. In order to cope with the problem on the electrolyte of $LiPF_6$ and to advance the electrolytes for lithium-ion batteries, several trials have been done during the past 20 years and the research is summarized in a doctoral thesis.

In Chapter 1, the preliminary results on the conductivity of fluoro-organic lithium salts in the mixed solvents of propylene carbonate (PC) and dimethoxyethane (DME) have been described, and the methods to improve the conductivity are discussed in terms of the concentration of free ions, the dissociation of a lithium salt, and the mobility of each ion. Bulky anions are difficult to move in a viscous liquid, which affects the mobility of anion. However, the electronic effect of fluoro-organic groups upon conductivity is clearly observed and it is positive, which compensates the negative effect derived from bulkiness of an anion. This clearly indicates that the electronic structures of fluoro-organic lithium salts are important in developing new fluoro-organic lithium salts for advanced lithium-ion batteries. Among fluoro-organic lithium salts examined, the fluoro-organic lithium salts of $(C_2F_5SO_2)_2NLi$, $((CF_3)_2CHOSO_2)_2NLi$, and $(C_4F_9SO_2)(CF_3SO_2)NLi$ show higher

conductivities than CF_3SO_3Li already known as a lithium battery electrolyte.

In Chapter 2, the oxidation potentials in an electrochemical window for fluoro-organic lithium salts are described together with the HOMO energy of each anion under consideration. One-to-one correspondence between the oxidation potentials empirically observed and the HOMO energies calculated by the computational methods for corresponding anions is observed for a series of fluoro-organic lithium salts, so that the HOMO energy calculation is used throughout the research. The oxidation potentials of $(RfSO_2)_2NLi$ and $(RfSO_2)_3CLi$ are higher than that of $(CF_3SO_2)OLi$, as is predicted by the HOMO energy calculation, in which Rf is a fluoro-alkyl group. A branched imide-ester salt $((CF_3)_2CHOSO_2)_2NLi$ shows the highest oxidation potential of 5.8 V among the imide-ester salts examined. Imide and methide salts with longer fluoro-alkyl groups show higher oxidation potentials, and they are resistive against aluminum corrosion, which is one of the problems in considering the application of imide salts to lithium-ion batteries. The aluminum dissolution potentials in PC electrolyte are observed to be 4.0 V vs. Li/Li^+ for $(CF_3SO_2)_2NLi$, 4.3 V for $((CF_3)_2CHOSO_2)_2NLi$, 4.8 V for $(C_4F_9SO_2)(CF_3SO_2)NLi$, 4.6 V for $(CF_3SO_2)_3CLi$, and 5.5 V for $(CF_3CH_2OSO_2)_3CLi$.

In Chapter 3, the lithium imide salts of $(C_2F_5SO_2)_2NLi$, $((CF_3)_2CHOSO_2)_2NLi$ and $(C_4F_9SO_2)(CF_3SO_2)NLi$ have been examined in prototype 14500 lithium-ion batteries consisting of a $LiCoO_2$-positive and graphite-negative electrodes. All the batteries are superior to the current lithium-ion batteries with a $LiPF_6$ electrolyte in terms of high-temperature storage and cycle performance. Among these electrolytes, $((CF_3)_2CHOSO_2)_2NLi$ shows the best performance in terms of capacity retention. In order to understand why the imide-ester salt of $((CF_3)_2CHOSO_2)_2NLi$ gives better cycle performance than $LiPF_6$ when it examined in lithium-ion batteries, detailed XPS analysis on the graphite-negative electrode has been performed, and it is shown that an effective solid electrolyte interface (SEI) derived from the imide-ester salt plays a crucial role to prevent a reaction of the electrolyte on the graphite-negative electrode and consequently it shows better capacity retention.

In Chapter 4, possible alternatives to $LiPF_6$ currently used in lithium-ion

batteries have been examined by modifying a PF_6^- anion. $LiPF_6$ shows excellent property to oxidation and good conductivity in polar aprotic solvents, as has been described throughout the thesis. The problem is the thermal stability of $LiPF_6$. In order to cope with the problem, the thermal stability of a $PF_{6-n}(CF_3)_n^-$ and $PF_{6-n}(C_2F_5)_n^-$ anion (n = 1, 2, or 3) is examined using isodesmic reactions by a computational method. Of these, a $PF_4(CF_3)_2^-$ anion is calculated to be highly stable, which is evidenced by a fact that the electrolyte containing $LiPF_4(CF_3)_2$ is colorless, transparent liquid even after 3-years storage at room temperature while that containing $LiPF_6$ is brown in color under the same condition. $LiPF_4(CF_3)_2$ also shows high oxidation potential, so that it have been examined in prototype 14500 lithium-ion batteries consisting of a $LiCoO_2$-positive and graphite-negative electrode. High-temperature storage is superior to that of $LiPF_6$ and cycle performance of the battery with $LiPF_4(CF_3)_2$ is better than these with $LiPF_6$ due to the formation of an effective SEI derived from $LiPF_4(CF_3)_2$.

As have been summarized above, fluoro-organic lithium salts show superior property to $LiPF_6$. Some of fluoro-organic lithium salts had been used in lithium batteries, and some of them have already been used as additives in lithium and lithium-ion batteries. The author hopes that the safe and reliable long-life high-energy density lithium batteries will grow through the research outlined herein in near future.

List of Publications

1. Fusaji Kita, Akira Kawakami, Takaaki Sonoda, and Hiroshi Kobayashi
   On the New Fluorinated Organic Lithium Salts for Lithium Batteries
   Proceedings of the Symposium on the New Sealed Rechargeable Batteries and Super Capacitors, ed. by B. M. Barmett, E. Dowgiallo, G. Halpert, Y. Matsuda, and Z.-I. Takehara, Proceeding Volume of The Electrochemical Society (PV93-23), p. 321-332, Penington, NJ, 1993.

   (Chapter 1)

2. Fusaji Kita, Akira Kawakami, Jin Nie, Takaaki Sonoda, and Hiroshi Kobayashi,
   On the Characteristics of Electrolytes with New Lithium Imide Salts,
   Journal of Power Sources, **68**, 307-310 (1997).

   (Chapter 2)

3. Fusaji Kita, Hideo Sakata, Sayaka Sinomoto, Akira Kawakami, Haruki Kamizori, Takaaki Sonoda, Hideo Nagashima, Jin Nie, Natalya V. Pavlenco, Yurii L. Yagupolskii,
   Characteristics of the Electrolyte with Fluoro Organic Lithium Salts,
   Journal of Power Sources, **90**, 27-32 (2000).

   (Chapter 3)

4. Fusaji Kita, Hideo Sakata, Akira Kawakami, Haruki Kamizori, Takaaki Sonoda, Hideo Nagashima, Natalya V. Pavlenco, and Yurii L. Yagupolskii,
   Electrocic Structures and Electrochemical Properties of $LiPF_{6-n}(CF_3)_n$
   Journal of Power Sources, **97-98**, 581-583 (2001).

   (Chapter 4)

Acknowledgments

This work was summarized under the guidance of Professor Tsutomu Ohzuku, Graduate School of Engineering, Osaka City University (OCU). I am greatly indebted to Professor Tsutomu Ohzuku for his suggestion and comments in preparing this manuscript. I would like to thank Professor Kouichi Tsuji (OCU) and Professor Seiya Kobatake (OCU) for reviewing this manuscript. I would like to thank Associate Professor Kingo Ariyoshi for the artwork of the final draft.

It is a pleasure to thank Dr. Takaaki Sonoda, former Associate Professor of Institute of Advanced Material Study at Kyushu University, for his cooperation and deep discussions on fluoro-organic lithium salts and also for his comments in preparing this manuscript. I also wish to thank Professor Hideo Nagashima and Professor Emeritus Hiroshi Kobayashi of Kyushu University for the assist of co-researching on fluoro-organic lithium salts.

I wish to thank Professor Yurii L. Yagupolskii, Institute of Organic Chemistry Ukrainian Academy of Science (Ukraine), and his members for the cooperation on the synthesis of following fluoro-organic lithium salts; $(CF_3CH_2OSO_2)_3CLi$, $(C_2F_5)_2P(=O)OLi$, and $LiPF_{6-n}(CF_3)_n$ (n = 1, 2, and 3). I wish to thank Professor Jin Nie, Huazhong University of Science and Technology (China), for the cooperation on the synthesis of following fluoro-organic lithium salts; $(C_4F_9SO_2)(CF_3SO_2)NLi$, $(C_8F_{17}SO_2)(CF_3SO_2)NLi$, $(FSO_2C_6F_4)(CF_3SO_2)NLi$, $((CF_3)_2CHOSO_2)_2NLi$, $(CF_3CH_2OSO_2)_2NLi$, $(CF_3CF_2CH_2OSO_2)_2NLi$, $(HCF_2CF_2CH_2OSO_2)_2NLi$, and polymer imide salts. I wish to thank Central Glass Co., Ltd., Mitsubishi Materials Electronic Chemicals Co., Ltd, Sumitomo 3M Limited, and NEOS Company Limited for supplying the fluoro-organic lithium salts.

I wish to thank Ms. Sayaka Sinomoto and Mr. Haruki Kamizori for their help on the computational methods for fluoro-organic lithium salts.

I also should like to thank Mr. Hideo Sakata, Mr. Kouji Murakami, Mr. Akira Kawakami and Mr. Kozo Kajita for their help on performing this work and their cooperation.

I wish to thank Dr. Kenji Sumiya for his encouragement of preparing this

manuscript. I would also like to express my gratitude to my family for their warm encouragements.

Finally, I wish to thank Hitachi Maxell Ltd. (HML) for giving me good opportunities to develop and study on lithium batteries with fluoro-organic lithium salts.

September, 2014

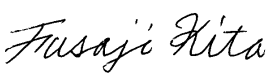

Fusaji Kita